THE UNIVERSITY OF
WAIKATO
Te Whare Wānanga o Waikato

Research Commons

http://waikato.researchgateway.ac.nz/
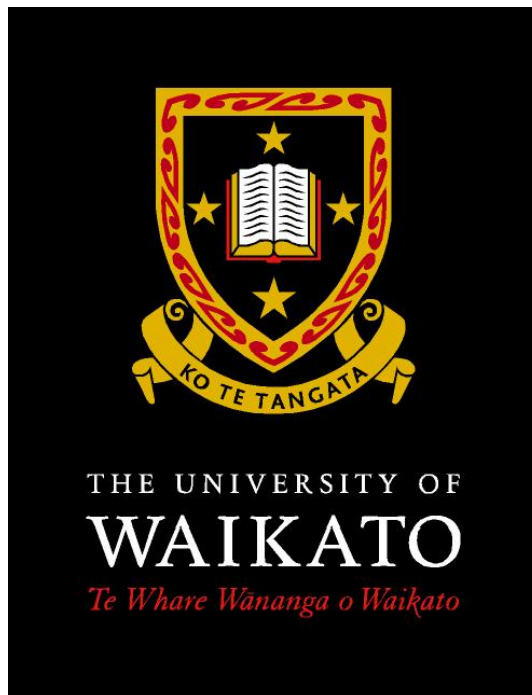
Research Commons at the University of Waikato

Copyright Statement:

Free vibration analysis of plates and shells by using the Superposition Method

A thesis
submitted in partial fulfillment
of the requirements for the degree
of
Doctor of Philosophy in Mechanical Engineering
at
The University of Waikato
by
Yusuke Mochida

The University of Waikato
2010

Abstract

This thesis is devoted to investigate the capability of the Superposition Method for obtaining the transient response of plates and the natural frequencies of thin doubly curved shallow shells. The Superposition Method gives accurate results with only a few terms and has proved to be efficient for both cases.

To investigate the transient response, all supports of a thin simply supported rectangular plate under self weight are suddenly removed. The resulting motion comprises a combination of the natural modes of a completely free plate. The modal superposition method is used for determining the transient response. The modes and natural frequencies of the plate are obtained using the Superposition Method and the Rayleigh-Ritz method with the ordinary and degenerated free-free beam functions. The W–W algorithm is then used to delimit the natural frequencies from the frequency equation derived in a determinantal form. There is an excellent agreement between the results from both approaches but the modes based on the Superposition Method result in more accurate values with fewer terms, and have shown faster convergence. The results from the Superposition Method may serve as benchmarks for the transient response of completely free plates. The transient response is found to be dominated by the lower modes. The centre of vibration is shifted parallel from the original xy plane by the distance of the first mode of the plate (a rigid body translation) multiplied by the first transient coefficient.

In the investigation of doubly curved shells, the natural frequency parameters of thin shallow shells with three different sets of boundary conditions were obtained for several different curvature ratios and two aspect ratios. The solutions to the building blocks, which are subject to simply-supported out-of-plane conditions and shear diaphragm in-plane conditions at all four edges, are represented by series of sine and cosine functions, generated using Galerkin's method since an exact solution is not available for the doubly curved shells. Once displacement functions for the building blocks are obtained, the prescribed boundary conditions of the actual shell under investigation are then satisfied using

the Superposition Method. The rate of convergence is found to be excellent and the results agree well with published results obtained using the Ritz method and those obtained using a Finite Element package, Abaqus. The computations show that it is possible to obtain the first 12 natural frequency parameters of the shallow shells on the rectangular planform with a rapid convergence rate.

<u>Acknowledgement</u>

The author would like to acknowledge the direction, guidance and advice by Associate Professor Sinniah Ilanko with respect of this thesis.

He also appreciates the panel of his supervisors, Dr. Mike Duke and Professor Yoshihiro Narita.

He specially thanks his family in their total support.

Table of Contents

List of Tables

List of Figures

1. Chapter I

Introduction

INTRODUCTION

1.1 Vibration of plates and shells

Thin plates and shells are two of the most common components in engineering machines and structures. Examples of applications include building walls, large-span roofs, turbine disks, pressure vessels, and airplane wings. In general, shell structures are more advantageous in engineering applications than plates in term of resistance to load. The engineering components must resist not only static loads but also dynamic loads. For instance, buildings must be designed to withstand dynamic forces such as earthquake excitations. Earthquake forces usually have low excitation frequency range. However, buildings must also be designed to minimise noise related problems. This means the structures must also be able to withstand acoustic excitations which extend to very high frequency range. Such engineering structures are also subjected to transient forces. One example is an airplane when it is exposed to gust. In engineering design, it is, therefore, important to use a method that is accurate and efficient for dynamic analysis including transient and steady state analyses of plates and shells.

Much research has been conducted into plate behaviour, using a wide range of methods. An excellent monograph of the early literature relating to vibration analysis of plates was published by Leissa [1]. Among the methods utilised for plate vibration analysis, it is known that the Superposition Method developed by Gorman is very efficient and accurate for a range of geometric shapes. The Superposition Method has been successfully applied for analysis of out-of-plane vibrations of a plate having classical boundary conditions, such as, clamped, free and cantilevered [2], and more complicated systems, such as elastic supported, orthotropic, and Mindlin plates [3-7]. The Superposition Method has also been utilised to analyse in-plane vibrations of plates [8,9]. In many cases the results from the Superposition Method are the benchmarks for the natural frequencies. Recently, the Superposition Method was shown to be applicable for the

determination of steady state response of plates [10], but until the commencement of this thesis, there has not been any publications dealing with the application of the Superposition Method for transient vibration analysis.

The Superposition Method mentioned above solves the plate problems using subsystems of the plates that have an exact solution, which are referred to as building blocks. However, Gorman and Wing obtained solutions for the free vibration of the fully clamped orthotropic and Mindlin plates using approximate modes for the building blocks, in a procedure they call the Superposition-Galerkin method [11]. Gorman also used the same method for the free vibration analysis of completely free orthotropic and Mindlin plates [12].

It is proven that the Superposition Method is very useful and efficient in solving various plate problems but the method is not limited only to plates. Yu, Cleghorn and Fenton extended the application of Gorman's Superposition Method to open circular cylindrical shells and investigated the analytical solutions for the free vibration of the shells with various boundary conditions [13].

The research about shells has a history as long as that of plates. An excellent review of the literature relating to vibration analysis of shells was also published by Leissa [14]. More recently, literature reviews on the vibration behaviour of shallow shells of various shapes and boundary conditions were published by Qatu [15], and Liew, Lim and Kitipornchai [16]. Although numerous publications that deal with vibration analyses of cylindrical and spherical shallow shells using various analytical and numerical methods, such as the Ritz method, the Finite Element Method and the Finite Strip Method are available, there are no articles on the vibration of shallow shells using Gorman's Superposition Method except for the paper on open cylindrical shells [13].

Research into the analysis of the transient response of plates and shells has spanned several decades. In one of the earliest papers on this subject, Forsyth and Warburton [17] predicted the transient response of cantilever plates to an impulse load using the natural frequencies and mode shapes obtained by applying the Rayleigh method. Craggs [18] solved the transient problems of simply supported,

clamped and cantilever plates using the transition matrix method. Nagaya [19] investigated the transient response of a continuous plate on elastic supports to an impact load using the Laplace transform method. The Finite Element Method was used by Rock and Hinton [20] to obtain the transient response of both simply supported thick and thin plates. Coleby and Mazumdar [21] analysed the large amplitude transient response of an elliptical plate using the Berger method. Celep [22] presented the transient response of a thin elastic plate supported on a foundation that reacts in compression only, where the plate displacement is approximated by the product of vibration modes of the free beam. Nath and Shukala [23] have carried out the non-linear transient analysis of moderately thick laminated composite plates with different combinations of clamped, simply supported, and free boundary conditions based on the Chebyshev approximation. In a recent publication, Abrate [24] examined the transient response of beams, plates and shells to certain pulse type loads using the modal expansion technique.

A review of literature at the commencement of this thesis, as presented above, indicated two potential areas for research, namely the applicability of the Superposition Method for obtaining natural frequencies of doubly curved shells and the effectiveness of this approach for solving transient vibration problems.

1.2 Research Questions

The general objectives of the study are to investigate the applicability of the Superposition Method for the transient response of plates and the free vibration analysis of doubly curved shells. The previous investigations [25-27] have shown that the Superposition Method has generally yielded results for frequencies and modes that are more accurate than those obtained using other competing methods. This observation has led to the question, whether transient response solutions obtained using modes generated from the Superposition Method would be significantly more accurate than those obtained using other methods.

Moreover, as mentioned, the applicability of the Superposition Method to doubly curved shells has not yet been explored. If the rapid rate of convergency and high level of accuracy of this method are also established for the doubly curved shells, it would prove to be a major contribution in the field of vibration of continuous systems. For doubly curved shells, exact solutions for natural frequencies and modes are not available. Therefore, the second research question is whether it is possible to use the Superposition Method, in conjunction with a suitable approximate method to compute the natural frequencies and modes of doubly curved shells of various boundary conditions.

1.3 Thesis Outline

In Chapter 2, it will be shown that the Superposition Method can also be used to accurately and efficiently determine the transient response of an undamped plate undergoing flexural vibration. The case considered is that the transient response of a thin rectangular plate with all edges simply supported, subject to an initial displacement corresponding to that of a plate under uniform load distribution, when all supports are suddenly removed. The natural frequencies and mode shapes of the plates used in this study are obtained by the Superposition Method. The results are compared with the response computed based on the natural frequencies and mode shapes given by the Rayleigh-Ritz method with the ordinary and degenerated free-free beam functions. This study, already reported in a recent paper [28] complements the recent publication on steady state response by the Superposition Method [10].

In Chapter 3, the applicability of the Superposition Method for the free vibration analysis of doubly curved shallow shells is investigated, and some numerical data for the natural frequencies of doubly curved thin shallow shells are presented for three different sets of boundary conditions. The procedure presented in this thesis and the Matlab code developed may be used to generate the solutions for many different combinations of boundary conditions but for brevity, results for only three cases are presented. In contrast to the application of the Superposition

Method for plates and cylindrical shells, for doubly curved shells in general, the Superposition Method requires approximate modes of the building blocks generated from other methods, such as Galerkin's method. The work shows that when the approximate modes of shells under one set of boundary conditions are known then the Superposition Method may be used to find the natural frequencies of shells subjected to other boundary conditions.

2. Chapter II

Transient vibration analysis of
a completely free plate using modes obtained
by Gorman's Superposition Method

Chapter II

Transient vibration analysis of a completely free plate using modes obtained by Gorman's Superposition Method

Nomenclature

a plate dimension in x direction

b plate dimension in y direction

D plate flexural rigidity, $(Eh^3/12)/(1-v^2)$

E elastic modulus of the material

h thickness of plate

w transient response of plate

W plate lateral deflection

x, y plate spatial co-ordinates

λ^2 $\omega a^2 \sqrt{\rho/D}$

η dimensionless plate spatial co-ordinates y/b

v Poisson's ratio of material

v^* $2-v$

ξ dimensionless plate spatial co-ordinates x/a

ρ density of plate

Φ aspect ratio of plate b/a

ω radian frequency of vibration

2.1 Introduction

In this chapter, it will be shown that the Superposition Method can also be applied accurately and efficiently to determine the transient response of an undamped plate undergoing flexural vibration. A thin rectangular plate whose edges are all simply supported is given an initial displacement corresponding to uniform load distribution, namely self weight. The transient response of the plate is investigated when all its supports are suddenly removed. The plate, after being released from its supports, is treated as a completely free plate. The natural frequencies and mode shapes of the plates used in this study are obtained by the Superposition Method. The results are compared with the response computed based on the natural frequencies and mode shapes given by the Rayleigh-Ritz method with the ordinary and degenerated free-free beam functions. The response generated from the Superposition Method agrees closely with the Rayleigh-Ritz results but it is noted that the Superposition Method converges faster. For the same matrix size, the Superposition Method gives more accurate results and it is believed that the results presented may be regarded as benchmarks for future comparisons.

2.2 Procedure

2.2.1 Natural frequencies and modes of vibration

Consider the motion of the completely free rectangular plate with the dimensions a and b as shown in Fig. 2. 1. The natural frequencies and modes will be calculated using both the variational method based on an energy functional and the partial differential equation, i.e. the Rayleigh-Ritz method and the Superposition Method. They are described in detail, in references [1,29] and [2,7] respectively.
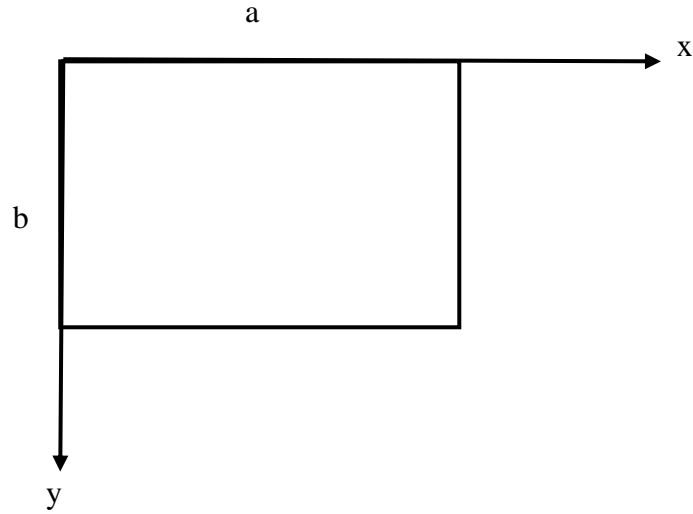
Fig. 2. 1 A completely free plate

2.2.2 The Rayleigh-Ritz Method

For the Rayleigh-Ritz method, it is assumed that the out-of-plane displacement, *W*(*x*, *y*), is taken in the form of the following series,

$$W(x, y) = \sum_{m}^{k} \sum_{n}^{k} G_{mn} X_m(x) Y_n(y) \qquad m, n = 1,2,3 \cdots k \qquad (2.1)$$

where $X_m(x)$ is ordinary free-free beam functions, which are expressed below [1].

$$X_1(x) = 1 \qquad (2.2)$$

$$X_2(x) = 1 - \frac{2x}{a} \qquad (2.3)$$

$$X_m(x) = \cos \gamma_1 \left(\frac{x}{a} - \frac{1}{2}\right) + \theta_{m1} \cosh \gamma_1 \left(\frac{x}{a} - \frac{1}{2}\right) \quad (m = 3, 5, 7, \dots) \quad (2.4)$$

and

$$X_m(x) = \sin \gamma_2 \left(\frac{x}{a} - \frac{1}{2}\right) + \theta_{m2} \sinh \gamma_2 \left(\frac{x}{a} - \frac{1}{2}\right) \quad (m = 4, 6, 8, \dots) \quad (2.5)$$

10

where $\theta_{m1} = -\sin(\gamma_1/2)/\sinh(\gamma_1/2)$ and $\theta_{m2} = \sin(\gamma_2/2)/\sinh(\gamma_2/2)$.

The ordinary beam functions satisfy all the boundary conditions of a free-free beam and are actually the natural modes of free-free beams. The values of γ_1 and γ_2 are obtained as roots of following Eq. (2.6) and Eq. (2.7) respectively.

$$\tan(\gamma_1/2) + \tanh(\gamma_1/2) = 0 \tag{2.6}$$

$$\tan(\gamma_2/2) - \tanh(\gamma_2/2) = 0 \tag{2.7}$$

$Y_n(y)$ is given by simply changing x to y and a to b in above equations.

Using the Rayleigh-Ritz method brings a set of equations expressed as [29]

$$\frac{\partial V_{max}}{\partial G_i} - \omega^2 \frac{\partial \Psi_{max}}{\partial G_i} = 0 \tag{2.8}$$

where ω is a natural frequency of the plate, V_{max} and $\omega^2 \Psi_{max}$ are maximum potential energy and maximum kinetic energy function respectively, which are given by

$$V_{max} = \frac{D}{2} \int_0^a \int_0^b \left[\left(\frac{\partial^2 W}{\partial x^2}\right)^2 + \left(\frac{\partial^2 W}{\partial y^2}\right)^2 + 2v\frac{\partial^2 W}{\partial x^2}\frac{\partial^2 W}{\partial y^2} + 2(1-v)\left(\frac{\partial^2 W}{\partial x \partial y}\right)^2 \right] dxdy \tag{2.9}$$

and

$$\Psi_{max} = \frac{\rho h}{2} \int_0^a \int_0^b W^2 dxdy = 0 \tag{2.10}$$

By inserting Eqs. (2.1), (2.9) and (2.10) into Eq. (2.8), one obtains a set of homogeneous linear algebraic equations in G_i, expressed in the following matrix form:

$$[K]\{G\} - \omega^2[M]\{G\} = 0 \tag{2.11}$$

where

$$K_{ij} = \frac{\partial^2 V_{max}}{\partial G_i \partial G_j} \text{ and } M_{ij} = \frac{\partial^2 \Psi_{max}}{\partial G_i \partial G_j} \tag{2.12}$$

The natural frequencies are determined by equating the determinant of the system to zero. The coefficients, G's, are given as the eigenvector corresponding to the natural frequency.

However, it has been noted that the ordinary free-free beam functions do not completely satisfy the free edge conditions of plate. The use of these functions to form the displacement of plates yields some residual moments and shear force at edges, wheares both should vanish at the extremities. Because of the above fact, the system is over-constrained, and hence, the calculated natural frequencies using the Rayleigh-Ritz method will converge to inaccurate values.

To overcome the above problem, Bassily and Dickinson introduced the concept of degenerated beam functions which effectively relaxes the end conditions [30]. This relaxation can be achieved by simply floating θ in Eqs (2.4) and (2.5). The θ is replaced by a coefficient, which will be determined during the usual minimisation procedure in the Rayleigh-Ritz method.

2.2.3 The Superposition Method

Determining the natural frequencies and mode shapes of the completely free plates by using the Superposition Method is described in detail by Gorman [2,7]. In this study, the Superposition Method is utilised with the W-W algorithm [31-33] to determine the natural frequencies to ensure that coincident roots of the frequency equation are not missed as explained later.

The partial differential equation governing the out-of-plane vibration of rectangular plates, may be expressed in non-dimensional form using dimensionless coordinates ξ and η, where $\xi = x/a$, $\eta = y/b$,. The equation is written as

$$\frac{\partial^4 W(\xi,\eta)}{\partial\eta^4} + 2\Phi^2 \frac{\partial^4 W(\xi,\eta)}{\partial\eta^2\partial\xi^2} + \Phi^4 \left\{ \frac{\partial^4 W(\xi,\eta)}{\partial\xi^4} - \lambda^4 W(\xi,\eta) \right\} = 0 \quad (2.13)$$

where $\lambda^2 = \omega a^2 \sqrt{\rho h/D}$ and Φ is the plate aspect ratio b/a. $\hspace{2cm}$ (2.14)

The bending moment distributed along the edges perpendicular to the ξ axis and the η axis are expressed as follows

$$\frac{b^2 M(\xi)}{aD} = -\left[\frac{\partial^2 W(\xi,\eta)}{\partial\eta^2} + \nu\Phi^2 \frac{\partial^2 W(\xi,\eta)}{\partial\xi^2} \right] \quad (2.15)$$

and

$$\frac{aM(\eta)}{D}$$
$$= -\left[\frac{\partial^2 W(\xi,\eta)}{\partial\xi^2} \right.$$
$$\left. + \frac{\nu}{\Phi^2} \frac{\partial^2 W(\xi,\eta)}{\partial\eta^2} \right] \quad (2.16)$$

The vertical edge reaction along the edges perpendicular to the ξ axis and the η axis are expressed as follows

$$\frac{b^3 V(\xi)}{aD} = -\left[\frac{\partial^3 W(\xi,\eta)}{\partial\eta^3} + \nu^*\Phi^2 \frac{\partial^3 W(\xi,\eta)}{\partial\eta\,\partial\xi^2} \right] \quad (2.17)$$

and

$$\frac{a^2 V(\eta)}{D} = -\left[\frac{\partial^3 W(\xi,\eta)}{\partial\xi^3} + \frac{\nu^*}{\Phi^2} \frac{\partial^3 W(\xi,\eta)}{\partial\xi\,\partial\eta^2} \right] \quad (2.18)$$

In the Superposition Method, the plate model is considered as consisting of four plate problems which have exact solutions [2,7], which are referred to as the building blocks as shown in Fig. 2. 2. The two small adjacent circles depict slip-shear condition, which is that there is no rotation normal to the edge and no transverse edge reaction. The rotation is applied on a driving edge of each building block. The displacement of the original plate, $W(x, y)$, is expressed as the sum of the displacement of these building blocks (Eq. (2.19)).
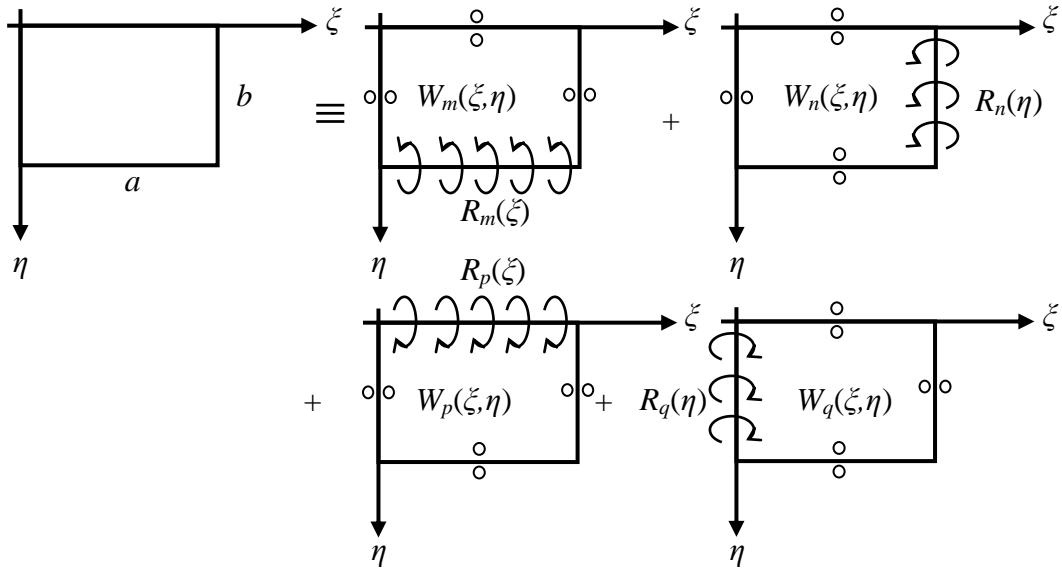
Fig. 2. 2 Building blocks used to analyse the completely free plate

$$W(\xi,\eta) = W_m + W_n + W_p + W_q \qquad (2.19)$$

The displacements of the first building block is taken to be in the form of the Lévy type solution,

$$W_m(\xi,\eta) = \sum_{m=0,1\cdots}^{k} Y_m(\eta) \cos m\pi\xi \qquad (2.20)$$

Substituting Eq. 2.20 into Eq. 2.13 one obtains

$$\frac{d^4 Y_m(\eta)}{d\eta^4} + 2\Phi^2(m\pi)^2 \frac{d^2 Y_m(\eta)}{d\eta^2} + \Phi^4\{(m\pi)^4 - \lambda^4\}Y_m(\eta) = 0 \qquad (2.21)$$

The solution for Eq. 2.21 depends on whether the eigenvalue λ^2 is greater than or less than $(m\pi)^2$. The typical solutions that satisfy Eq. 2.21 are

for $\lambda^2 > (m\pi)^2$

$$Y_m(\eta) = A_m \sinh\beta_m\eta + B_m \cosh\beta_m\eta + C_m \sin\gamma_m\eta + D_m \cos\gamma_m\eta \qquad (2.22)$$

and, for $\lambda^2 < (m\pi)^2$,

14

$$Y_m(\eta) = A_m \sinh \beta_m \eta + B_m \cosh \beta_m \eta + C_m \sinh \gamma_m \eta + D_m \cosh \gamma_m \eta \qquad (2.23)$$

where $\beta_m = \Phi\sqrt{\lambda^2 + (m\pi)^2}$

and $\gamma_m = \Phi\sqrt{\lambda^2 - (m\pi)^2}$ or $\gamma_m = \Phi\sqrt{(m\pi)^2 - \lambda^2}$, whichever is real.

Here, A_m, B_m, C_m, and D_m are constants to be determined.

Since there is no edge rotation and transverse edge reaction at the edge $\eta = 0$, sine and hyperbolic sine terms will be eliminated. The other two coefficients are determined by enforcing the boundary condition of zero vertical edge reaction and the equilibrium of edge rotation along the edge $\eta = 1$. The edge rotation is expressed as following Fourier expansion

$$R_m(\xi) = \frac{\partial W_m(\xi, \eta)}{\partial \eta} = \sum_{m=0,1\cdots}^{k} E_m \cos m\pi\xi \qquad (2.24)$$

The analytical function $Y_m(\eta)$ is readily determined. The solutions for $Y_m(\eta)$ are expressed in terms of the coefficients E_m, [7] as

for $\lambda^2 > (m\pi)^2$

$$Y_m(\eta) = E_m(\theta_{m11} \cosh \beta_m \eta + \theta_{m12} \cos \gamma_m \eta) \qquad (2.25)$$

where $\theta_{m11} = 1/\{(\beta_m - ZZ_1\gamma_m/ZZ_2) \sinh \beta_m\}$

and $\theta_{m12} = ZZ_1/\{ZZ_2(\beta_m - ZZ_1\gamma_m/ZZ_2) \sin \gamma_m\}$

with $ZZ_1 = -\beta_m\{\beta_m^2 - v^*\Phi^2(m\pi)^2\}$

and $ZZ_2 = \gamma_m\{\gamma_m^2 + v^*\Phi^2(m\pi)^2\}$

and, for $\lambda^2 < (m\pi)^2$

$$Y_m(\eta) = E_m(\theta_{m21} \cosh \beta_m \eta + \theta_{m22} \cosh \gamma_m \eta) \qquad (2.26)$$

where $\theta_{m21} = 1/\{(\beta_m - ZZ_1\gamma_m/ZZ_2) \sinh \beta_m\}$

and $\theta_{m22} = ZZ_1/\{ZZ_2(\beta_m + ZZ_1\gamma_m/ZZ_2) \sinh \gamma_m\}$

with $ZZ_1 = -\beta_m\{\beta_m^2 - v^*\Phi^2(m\pi)^2\}$

and $ZZ_2 = \gamma_m\{\gamma_m^2 - v^*\Phi^2(m\pi)^2\}$

Next, the analytical function $Y_n(\xi)$ for the second building block can be deduced from the first building block by interchange of coordinate variables η and ξ. The aspect ratio must be replaced by its inverse and λ^2 must be multiplied by Φ^2. The subscript should be change from m to n.

Once the solutions to the first and second building blocks are obtained, solutions to the third and forth building blocks are determined by simply replacing η in the first building block solution to $1-\eta$, ξ in the second building block solution to $1-\xi$, and changing subscripts to p and q respectively, i.e.

$$Y_p(\eta) = Y_m(1 - \eta) \qquad (2.27)$$

$$Y_q(\xi) = Y_n(1 - \xi) \qquad (2.28)$$

These building blocks are superimposed in order to solve the original plate problem. Applying the boundary conditions of original plate problem, i.e. zero bending moment at the edges, using k terms in each building block, yields a set of $4k$ homogeneous algebraic equations relating $4k$ coefficients, E_m, E_n, E_p and E_q which can be expressed in matrix form as follows:

$$[A]\{E_x\} = \{0\} \qquad (2.29)$$

where $[A]$ is $4k \times 4k$ matrix, $\{E_x\}$ is $4k \times 1$ column vector of coefficients, E_m, E_n, E_p and E_q.

The natural frequencies are determined by searching for the λ values which make the determinant of the system vanish by trial and error. Once the λ values are found, the coefficients, E's, are found by substituting into Eq. (2.29) and these give the natural modes of the plate. However, this procedure also picks up some unexpected values when the determinant goes through a pole (case (b) in Fig. 2. 3), and misses the values associated with coincident modes of a square plate (case(c)), i.e. the symmetric-antisymmetric modes and the antisymmetric-symmetric modes about x and y axes.
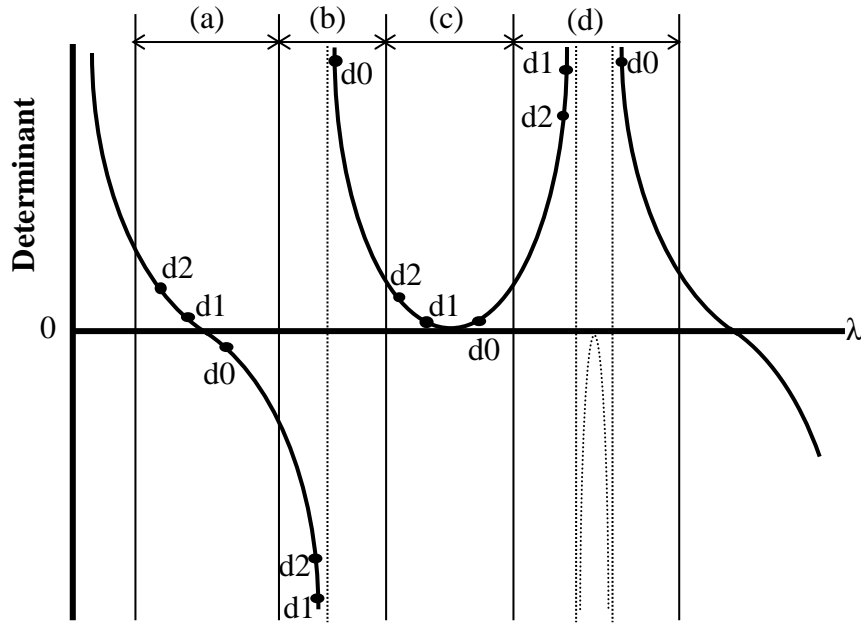
Fig. 2. 3 Plot of the determinant vs. trial λ

To ensure that coincident roots are not missed, the W-W algorithm [31-33] has been used. The coefficient matrix generated with the trial value is modified to an upper triangular matrix according to the W-W algorithm. The number of negatives along the diagonal of the matrix is counted for each trial frequency. Any change in this number gives the number of roots that exist between the previous trial frequency and the current trial frequency, therefore, the natural frequency parameters λ can be defined in this way. If the number changes in two, then the value of λ is considered as associating with a coincident mode. However, using this procedure still gives some unexpected values when the determinant changes sign through zero at the poles and the values of λ corresponds to the eigenvalues of the square plate having all edges fully constrained against rotation (case (d)). Technically, the application of the W-W algorithm requires the knowledge of the natural frequencies of the fully constrained plate and each time such frequencies are passed the number of such frequencies should be accounted into the sign count. This was effectively achieved using the following procedure. The distances of the determinant from the zero line are stored at a given trial frequency which gives a determinant d_0. The previous two determinants are examined when the number of negatives changed. Let the previous two values of determinant d_1 and d_2 as shown in Fig. 2. 3. If d_1 is closer to the zero line than d_2, then λ is considered as the value associating with a natural frequency or coincident natural frequencies (when

17

change of the negatives is two), otherwise the value of λ is omitted. This procedure has eliminated the false roots and given only the required set of natural frequency parameters. These results agree closely with those in the literature [2,7,25-27].

2.2.4 Transient vibrations

In the transient analysis studied here, the effect of damping has not been considered. The response due to an initial disturbance is then expressed in term of its modes as follows:

$$w(x, y, t) = \sum a_i W_i(x, y) \sin(\omega_i t) + \sum b_i W_i(x, y) \cos(\omega_i t) \quad (2.30)$$

where $W_i(x,y)$ is i^{th} normal mode and ω_i is the ith natural frequency. $W_i(x,y)$ is given by Eq. (2.1) or (2.19). Eq. (2.30) has to satisfy the prescribed initial conditions, i.e. the displacement and/or velocity at $t = 0$. An expression for the velocity may be obtained by differentiating Eq. (2.30) with respect to t.

$$\dot{w}(x, y, t) = \sum \omega_i (a_i W_i(x, y) \cos(\omega_i t) - b_i W_i \sin(\omega_i t)) \quad (2.31)$$

Let the displacement and the velocity at $t = 0$ be following equations,

$$w(x, y, 0) = w_0(x, y) \quad (2.32)$$
$$\dot{w}(x, y, 0) = \dot{w}_0(x, y) \quad (2.33)$$

At $t = 0$, Eqs. (2.30) and (2.31) become,

$$w_0(x, y) = \sum b_i W_i(x, y) \quad (2.34)$$

$$\dot{w}_0(x, y) = \sum \omega_i a_i W_i(x, y) \quad (2.35)$$

18

The coefficients a_i and b_i may be determined by multiplying both sides of Eqs. (2.34) and (2.35) by W_j and integrating over the area of plate, i.e.,

$$\iint w_0(x,y)W_j(x,y)dxdy = \iint \sum_i b_i W_i(x,y)W_j(x,y)dxdy \qquad (2.36)$$

and

$$\iint \dot{w}_0(x,y)W_j(x,y)dxdy = \iint \sum_i \omega_i a_i W_i(x,y)W_j(x,y)dxdy \qquad (2.37)$$

However, from the orthogonality condition,

$$\iint W_i(x,y)W_j(x,y)dxdy = 0 \qquad (i \neq j) \qquad (2.38)$$

From Eqs. (2.36), (2.37) and (2.38), the coefficients a_i and b_i are given by,

$$a_j = \frac{\iint \dot{w}_0(x,y)W_j(x,y)dxdy}{\omega_i \iint \{W_j(x,y)\}^2 dxdy} \qquad (2.39)$$

and

$$b_j = \frac{\iint w_0(x,y)W_j(x,y)dxdy}{\iint \{W_j(x,y)\}^2 dxdy} \qquad (2.40)$$

2.2.5 Initial conditions

The initial conditions given in this study are that there is an imposed deflection which is equal to that of a plate with all edges simply supported, and subject to a uniformly distributed load such as self weight and that the velocity is zero everywhere. The deflection expression for this case which is readily available in the literature [34] is,

$$w_0(x,y) = \frac{16q_0}{\pi^6 D} \sum_k \sum_l \frac{\sin\frac{k\pi x}{a}\sin\frac{l\pi y}{b}}{kl\left(\frac{k^2}{a^2}+\frac{l^2}{b^2}\right)^2} \qquad (k = 1,3,5,\dots\; l = 1,3,5,\dots) \qquad (2.41)$$

19

where q_o is a load per area. The load is assumed as the weight of the plate per area, which is given by $q_o = \rho h g$. Five terms in each direction were found to be sufficient to ensure that the results for the displacement have converged to four significant figures, and therefore k and l in Eq (2.41) were set for nine in computation. It should be noted here that if the transient response of a plate that is freely falling under gravity after removal of its simple supports is required, the rigid body motion of the plate due to the gravity force $gt^2/2$ should be added. The above initial condition was chosen as a convenient case to remember for the purpose of benchmarking and not due to any engineering significance.

2.3 Result and discussion

The transient response of a completely free plates has been calculated when the plates having all the edges simply supported are suddenly released from the all supports. The computation of the response of the plates for the various aspect ratios was done using the natural frequencies and modal shapes given by the Superposition method and the Rayleigh-Ritz method with the ordinary and degenerated free-free beam functions. The first 50 modes were used in the calculation. The displacement and time are given in dimensionless forms, which are $w/\left(\frac{16q_0a^4}{\pi^6 D}\right)$ and $t/\left(a^2\sqrt{\rho h/D}\right)$ respectively. All responses were calculated by using the software MATLAB in default double precision. However, the maximum number of terms used in the degenerated beam functions to compute the natural frequencies and mode shapes is limited to eight terms in each direction because the computing procedure showed numerical instability when using more than nine terms.

Firstly, the convergence tests were carried out for the results computed by all the methods mentioned above. The responses at the centre of the square plate obtained using the natural frequencies and modes given by the Superposition Method are plotted in Fig. 2. 4 for various values of number of terms used in each

building block. It may be seen that except for the four term solution, all other results agree well even for non-dimensional time of 100 units, showing that convergence has been reached with only six terms. Figs. 2. 5 and 2. 6 show the response at the same point calculated based on the natural frequencies and modes given by the Rayleigh-Ritz method in respect of the terms used in the ordinary beam functions and the degenerated beams functions respectively. As can be seen from Part (a) of these figures, there are no significant differences between the results for different number of terms for either method, immediately after the plates were released. However, the differences become larger as time increases as can be seen from Part (b) of the figures. While almost no differences are found between the results obtained using 10 and 15 terms in Eq.(2.20) for the Superposition Method, and six and eight terms in each direction of Eq.(2.1) for the degenerated beam functions, there are obvious disagreements between the results obtained using the ordinary beam functions. For a fair comparison between the convergence rates of the Superposition Method and the Rayleigh-Ritz method with degenerated beam functions, it is useful to note that to get convergence to the same level of agreement, the Superposition Method uses a matrix size of 40×40 where as the Rayleigh-Ritz method requires about 100×100. The rates of convergence of the Superposition Method and the Rayleigh-Ritz method with the degenerated beam functions are considerably better than that of the Rayleigh-Ritz method with the ordinary beam functions. Results of the convergence test presented here are only for the square plate, but the same occurrences were observed for plates of other aspect ratios.

Fig. 2. **7** shows the transient response of the completely free square plate at (a) the centre, (b) the point $x=0.75a$ and $y=0.75b$ and (c) the corner. The natural frequencies and mode shapes used in the computation were obtained using 15 terms in the Superposition Method, eight-term degenerated beam functions and 50-term ordinary beam functions in the Rayleigh-Ritz method. Initially, there is an excellent agreement between the results given by all three methods. However, the difference becomes noticeable as time increases. Fig. 2. 8 shows that the response at the corner of the plate at the time of 98 to 100. While the results obtained based on the Superposition Method and the degenerated beam functions are in excellent agreement with each other, there is a large discrepancy between the result based

on the ordinary beam functions and others. This is due to the fact that the Rayleigh-Ritz method using the ordinary free-free beam functions gives higher values for the natural frequencies of the completely free plates than those given by the Superposition Method and the Rayleigh-Ritz method with the degenerated free-free beam functions. Similar differences were also found in the responses at other points of the plate and of the plates for other aspect ratios.

It can also be seen from Fig. 2. **7** that the plates vibrate about a shifted plane parallel to the original xy plane representing the undeformed state of the plate. The plane shift was also discovered in the responses of the plates for the aspect ratios 1.5 and 2.0. The distance between the planes that are at the centre of vibration and the xy plane almost agree with the displacement contribution of the first mode, which is the rigid body motion in dimensionless distance of 1.0, multiplied by the first transient coefficient of the plates, which is 0.1023 for the square plate (Table 2. 1).

The modal superposition method used in this thesis to investigate the transient response of the plate gives an insight into how modes participate in the response, as mentioned in the reference [24]. Fig. 2. 9 shows the proportions of modes participating in the transient responses. Since, in the case studied here, the initial disturbance is symmetric about both centre lines of the plate parallel to x and y axes, only doubly symmetric modes participate. The first three participating modes dominate about 90-percent of the responses for the square plate. The transient responses of the plates with aspect ratios 1.5 and 2.0 are governed in similar rates by the first four and five participating modes respectively. The figures also show that the proportion of higher modes contributing to the transient response of the plates with aspect ratios 1.5 and 2.0 are larger than that of a square plate.

It is known that both the Superposition Method and the Rayleigh-Ritz method give upper bounds for the natural frequencies of completely free plates [1,26,27] and lowest values would be considered as benchmarks. The Superposition Method and the Rayleigh-Ritz method using the degenerated free-free beam functions give lower values of natural frequencies than those given by

the Rayleigh-Ritz method using the ordinary free-free beam functions for the completely free plates. Those methods also give faster convergence rates. For the same matrix size, however, the Superposition Method gives lower values than those obtained using the degenerated beam functions, and also use of the degenerated beam functions exhibits numerical instability in the results when using more than nine terms in the series. Therefore, it is preferable to use the Superposition Method. It seems appropriate at this stage to treat the transient responses obtained using the natural frequencies and modes given by the Superposition Method as benchmark results for the response of the plates with all edges simply supported when being suddenly released from all the supports after being subject to an initial displacement corresponding to that due to a uniformly distributed load. The first few participating modes, transient coefficients, corresponding natural frequency parameters, λ^2 [26,27] and modal displacements at the centre, the point of *0.75a, 0.75b* and the corner are given in Table 2. 1. It should be noted that the numerical results may serve as benchmarks for transient response of plates.
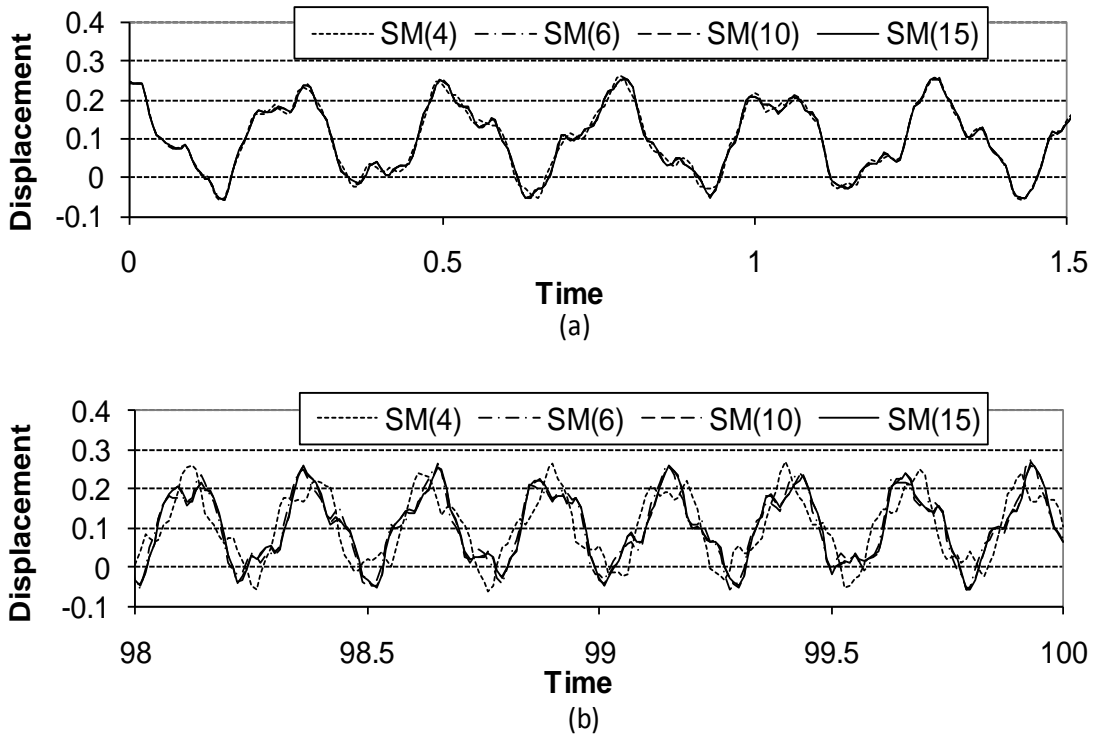
Fig. 2. 4 The transient response of the completely free square plate at the centre, based on the natural frequencies and modes given by the Superposition Method at the time of (a) 0 to 1.5 and (b) 98 to 100.
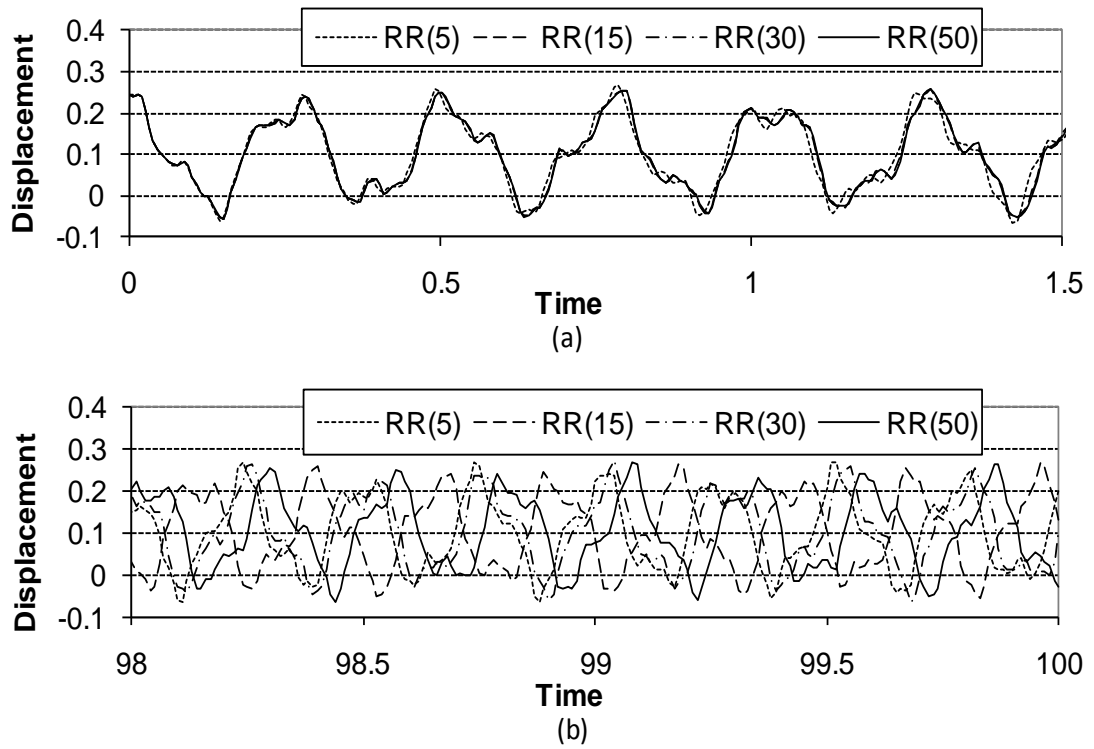
Fig. 2. 5 The transient response of the completely free square plate at the centre, based on the natural frequencies and modes given by the Rayleigh-Ritz method with the ordinary beam functions at the time of (a) 0 to 1.5 and (b) 98 to 100.
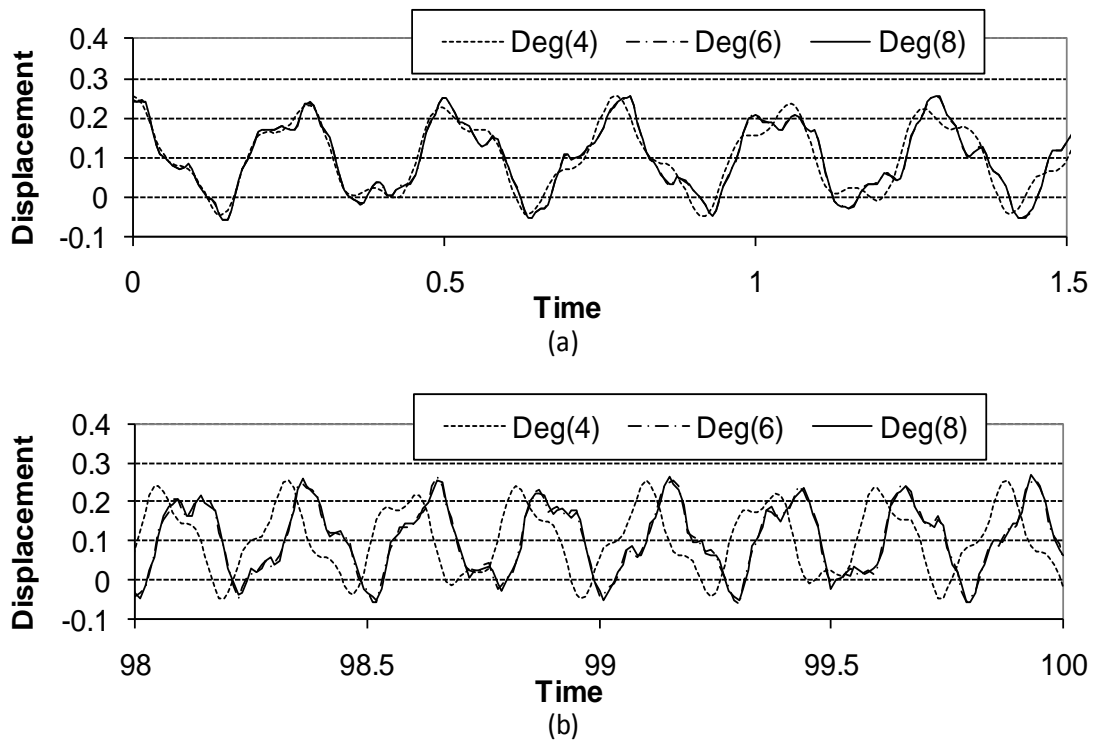
Fig. 2. 6 The transient response of the completely free square plate at the centre, based on the natural frequencies and modes given by the Rayleigh-Ritz method with the degenerated beam functions at the time of (a) 0 to 1.5 and (b) 98 to 100.
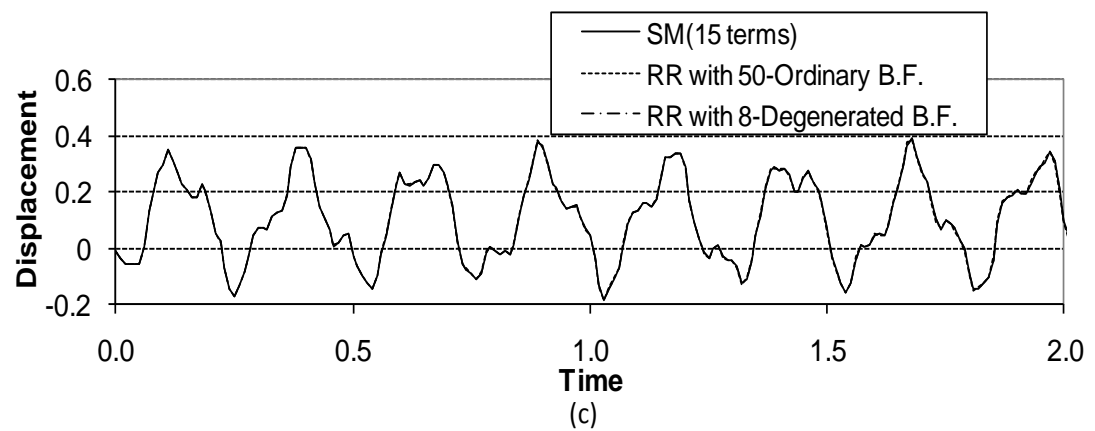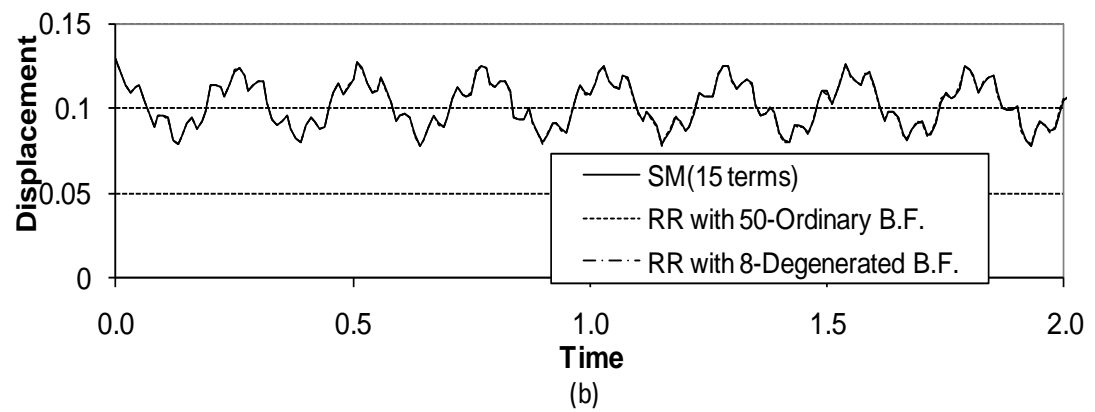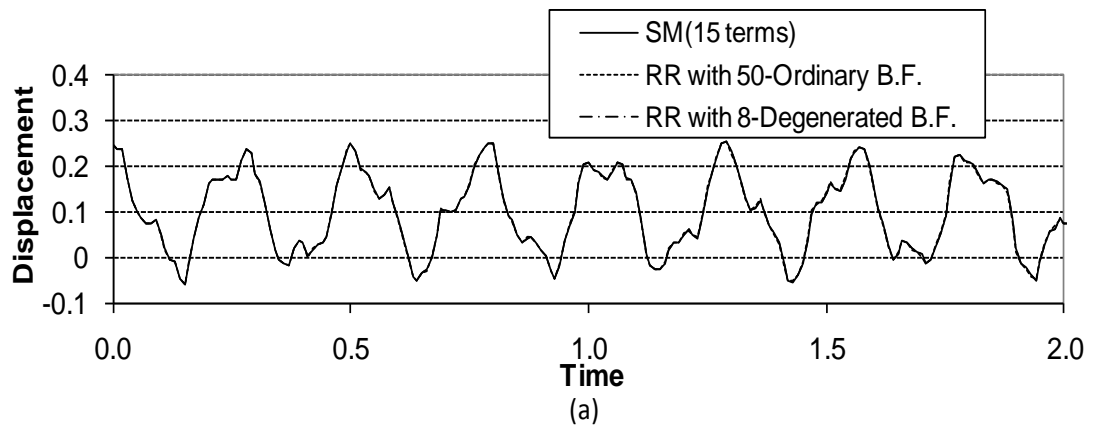
Fig. 2. 7 The transient response of the completely free square plate at (a) the centre, (b) the point *x=0.75a y=0.75b* and (c) the corner, obtained using the natural frequencies and modes given by the Superposition Method and the Rayleigh-Ritz method with the ordinary and degenerated beam functions.

27
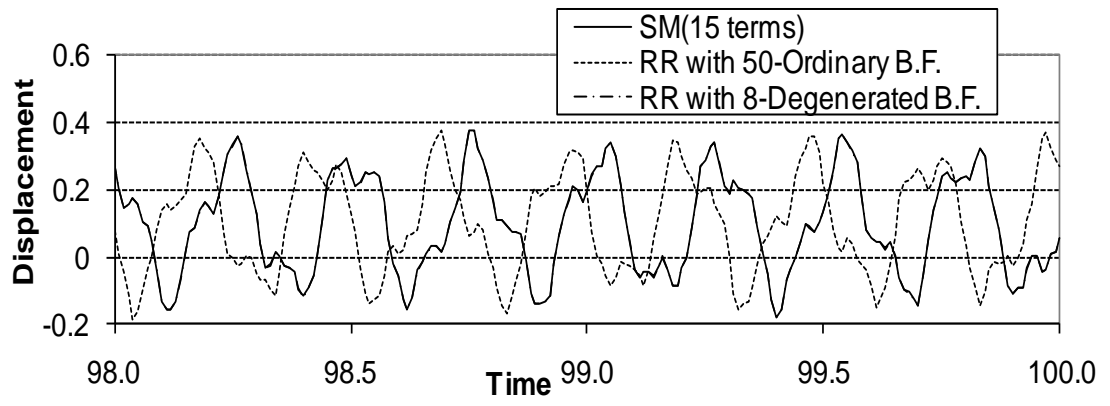
Fig. 2. 8 The transient response of the completely free square plate at the corner at the time of 98 to 100.
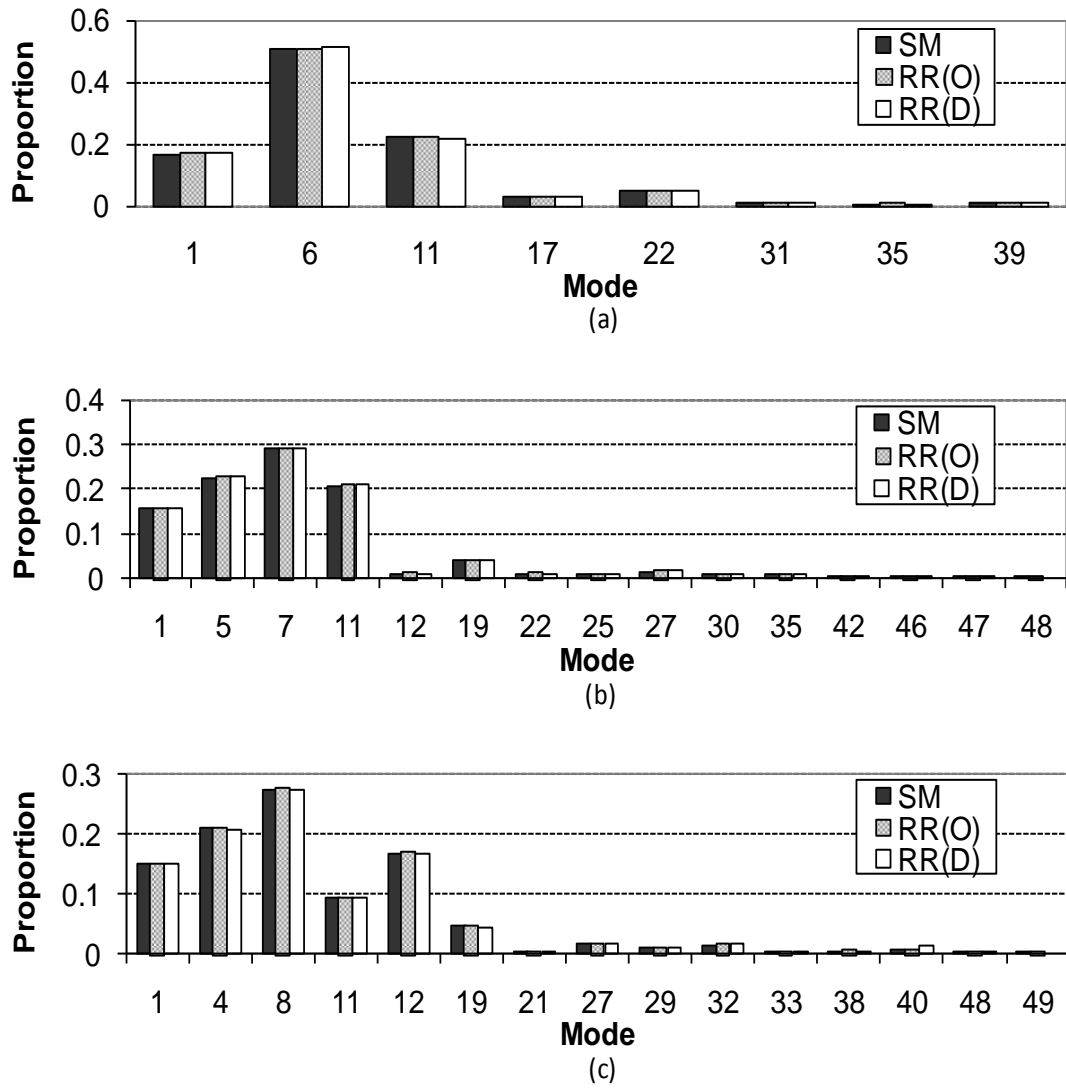
Fig. 2. 9 The proportion of the participating modes of completely free plates with aspect ratio of (a) 1.0, (b) 1.5 and (c) 2.0

Table 2. 1 Contribution of participating modes.

Φ = 1.0

Participating Modes		1	6	11		
λ^2		0	24.27	63.69		
Transient Coefficients		0.1023	0.8051	-0.5145		
Modal displacement	Centre	1.000	0.1433	-0.0795		
	0.75a,					
	0.75b	1.000	0.0213	-0.0031		
	Corner	1.000	-0.2411	-0.1420		

Φ= 1.5

Participating Modes		1	5	7	11	12
λ^2		0	9.517	22.18	43.93	53.35
Transient Coefficients		0.1968	-1.0559	-1.3461	-1.0306	-0.1060
Modal displacement	Centre	1.000	-0.0780	-0.1032	-0.0696	0.0512
	0.75a,					
	0.75b	1.000	-0.0126	-0.0128	-0.0090	-0.0386
	Corner	1.000	0.1333	0.1667	-0.1215	0.0838

Φ = 2.0

Participating Modes		1	4	8	11	12
λ^2		0	5.366	22.00	29.68	36.04
Transient Coefficients		0.2646	-1.4421	1.9101	1.3581	1.0745
Modal displacement	Centre	1.000	-0.0844	0.0929	-0.0255	0.0986
	0.75a,					
	0.75b	1.000	-0.0139	0.0022	0.0388	-0.0129
	Corner	1.000	0.1440	-0.1244	-0.0559	0.1650

2.4 Concluding Remarks

It has been shown that the natural frequencies and modes determined by applying the Superposition Method can be used to calculate the transient response of completely free plates accurately and efficiently. The results agree well with those obtained using the frequencies and modes found by applying the Rayleigh-Ritz method for short periods of time. The response based on the Rayleigh-Ritz modes based on ordinary beam functions are slower to converge compared to the corresponding results based on the degenerated beam functions. The results based on the Superposition Method prove to be the fastest to converge. This means that for a given matrix size, the Superposition Method gives the most accurate results for the response. The difference between the results found using the Superposition Method and the Rayleigh-Ritz modes increase with time and the use of the degenerated beam functions shows numerical instability during the computation when using more than nine terms in the series. Therefore, the results calculated using the natural frequencies and modes given by the Superposition Method are more accurate and reliable, and may be considered as benchmark data for the transient response of the completely free plates.

As expected the transient response is dominated by the lower modes. The plates vibrate about the shifted plane parallel to the original xy plane. The distances between these two planes agree with the displacements for the first mode of the plate (a rigid body translation) multiplied by the first transient coefficient.

3. Chapter III

Free vibration analysis of

thin shallow shells using

the Superposition-Galerkin Method

Chapter III

Free vibration analysis of thin shallow shells using the Superposition-Galerkin Method

Nomenclature

a	planform dimension in x direction
b	planform dimension in y direction
D	plate flexural rigidity, $(Eh^3/12)/(1-v^2)$
E	elastic modulus of the material
h	thickness of shell
R_x	radius of curvature parallel to x axis
R_y	radius of curvature parallel to y axis
u	in-plane displacement in x direction
U	dimensionless displacement, u/a
v	in-plane displacement in y direction
V	dimensionless displacement, v/a
w	out-plane displacement
W	dimensionless displacement, w/a
x, y	platform spatial co-ordinates
β	curvature ratio, a/R_x
γ	Gaussian curvature, R_x/R_y
δ	thickness ratio, a/h
η, ξ	dimensionless co-ordinates; y/b, x/a
v	Poisson's ratio of material
$\bar{v}$	$(1-v)/2$
ρ	density of shell
Φ	aspect ratio of planform b/a
ω	radian frequency of vibration
Ω	frequency parameter $\omega a^2 \sqrt{\rho h/D}$

3.1 Introduction

This chapter shows that the Superposition Method is applicable for the free vibration analysis of doubly curved shallow shells with any combinations of simply-supported and clamped edges, which leads to 55 possible combinations. Some numerical data of the natural frequencies are presented for singly and doubly curved thin shallow shells with three different sets of boundary conditions described later. The computed results for fully clamped shells are compared with the data obtained using the Ritz method in the earlier literature, and the results for other boundary conditions are compared with results generated using a Finite Element package Abaqus. While the application of the Superposition Method for plates and cylindrical shells generally requires an exact solution for the building blocks, the present work utilises approximate modes of the building blocks generated using the Galerkin method because, in general, an exact solution is not yet available for doubly curved shells. Consequently, it is shown that when the approximate modes of shells under one set of boundary conditions are known then the Superposition Method may be used to find the natural frequencies of the same shells subjected to other boundary conditions.

3.2 Procedure

In the Superposition Method, a free vibration problem was solved by superimposing plural forced vibration solutions. They are referred to as building blocks. The vibration analysis of plates using the ordinary Superposition Method and the Superposition-Galerkin Method has been described in detail in literature [2,7] and [11,12] respectively.
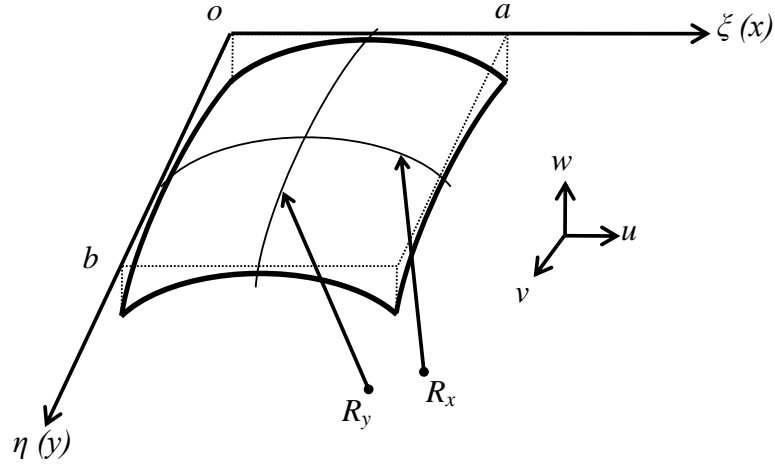
Fig. 3. 1 A shallow shell on rectangular planform

Fig. 3. 1 shows the middle surface of a shallow shell on a rectangular planform. The governing equations based on Donnell - Mushtari - Vlasov theory for free vibration of thin shallow shells are given in reference [35] and the dimensionless form of the governing equations is expressed as follows.

$$
\begin{cases}
12\delta^2\dfrac{\partial^2 U}{\partial\xi^2} + 12\bar{v}\dfrac{\delta^2}{\Phi^2}\dfrac{\partial^2 U}{\partial\eta^2} + 12(v+\bar{v})\dfrac{\delta^2}{\Phi}\dfrac{\partial^2 V}{\partial\xi\partial\eta} + 12\delta^2\beta(1+v\gamma)\dfrac{\partial W}{\partial\xi} + \Omega^2 U = 0 \\[3mm]
12(v+\bar{v})\dfrac{\delta^2}{\Phi}\dfrac{\partial^2 U}{\partial\xi\partial\eta} + 12\bar{v}\delta^2\dfrac{\partial^2 V}{\partial\xi^2} + 12\dfrac{\delta^2}{\Phi^2}\dfrac{\partial^2 V}{\partial\eta^2} + \dfrac{12\delta^2\beta}{\Phi}(1+\gamma)\dfrac{\partial W}{\partial\eta} + \Omega^2 V = 0 \\[3mm]
12\delta^2\beta(1+v\gamma)\dfrac{\partial U}{\partial\xi} + \dfrac{12\delta^2\beta}{\Phi}(1+\gamma)\dfrac{\partial V}{\partial\eta} + \left(\dfrac{\partial^4 W}{\partial\xi^4} + \dfrac{2}{\Phi^2}\dfrac{\partial^4 W}{\partial\xi^2\partial\eta^2} + \dfrac{1}{\Phi^4}\dfrac{\partial^4 W}{\partial\eta^4}\right) \\[3mm]
\qquad\qquad + 12\delta^2\beta^2(1+2\gamma v+\gamma^2)W - \Omega^2 W = 0
\end{cases} \tag{3.1}
$$

where the symbols are given in the nomenclature.

The dimensionless bending moment, *M*, and membrane force, *N*, are given in terms of displacements as

$$
\begin{Bmatrix} M_\xi \\ M_\eta \\ M_{\xi\eta} \end{Bmatrix} =
\begin{Bmatrix}
-\left(\dfrac{\partial^2 W}{\partial\xi^2} + \dfrac{v}{\Phi^2}\dfrac{\partial^2 W}{\partial\eta^2}\right) \\[3mm]
-\left(\dfrac{\partial^2 W}{\partial\eta^2} + v\Phi^2\dfrac{\partial^2 W}{\partial\xi^2}\right) \\[3mm]
-(1-v)\dfrac{\partial^2 W}{\partial\xi\partial\eta}
\end{Bmatrix} \tag{3.2}
$$

and

$$\begin{Bmatrix} N_\xi \\ N_\eta \\ N_{\xi\eta} \end{Bmatrix} = \begin{Bmatrix} \dfrac{\partial U}{\partial \xi} + \dfrac{\nu}{\Phi}\dfrac{\partial V}{\partial \eta} + \beta(1+\gamma\nu)W \\ \dfrac{\partial U}{\partial \xi} + \Phi\nu\dfrac{\partial V}{\partial \eta} + \beta\phi(\gamma+\nu)W \\ \dfrac{1-\nu}{2}\left(\dfrac{\partial U}{\partial \eta} + \Phi\dfrac{\partial V}{\partial \xi}\right) \end{Bmatrix} \qquad (3.3)$$

At each edge of the three classical boundary conditions, namely, free, simply supported, and clamped conditions, in this study only simply-supported and clamped cases are considered. For in-plane conditions, of the four common combinations of tangentially free or restrained and normally free or restrained, it is tangentially restrained and normally free or restrained conditions that are considered. With the selected boundary conditions, it is possible to have 55 different combinations for a shell of rectangular planform with arbitrary curvature, and for certain special cases such as cylindrical shells, there are 100 different combinations of the above boundary conditions. The Superposition scheme developed here is easily applicable to solve any of these cases but for brevity, results for only three combinations are presented. The boundary conditions treated are: (a) all edges are fully clamped; (b) a pair of opposite edges is simply-supported out-of-plane, shear diaphragm in-plane and others are clamped; (c) two adjacent edges are simply-supported out-of-plane, shear diaphragm in-plane and others are clamped. Let us begin by explaining the procedure for the fully clamped case.

The analysis of fully clamped shallow shells is accomplished by using eight building blocks whose edges are all simply supported with shear diaphragm in-plane conditions, as shown in Fig. 3. 2. The boundary conditions of a simply supported shallow shell with shear diaphragm in-plane conditions are given by Eq. (3.4).
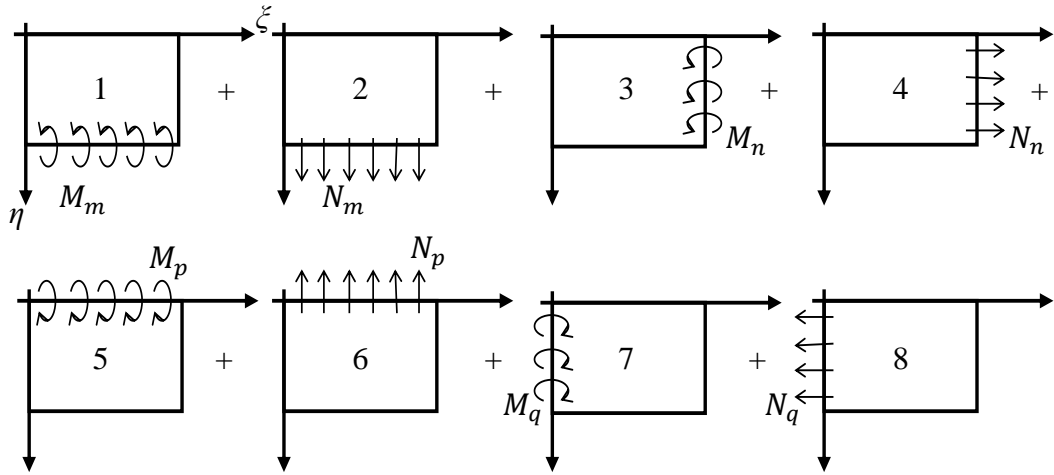
Fig. 3. 2 Building blocks used for the free vibration analysis of the shell

$$\left.\begin{array}{ll} V = W = 0, N_\xi = 0 \ and \ M_\xi = 0 & (at \ \xi = 0 \ and \ 1) \\ U = W = 0, N_\eta = 0 \ and \ M_\eta = 0 & (at \ \eta = 0 \ and \ 1) \end{array}\right\} \qquad (3.4)$$

First let us consider the first two building blocks. The first and second building blocks are subjected to bending moments, M, and an in-plane force parallel to η-axis, N, respectively on its driving edges. These moment and in-plane force terms are expressed in a series form (Eq. (3.5)).

$$\left.\begin{array}{l} M_m = \displaystyle\sum_{m=1}^{k} E_m \sin m\pi\xi \\ N_m = \displaystyle\sum_{m=1}^{k} F_m \sin m\pi\xi \end{array}\right\} \qquad (3.5)$$

The in-plane displacements U and V, and out-of-plane displacement W are expressed by Eq. (3.6). The specific set of functions that satisfy the governing differential equations and the boundary conditions approximately for building blocks 1 and 2 are given by Eqs. (3.7) and (3.8), respectively.

$$U_m = \sum_{m=1}^{k} X_m(\eta) \cos m\pi\xi$$

$$V_m = \sum_{m=1}^{k} Y_m(\eta) \sin m\pi\xi \qquad (3.6)$$

$$W_m = \sum_{m=1}^{k} Z_m(\eta) \sin m\pi\xi$$

$$X_m(\eta) = \sum_{i=1}^{K} A_{mi} \sin i\pi\eta$$

$$Y_m(\eta) = \sum_{j=1}^{K} A_{mj} \cos(j-1)\pi\eta \qquad (3.7)$$

$$Z_m(\eta) = \sum_{l=1}^{K} A_{ml} \sin l\pi\eta + \frac{E_m}{6}(\eta - \eta^3)$$

$$X_m(\eta) = \sum_{i=1}^{K} B_{mi} \sin i\pi\eta$$

$$Y_m(\eta) = \sum_{j=1}^{K} B_{mj} \cos(j-1)\pi\eta + F_m \frac{\eta^2}{2} \qquad (3.8)$$

$$Z_m(\eta) = \sum_{l=1}^{K} B_{ml} \sin l\pi\eta$$

Eqs.(3.6) and (3.7) are substituted into Eq. (3.1) and differentiated term-by-term. This creates an algebraic equation relating the $3 \times K$ Fourier unknowns, A_{mi}, A_{mj}, A_{ml} and driving coefficient E_m, which is given as follows.

$$\sum \left\{ -12\delta^2(m\pi)^2 - 12\bar{v}\frac{\delta^2}{\Phi^2}(i\pi)^2 + \Omega^2 \right\} A_{mi} \sin i\pi\eta$$

$$+ \sum \left\{ -12(v + \bar{v})\frac{\delta^2}{\Phi}(m\pi)(j-1)\pi \right\} A_{mj} \sin(j-1)\,\pi\eta$$

$$+ \sum \{12\delta^2\beta(1 + v\gamma)(m\pi)\} A_{ml} \sin l\pi\eta$$

$$+ 12\delta^2\beta(1 + v\gamma)(m\pi)\frac{E_m}{6}(\eta - \eta^3) = 0 \qquad (3.9)$$

38

$$\sum\left\{-12(\nu+\bar{\nu})\frac{\delta^2}{\Phi}(m\pi)(i\pi)\right\}A_{mi}\cos i\,\pi\eta$$

$$+\sum\left\{-12\bar{\nu}\delta^2(m\pi)^2-12\frac{\delta^2}{\Phi^2}(j-1)^2\pi^2+\Omega^2\right\}A_{mi}\cos(j-1)\pi\eta$$

$$+\sum\left\{\frac{12\delta^2\beta}{\Phi}(1+\gamma)(l\pi)\right\}A_{ml}\cos l\pi\eta$$

$$+\frac{12\delta^2\beta}{\Phi}(1+\gamma)\frac{E_m}{6}(1-3\eta^2)=0 \qquad\qquad (3.10)$$

$$\sum\{-12\delta^2\beta(1+\nu\gamma)(m\pi)\}A_{mi}\sin i\pi\eta$$

$$+\sum\left\{-\frac{12\delta^2\beta}{\Phi}(1+\gamma)(j-1)\pi\right\}A_{mj}\sin(j-1)\pi\eta$$

$$+\sum\left\{(m\pi)^4+\frac{2}{\Phi^2}(m\pi)^2(l\pi)^2+\frac{1}{\Phi^4}(l\pi)^4\right.$$

$$\left.+12\delta^2\beta^2(1+2\gamma\nu+\gamma^2)-\Omega^2\right\}A_{ml}\sin l\pi\eta+\left[\frac{2}{\Phi^2}(m\pi)^2\eta\right.$$

$$\left.+\{(m\pi)^4+12\delta^2\beta^2(1+2\gamma\nu+\gamma^2)-\Omega^2\}\frac{(\eta-\eta^3)}{6}\right]E_m=0 \;(3.11)$$

By following the Galerkin method, these equations are expanded in an appropriate trigonometric function of K terms, which gives a set of $3\times K$ simultaneous non-homogeneous algebraic equations [11,12]. These Fourier unknowns are obtained by solving the algebraic equations, and thus a solution for the first building blocks is expressed in terms of E_m. A schematic explanation of the algebraic equations in a matrix form is shown in Fig. 3. 3. The short bars depict non-zero elements. It is noted that it is advantageous to use sine functions for out-of-plane and tangential displacements, and cosine functions for perpendicular displacements because of their simplicity and orthogonality. A solution for the second block is obtained similarly and expressed in term of F_m.

$$
\begin{array}{ccccccccc}
A_{mi} & & & A_{mj} & & & A_{ml} & & & E_m \\
1 & 2 & 3 & 1 & 2 & 3 & 1 & 2 & 3 &
\end{array}
$$
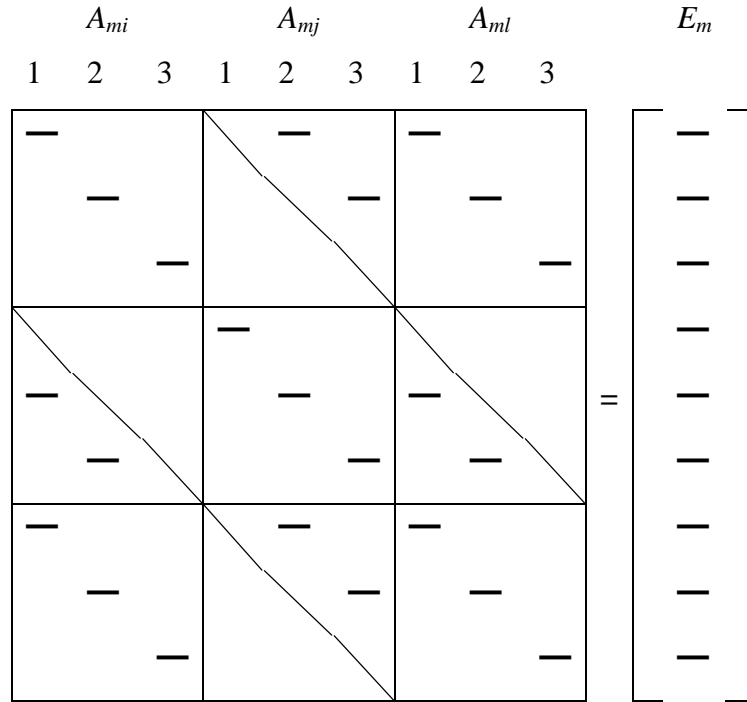
Fig. 3. 3 A Schematic explanation of the algebraic equations given by Galerkin method in matrix form

The solution for the third and fourth building block will be obtained by interchanging η and ξ, as well as X and Y of Eqs (3.7) and (3.8), and substituting into Eq.(3.1) followed by Galerkin's procedure used to solve the first two building blocks. Once the solutions to the first four building blocks are available, solutions for the other building blocks can be generated from the first four building blocks by simply replacing η in the first two building block solution to $1\text{-}\eta$, ξ in the third and fourth building block solution to $1\text{-}\xi$, and changing subscripts from m to p and n to q respectively. The solution for X_p, Z_p, Y_q and Z_q should be preceded with negative sign, i.e.

$$
\left.\begin{array}{l}
X_p(\eta) = -X_m(1 - \eta) \\
Y_p(\eta) = Y_m(1 - \eta) \\
Z_p(\eta) = -Z_m(1 - \eta)
\end{array}\right\} \tag{3.12}
$$

$$
\left.\begin{array}{l}
X_q(\xi) = X_n(1 - \xi) \\
Y_q(\xi) = -Y_n(1 - \xi) \\
Z_q(\xi) = -Z_n(1 - \xi)
\end{array}\right\} \tag{3.13}
$$

40

Once the solutions for all building blocks are obtained, these building blocks are superimposed and the coefficients in the solutions of building blocks are adjusted so as to satisfy the boundary conditions of the original clamped shell. In other words, the flexional rotation and in-plane displacement perpendicular to edges of the superimposed set of building blocks should vanish. The boundary conditions of fully clamped shell are given by the following equations.

$$\left. \begin{array}{ll} U = V = W = 0, & and \quad \dfrac{\partial W}{\partial \xi} = 0 \quad (at \; \xi = 0 \; and \; 1) \\[2mm] U = V = W = 0, & and \quad \dfrac{\partial W}{\partial \eta} = 0 \quad (at \; \eta = 0 \; and \; 1) \end{array} \right\} \tag{3.14}$$

These flexional rotation and in-plane displacement contributions are expanded in an appropriate trigonometric series and this yields a set of $8k$ homogeneous algebraic equations relating $8k$ coefficients, E's and F's which can be expressed in matrix form as follows:

$$[A]\begin{Bmatrix} E \\ F \end{Bmatrix} = \{0\} \tag{3.15}$$

where $[A]$ is $8k \times 8k$ matrix, $\begin{Bmatrix} E \\ F \end{Bmatrix}$ is $8k \times 1$ column vector of coefficients, E's and F's.

A schematic representation of the matrix $[A]$ of Eq. (3.15) when $k=3$ is given in Fig. 3. 4. The dots in the figure depict non-zero components. The matrix is divided into 8×8 segments, and each column and row the segment denote the building block and its contribution to the boundary condition at the edge respectively. The natural frequencies are determined by searching for the Ω values for which the determinant of the system vanishes by trial and error. Once the Ω values are found, the coefficients, E's, and F's are found by substituting into Eq.(3.15) and these give the natural modes.
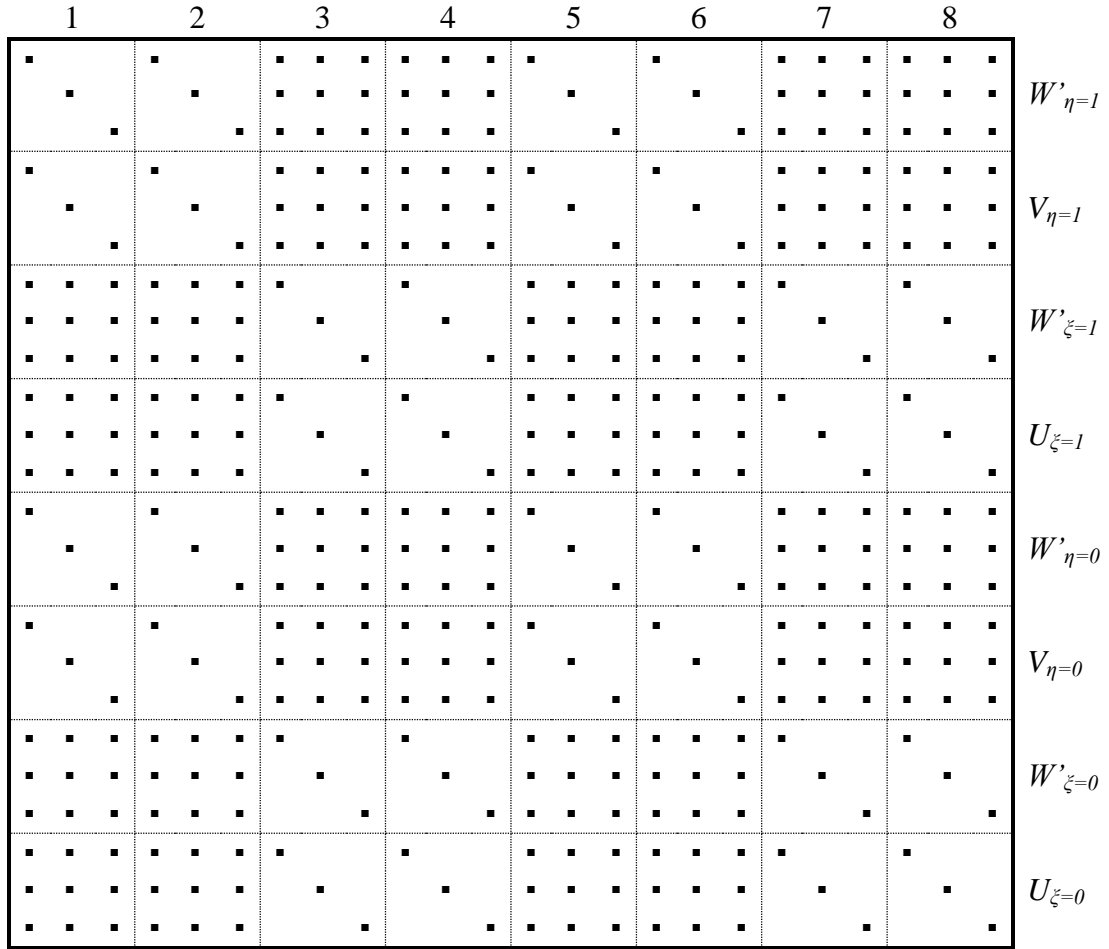
Fig. 3. 4 A schematic representation of matrix [*A*] for *k* = 3.

The preceding paragraphs explain how to obtain the natural frequency parameters of fully clamped shallow shells using eight building blocks whose edges are all simply-supported with in-plane shear diaphragm. However, shells with any combination of boundary conditions of simply-supported and clamped in the out-of-plane case, and shear diaphragm or fully constrained in the in-plane case, can be solved using the same building blocks employed here. In other words, each edge of a shell is imposed four different boundary conditions, depending on whether or not the out-of-plane rotation and/or the in-plane displacement normal to the edge are prohibited. As mentioned earlier, this leads to 55 possible different combinations of boundary conditions. Solutions for shells with any of these combinations can be obtained by simply eliminating certain building blocks and corresponding sub-matrices from the matrix [*A*]. For example, a shell whose edges are simply supported and on shear diaphragm at $\xi = 1$ and 0, and others are clamped can solved by removing

42

the building blocks 3, 4, 7, and 8, namely third, forth, seventh and eighth columns and rows of segments of the matrix [*A*]. This shows the versatility of the Superposition Method.

3.3 Result and discussion

The numerical results are presented for three type of shallow shells, which are cylindrical ($R_x/R_y = 0$), spherical ($R_x/R_y = 1$), and hyperbolic-paraboloidal ($R_x/R_y = -1$) shells and for three different sets of boundary conditions. The results are compared to the results in earlier literature and those obtained using an FEA package, Abaqus. The natural frequencies are given in a dimensionless form, which will be referred to as the natural frequency parameter. The Poisson's ratio and the ratio of planform dimension to thickness (*a/h*) are set to 0.3 and 100 respectively for all calculations in this thesis. All natural frequency parameters were obtained for the curvature ratios (*a/R_x*) of 0.1 to 0.5. A shell, in general, is considered as thin and shallow if the ratio of thickness to radius of curvature is less than 1/20 [36] and a subtended angle is not more than 40° [37], which means the curvature ratio is less than 0.68, respectively. Since all shells studied here are in the above criteria, the thin shallow shells theory is valid for this study. The present results were calculated by using the software MATLAB in default double precision. The spec of the computer used for this study is that Intel® Pentium® D CPU 2.80GHz 2.79GHz and 1.00 GB of RAM.

Convergence tests were carried out to determine the number of terms which are used in the series expansions. The Superposition-Galerkin method requires two numbers for the series summations. One is the number of terms for the series expansions in Eqs. (3.7) and (3.8), which is "*K*" and the other is the number of terms for the driving coefficients *E*'s and *F*'s, which is "*k*". Table 3. 1 shows that computed fundamental natural frequency parameters of the fully clamped cylindrical shallow shell on the square planform for various number of *K*. There is no change in four significant digits beyond 11 terms.

Table 3. 2 presents the fundamental natural frequency parameters of the same type of shell for various values of k. No change in fourth digit is found after using more than five terms. It may be seen that there is no difference in the parameters for the number of k between 1 and 2, and also 3 and 4. This is because the solution includes both symmetrical and anti-symmetrical terms but Table 3. 2 presents results for a mode which is symmetrical and therefore not influenced when adding an anti-symmetrical term. After convergence tests for other modes and other shells with different curvature ratios, the values of $k = 10$ and $K = 20$ are chosen. These numbers could be considered large enough to obtain four significant digits in the natural frequency parameters although using more terms gives results which converged to more significant digits. The work also shows that the Superposition-Galerkin method gives excellent convergence in its results for the fundamental natural frequency parameters.

In Table 3. 3, the frequency parameters obtained using the Superposition - Galerkin method for cylindrical shallow shells having an aspect ratio of 1.0 and a curvature ratio of 0.1 are compared with those in the reference published by Monterrubio [38]. He uses the Rayleigh-Ritz method and the penalty function method to obtained true upperbound results [39]. There is an excellent agreement between the results but the present results are lower. This is reasonable since the present results seem to be lowerbound as can be seen from Table 3. 2. However, it may not possible to declare that the Superposition-Galerkin Method gives lowerbounds for the results obtained for the fully clamped shell because of the following reason. If one were to use exact modes of the building blocks, one would expect the Superposition Method to yield lowerbound results, but if the modes of the building blocks are approximate this is not guaranteed. In the present case the Superposition Method gives higher values if fewer terms were used for K. For example, using three terms only for K gives the higher value than that of published upperbound frequency parameters.

Table 3. 1 The fundamental frequency parameter of the fully clamped square cylindrical shallow shell for various number of K ($a/R_x = 0.1$).

K	3	4	5	6	7	8	9	10	11
Ω_1	46.86	46.26	46.33	46.26	46.29	46.27	46.28	46.27	46.28
K	12	13	14	15	16	17	18	19	20
Ω_1	46.28	46.28	46.28	46.28	46.28	46.28	46.28	46.28	46.28

Table 3. 2 The fundamental frequency parameter of the fully clamped square cylindrical shallow shell for various number of k ($a/R_x = 0.1$).

k	1	2	3	4	5	6
Ω_1	45.84	45.84	46.26	46.26	46.28	46.28
k	7	8	9	10	11	12
Ω_1	46.28	46.28	46.28	46.28	46.28	46.28

Table 3. 3 Comparison of present results and those in the reference [38] for fundamental frequency parameter of the fully clamped square spherical shallow shell

	$\Omega 1$	$\Omega 2$	$\Omega 3$	$\Omega 4$	$\Omega 5$	$\Omega 6$	$\Omega 7$	$\Omega 8$
Ref. [38]	46.292	74.748	79.376	110.58	132.78	135.78	166.28	167.42
Present	46.28	74.65	79.28	110.3	132.5	135.5	165.7	166.9

Fig. 3. 5, 3. 6 and 3. 7 show the first natural frequency parameter of shallow shells for $K = 10$, 15 and 20 with boundary conditions of CCCC (all edges are clamped out-of and in-plane), SCSC (simply supported out-of-plane and shear diaphragm in-plane at $\xi = 0$, 1 and clamped at $\eta = 0$, 1), and CCSS respectively. As can be seen from these figures, the natural frequency parameters increase with number of driving coefficients, k. This has been confirmed for all shells studied. However, since the Galerkin's solution is an upperbound it is not possible to assure lowerboundedness for the final solution to the original problem. For a given number of driving coefficients k, increasing the number of terms in the Galerkin's series K generally shows upperbound behaviour but it is not consistent. On the boundedness, it should be noted here that even for plates, Superposition Method gives bounded solutions only for some boundary conditions. It is not possible to get bounded solutions for CFCF plates for

45

example, as any usable building block would have some boundaries that are stiffer and others that are more flexible compared to the final solution.
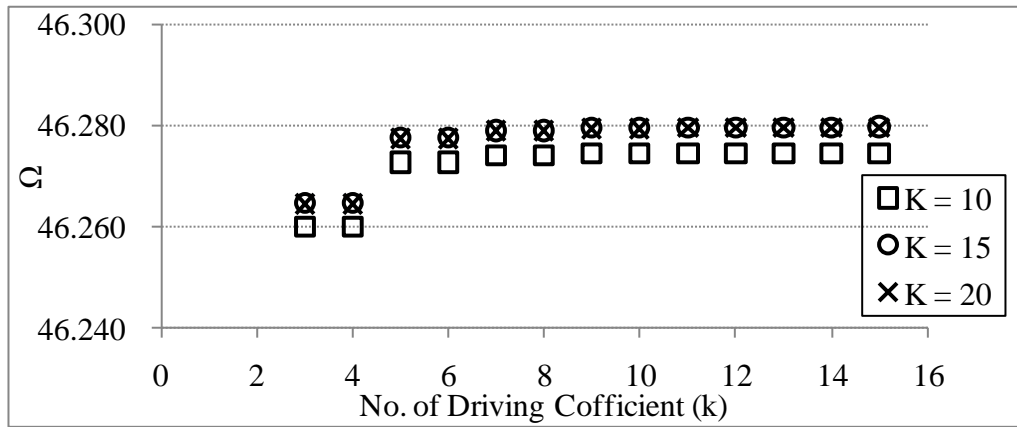
Fig. 3. 5 First frequency parameter of CCCC shallow shell ($\Phi = 1.0$, $a/R_x = 0.1$, $R_x/R_y = 0$)
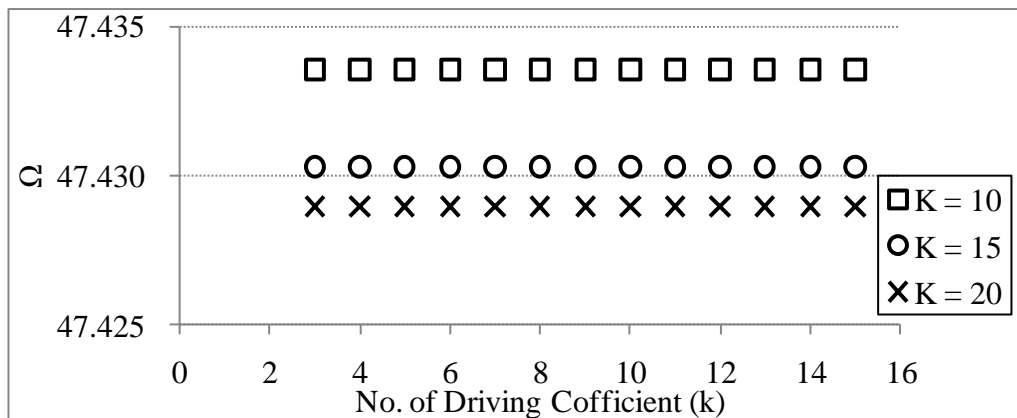
Fig. 3. 6 First frequency parameter of SCSC shallow shell ($\Phi = 1.0$, $a/R_x = 0.1$, $R_x/R_y = 1$)
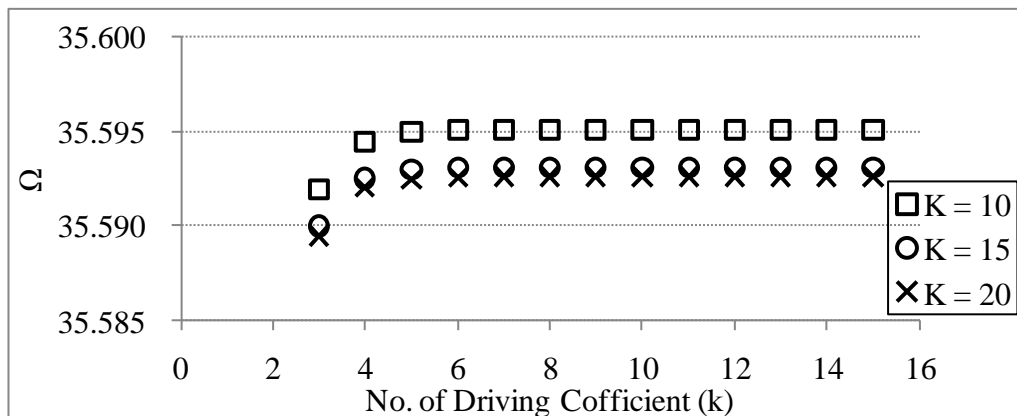
Fig. 3. 7 First frequency parameter of CCSS shallow shell ($\Phi = 1.0$, $a/R_x = 0.1$, $R_x/R_y = -1$)

Tables 3. 4 and 3. 5 give the first 12 natural frequency parameters of SCSC and CCSS shallow shell on the square planform respectively. Those values are compared with the results obtained using Abaqus as the results for the shells having the same combination of boundary conditions were not found in published literature. The Abaqus results were calculated using 10000 quadric elements. The element used is the doubly curved, reduced integration, thin shell element with five degree of freedom at each node, (S8R5).

Table 3. 6 shows the first 12 natural frequencies parameters of fully clamped shallow shells with the aspect ratio of 1.0 and curvature ratios of 0 (flat plate) to 0.5. Table 3. 7 gives results for the shallow shells having the aspect ratio of 2.0. The obtained results are compared with the natural frequency parameters available in reference [40] and [41]. The results in reference [40] are based on the *pb*-2 Ritz method and those in reference [41] were computed using the Ritz method with the displacement functions expressed by polynomials in Eqs. (3.16) and (3.17) [42].

$$
\left.
\begin{aligned}
U &= \sum_{i=0}^{M-1}\sum_{j=0}^{N-1} P_{ij}X_i(\xi)Y_j(\eta) \\
V &= \sum_{k=0}^{M-1}\sum_{l=0}^{N-1} Q_{kl}X_k(\xi)Y_l(\eta) \\
W &= \sum_{m=0}^{M-1}\sum_{n=0}^{N-1} R_{mn}X_m(\xi)Y_n(\eta)
\end{aligned}
\right\}
\tag{3.16}
$$

$$
\left.
\begin{aligned}
X_i(\xi) &= \xi^i(1+\xi)^{Bu1}(1-\xi)^{Bu3} \\
Y_j(\eta) &= \eta^j(1+\eta)^{Bu2}(1-\eta)^{Bu4} \\[6pt]
X_k(\xi) &= \xi^k(1+\xi)^{Bv1}(1-\xi)^{Bv3} \\
Y_l(\eta) &= \eta^l(1+\eta)^{Bv2}(1-\eta)^{Bv4} \\[6pt]
X_m(\xi) &= \xi^m(1+\xi)^{Bw1}(1-\xi)^{Bw3} \\
Y_n(\eta) &= \eta^n(1+\eta)^{Bw2}(1-\eta)^{Bw4}
\end{aligned}
\right\}
\tag{3.17}
$$

where $\xi = 2x/a$, $\eta = 2y/b$, and P_{ij}, Q_{kl} and R_{mn} are unknown coefficients. B_{rs} ($r = u$, v, w; $s = 1, 2, 3, 4$) is called the boundary index.

These polynomials satisfy arbitrary kinematic boundary condition by changing the boundary index [42]. For a fully clamped shell, the boundary indices are as follows:

$$B_{us} = B_{vs} = 1, \qquad B_{ws} = 2 \qquad\qquad (3.18)$$

From the results it may be noted that for the fully clamped shells, the agreement between the Superposition-Galerkin Method and the Rayleigh-Ritz method is excellent. However, the Superposition Method is more efficient than the Rayleigh-Ritz method in term of matrix size. Once the steady state solutions of building blocks are obtained, the Superposition Method requires a smaller size of eigenmatrix than that required by the Rayleigh-Ritz method. For example, the Superposition Method using 10 terms raises a matrix of 8×10 rows and columns while the Rayleigh-Ritz method raises 3×10×10 rows and columns. In addition, it should be noted that the same procedure and functions can be used to solve shell problems with any combination of clamped or simply-supported (out-of-plane), and shear diaphragm or fully constrained (in-plane) edge conditions by only eliminating building blocks which are not necessary.

For the same boundary conditions, there exists some noticeable discrepancy between the Abaqus results and the present results. This may be partly due to the difference between the Abaqus model which is based on the classical thin shell theory and the present results which are based on the thin shallow shell theory (DMV theory). The shallow shell theory, neglecting in-plane displacements in bending and twisting, leads to a stiffer condition. It may be seen that the differences generally increase as the curvature ratio, a/R_x, and aspect ratio increase [37].

While we acknowledge that the application of the Superposition Method for doubly curved shells requires approximate solutions for another set of boundary conditions, this chapter illustrates how the solution for different

boundary conditions may be generated without the need to go through a procedure that requires satisfying the governing equations of motion for the entire shell. Instead, only the boundary conditions are used to compose the final solution from functions that already satisfy the governing differential equations of motion.

Table 3. 4 Natural frequency parameters of the SCSC shallow shell ($\Phi = 1.0$)

	a/R_x	Ω_1	Ω_2	Ω_3	Ω_4	Ω_5	Ω_6	Ω_7	Ω_8	Ω_9	Ω_{10}	Ω_{11}	Ω_{12}	
$R_y/R_x = 0$	0.1	34.03	55.51	74.27	96.14	102.3	132.5	140.6	156.5	170.4	200.5	206.8	210.7	Present
		34.01	55.43	74.15	95.94	102.1	132.1	140.2	156.0	169.8	199.7	206.0	209.8	Abaqus
	0.3	60.66	61.31	103.5	105.7	107.9	144.3	156.9	169.6	170.6	206.2	208.0	228.2	Present
		60.77	61.13	102.8	105.7	107.6	143.4	156.5	169.0	169.1	205.0	206.2	227.4	Abaqus
	0.5	71.32	92.63	105.7	127.9	149.8	151.3	171.1	193.1	196.9	210.3	217.2	258.8	Present
		71.20	93.27	104.1	127.9	149.6	150.4	167.7	192.6	196.8	206.8	215.4	252.8	Abaqus
$R_y/R_x = 1$	0.1	47.43	64.47	77.54	100.7	107.5	133.8	144.2	158.5	173.5	202.6	209.3	211.1	Present
		47.41	64.39	77.39	100.5	107.3	133.4	143.8	158.0	173.0	201.8	208.5	210.1	Abaqus
	0.3	114.9	115.7	125.0	140.1	143.0	167.3	173.0	186.2	197.2	224.2	229.6	231.8	Present
		114.7	115.2	123.8	138.9	141.5	165.7	171.0	184.2	194.0	221.3	226.2	229.0	Abaqus
	0.5	177.6	182.8	185.8	195.2	196.1	219.2	221.7	231.8	237.5	262.1	265.6	268.2	Present
		176.4	180.9	181.1	192.0	192.5	214.3	217.4	226.2	229.9	254.8	257.1	260.8	Abaqus
$R_y/R_x = -1$	0.1	41.52	61.49	73.03	96.18	106.3	132.3	141.6	156.0	173.0	200.3	208.0	210.5	Present
		41.48	61.39	72.84	95.88	106.0	131.8	141.1	155.3	172.4	199.3	207.1	209.3	Abaqus
	0.3	92.02	97.58	98.13	108.0	133.6	152.5	156.4	166.5	192.8	205.2	218.1	226.4	Present
		92.04	97.06	98.24	107.6	133.9	152.1	155.3	165.3	193.2	203.8	217.6	224.3	Abaqus
	0.5	127.9	133.3	135.9	142.7	170.7	171.0	192.8	199.0	218.4	226.0	236.3	255.3	Present
		127.5	132.0	135.8	142.7	171.8	172.3	190.9	197.5	216.5	229.1	237.8	251.6	Abaqus

Table 3. 5 Natural frequency parameters of the CCSS shallow shell ($\Phi = 1.0$)

	a/R_x	Ω_1	Ω_2	Ω_3	Ω_4	Ω_5	Ω_6	Ω_7	Ω_8	Ω_9	Ω_{10}	Ω_{11}	Ω_{12}	
$R_y/R_x = 0$	0.1	34.45	62.02	66.71	94.86	114.9	118.5	146.5	147.9	188.6	191.1	198.9	219.5	Present
		34.44	61.90	66.63	94.66	114.6	118.3	146.1	147.5	187.8	190.4	198.1	218.5	Abaqus
	0.3	59.37	78.78	99.86	111.8	118.3	145.7	152.1	163.0	189.5	205.8	210.5	221.5	Present
		59.31	78.51	99.79	111.4	117.4	145.5	151.1	162.4	187.5	204.4	209.9	219.4	Abaqus
	0.5	72.37	105.5	127.2	133.0	147.5	168.6	184.6	191.9	192.1	219.7	226.2	244.5	Present
		72.24	104.1	127.1	132.4	146.6	167.4	184.4	187.8	191.3	217.5	222.0	243.9	Abaqus
$R_y/R_x = 1$	0.1	45.19	69.57	70.38	99.06	119.4	119.8	149.7	150.0	191.4	191.6	200.9	221.7	Present
		45.17	69.47	70.26	98.85	119.1	119.4	149.2	149.6	190.6	190.8	200.2	220.8	Abaqus
	0.3	108.3	119.1	123.6	139.1	153.0	154.9	177.8	178.9	213.6	214.3	222.8	241.4	Present
		108.0	118.3	122.7	137.9	151.3	153.5	175.8	176.9	210.0	211.7	219.8	237.7	Abaqus
	0.5	171.6	180.3	187.0	195.3	204.1	210.1	223.5	226.0	252.1	254.2	260.9	276.5	Present
		170.9	177.9	184.0	192.7	199.7	208.2	219.9	222.0	243.6	246.7	253.4	267.3	Abaqus
$R_y/R_x = -1$	0.1	35.59	65.72	65.83	94.61	118.0	118.1	147.1	147.3	190.8	190.9	198.6	220.4	Present
		35.57	65.60	65.71	94.34	117.7	117.8	146.5	146.8	190.0	190.1	197.7	219.3	Abaqus
	0.3	69.31	92.45	97.60	112.7	141.7	142.1	157.9	158.2	203.4	208.7	208.8	229.8	Present
		69.49	92.08	97.30	112.1	141.0	141.2	156.7	156.9	201.4	206.8	206.9	227.2	Abaqus
	0.5	94.18	122.4	137.0	149.2	173.0	173.6	183.1	187.1	216.3	239.0	239.3	247.8	Present
		94.36	122.0	136.4	148.5	170.9	172.7	181.4	185.7	212.6	235.4	235.9	243.4	Abaqus

Table 3. 6 Natural frequency parameters of the fully clamped shallow shell ($\Phi = 1.0$)

	a/R_x	Ω_1	Ω_2	Ω_3	Ω_4	Ω_5	Ω_6	Ω_7	Ω_8	Ω_9	Ω_{10}	Ω_{11}	Ω_{12}	
	0	35.98	73.38	73.38	108.2	131.6	132.2	164.9	164.9	210.5	210.5	219.8	242.0	
$R_y/R_x = 0$	0.1	46.28	74.65	79.28	110.3	132.5	135.5	165.7	166.9	210.6	212.9	220.8	242.7	Present
		46.28	74.66	79.29	110.4	132.5	135.6	165.8	167.0					Ref. [40]
		46.24	74.46	79.14	110.0	132.0	135.1	165.1	166.3	209.5	211.9	219.8	241.4	Abaqus
	0.3	83.92	90.39	115.0	125.9	140.5	161.2	172.8	181.8	211.7	228.3	230.8	245.5	Present
		83.92	90.40	115.1	125.9	140.5	161.3	172.8	181.8					Ref. [40]
		83.42	90.20	114.9	125.3	139.3	160.8	171.4	180.9	209.2	226.6	229.9	242.8	Abaqus
	0.5	99.26	119.0	151.1	156.3	172.5	192.4	201.7	207.8	213.9	243.4	251.1	262.9	Present
		99.26	119.0	151.1	156.4	172.5	192.4	201.7	207.8					Ref. [40]
		98.48	117.2	150.3	155.5	171.3	190.4	201.2	206.6	208.8	240.6	246.0	261.9	Abaqus
$R_y/R_x = 1$	0.1	58.30	81.75	81.75	114.1	136.0	137.7	168.7	168.7	213.2	213.2	222.7	244.5	Present
		58.30	81.76	81.76	114.2	136.0	137.7	168.8	168.8					Ref. [40]
		58.24	81.55	81.55	113.8	135.4	137.2	167.9	167.9	212.0	212.0	221.4	243.0	Abaqus
	0.3	130.2	130.2	134.0	153.4	167.2	181.2	196.3	196.3	234.0	234.0	244.0	262.9	Present
		130.2	130.2	134.0	153.4	167.2	181.2	196.4	196.4					Ref. [40]
		129.0	129.4	133.2	152.1	165.8	179.8	194.4	194.5	231.2	231.5	241.3	260.1	Abaqus
	0.5	192.0	192.0	196.9	210.0	216.2	242.2	242.2	257.4	270.7	270.7	282.4	296.4	Present
		192.0	192.0	196.9	210.0	216.2	242.2	242.2	257.4					Ref. [40]
		187.4	189.5	193.3	206.2	212.3	237.1	237.9	253.2	263.6	265.9	276.6	290.1	Abaqus
$R_y/R_x = -1$	0.1	50.75	79.14	79.14	110.7	135.2	135.7	166.7	166.7	212.7	212.7	220.8	243.4	Present
		50.75	79.15	79.15	110.7	135.3	135.7	166.8	166.8					Ref. [40]
		50.70	78.95	78.95	110.3	134.7	135.2	165.9	166.0	211.6	211.6	219.6	242.0	Abaqus
	0.3	110.8	114.1	114.1	128.6	161.6	162.0	180.6	180.6	228.7	229.7	229.7	254.1	Present
		110.8	114.1	114.1	128.6	161.6	162.0	180.7	180.7					Ref. [40]
		111.0	113.7	113.7	127.7	160.5	160.9	179.0	179.0	226.1	227.4	227.5	251.0	Abaqus
	0.5	157.3	157.3	157.4	166.5	204.0	208.7	208.7	208.9	247.1	259.7	259.7	272.8	Present
		157.4	157.4	157.4	166.5	204.0	208.7	208.7	208.8					Ref. [40]
		156.4	156.9	157.0	166.8	202.8	206.1	206.2	208.0	242.7	255.3	255.9	267.6	Abaqus

Table 3. 7 Natural frequency parameters of the fully clamped shallow shell ($\Phi = 2.0$)

	a/R_x	Ω_1	Ω_2	Ω_3	Ω_4	Ω_5	Ω_6	Ω_7	Ω_8	Ω_9	Ω_{10}	Ω_{11}	Ω_{12}	
	0	24.58	31.82	44.76	63.31	63.98	71.06	83.23	87.22	100.7	116.3	123.2	123.6	
$R_y/R_x = 0$	0.1	37.75	42.97	53.53	64.34	70.02	72.27	85.16	92.38	103.0	120.4	123.9	125.8	Present
		37.75	42.97	53.54	64.35	70.05	72.29							Ref. [41]
		37.72	42.93	53.48	64.18	69.94	72.10	84.98	92.25	102.8	120.1	123.5	125.6	Abaqus
	0.3	67.15	81.13	83.64	88.20	96.35	98.99	108.6	119.2	125.7	132.7	138.5	142.5	Present
		67.15	81.14	83.65	88.21	96.37	99.03							Ref. [41]
		66.58	80.64	83.39	88.00	96.21	98.53	108.4	118.7	125.5	131.6	137.4	141.9	Abaqus
	0.5	72.27	95.78	106.4	116.4	120.9	132.0	145.2	150.6	168.5	170.0	170.0	170.3	Present
		72.28	95.8	106.4	116.4	121.0	132.1							Ref. [41]
		71.07	94.99	104.4	114.6	120.3	130.7	144.5	149.8	167.4	169.0	169.2	169.5	Abaqus
$R_y/R_x = 1$	0.1	51.11	51.54	59.38	72.41	72.81	79.32	90.54	94.09	106.8	121.3	128.4	128.6	Present
		51.11	51.54	59.38	72.41	72.95	79.33							Ref. [41]
		51.05	51.50	59.27	72.24	72.58	79.12	90.29	93.73	106.4	120.8	128.0	128.1	Abaqus
	0.3	115.5	116.6	119.8	127.0	128.3	130.1	135.1	141.8	146.2	155.9	162.2	170.1	Present
		115.5	116.7	119.8	127.0	129.2	130.7							Ref. [41]
		114.9	115.8	118.5	125.7	127.2	128.8	133.7	140.3	144.4	153.1	159.7	168.4	Abaqus
	0.5	179.4	179.9	180.5	187.9	189.6	192.5	194.5	200.4	202.5	208.1	214.0	224.5	Present
		179.4	180.2	180.6	187.9	190.8	194.5							Ref. [41]
		173.6	177.4	178.0	182.9	185.7	188.3	190.0	195.1	197.5	202.1	207.9	216.5	Abaqus
$R_y/R_x = -1$	0.1	43.58	44.85	54.15	69.80	70.94	75.61	86.18	92.12	102.9	120.1	125.4	127.6	Present
		43.55	44.80	54.03	69.57	70.78	75.40	85.91	91.73	102.5	119.5	124.9	127.1	Abaqus
	0.3	94.90	96.03	102.3	102.6	108.8	111.4	114.2	120.6	125.6	140.0	146.4	158.1	Present
		94.79	96.02	101.8	102.0	108.4	111.4	113.8	119.4	124.8	138.2	144.7	157.0	Abaqus
	0.5	131.0	131.2	139.2	139.9	154.4	155.5	158.4	159.0	175.1	183.5	186.1	189.9	Present
		130.4	130.5	139.0	139.1	153.0	153.5	157.3	158.6	173.8	183.1	184.6	184.9	Abaqus

3.4 Concluding Remarks

The applicability of the Superposition Method for free vibration analysis of doubly curved thin shallow shells has been demonstrated. In addition, the natural frequencies of thin shallow shells with various curvature ratios and aspect ratios were computed for three different sets of boundary conditions using the Superposition-Galerkin method. The procedure described here and the code developed for this study could be used to generate any of the 55 different combinations of in-plane/out-of-plane boundary conditions. This is achieved simply by removing appropriate rows and columns from the eigenmatrix of the shell with all four edges fully clamped. Displacements of the shells were represented by series of sine and cosine functions, generated using the Galerkin method. These functions are simple, orthogonal and the final series approximately satisfy the governing equations but correspond to a different set of boundary conditions. The prescribed boundary conditions are then satisfied using the Superposition Method.

There is an excellent agreement between the results obtained by the Superposition-Galerkin Method and the values found in earlier literature for the fully clamped shell. For the other two boundary conditions, the results showed reasonable agreement with FEA results obtained using Abaqus. The Superposition - Galerkin Method shows very good convergence for the fundamental natural frequencies with only five terms.

4. Chapter IV

Conclusions

CONCLUSIONS

4.1 General Conclusions

The applicability of the Superposition Method for the transient vibration analysis of the plates and the free vibration analysis of the doubly curved shells has been investigated. It has been shown that the use of the natural frequencies and the modes obtained using the Superposition Method can provide accurate and efficient predictions of the transient response of an undamped plate. The results based on the Superposition Method require a smaller size of matrix to converge than that of the matrix which is required for the results based on the natural frequencies and the modes determined using the Rayleigh-Ritz method with either the ordinary or the degenerated beam functions. The values obtained using the natural frequencies and modes given by the Superposition Method are more accurate and reliable, and may be considered as benchmark data for the transient response of completely free plates.

More interestingly, it is the first time that the Superposition Method is employed to determine the natural frequencies of thin doubly curved shallow shells. The approximate modes given by the Galerkin method are used for the building blocks since an exact solution is not available for doubly curved shells. The work shows that the present method gives a fast convergence rate in its results. The obtained results have an excellent agreement with those in the literature published earlier and a reasonable agreement with FEA results obtained using Abaqus.

4.2 Future Research

It has been shown so far that the Superposition Method is an accurate and efficient method for vibration analyses of plates, including steady states and transient analyses of plates with various boundary conditions, and free vibration analysis of the open cylindrical shells and thin doubly curved shallow shell. The Superposition Method may be able to be applied for free vibration analysis of thin shallow shells having more complicated geometry, or other combinations of boundary conditions such as completely free, elastically supported, and various types of shells such as orthotropic, and composite shells. Transient and steady state vibration analyses of those shells are also a worthwhile area for research. The Superposition Method could also be applied for any other linear eigenvalue problem, such as buckling or aeroelastic analysis of the plates and shells.

The Superposition Method will not be limited to only two-dimensional vibration problems. Three-dimensional problems can also be solved. In the thin plate theory, the effects of shear deformation and/or rotatory inertia are neglected, and therefore the obtained solution will be inaccurate when the plates become thicker. Since the three-dimensional theory provides more reliable and accurate results for thick plates, the three-dimensional solutions attract many researchers' attention. A literature review on the vibration analysis of thick plates was published by Liew, Xiang and Kitipornchai [43].

Mindlin assumed that a shear stress distribution is constant through the thickness and took account of both the shear deformation and rotatory inertia in an analysis of thick plates [44]. Gorman successfully applied the Superposition Method for the Mindlin plates with some boundary conditions [45-47]. Srinivas, Joga Rao, and Rao used a three-dimensional linear, small deformation theory to investigate the free vibration of simply-supported, homogeneous, isotropic thick plates as shown in Fig. 4. 1. and obtained an exact solution by solving the characteristic equations that are derived from a double trigonometric series of displacement functions [48]. Liew, Hung and Lim predicted the vibration behaviours of the thick plates based on the same theory for various boundary

conditions, namely a combination of simply-supported, clamped and free conditions, using the Ritz method with a set of orthogonal polynomial functions [49]. The boundary conditions on simply-supported, clamped and free straight edges, x = constant, are expressed as Eqs (4.1), (4.2) and (4.3) respectively [49]. These boundary conditions are effectively the same as the boundary conditions of the shells studied in this thesis. Filipich, Rosales and Belles considered rectangular plates as tridimensional solids and analysed the case where the plates are simply-supported using the variational method developed by the authors, which is named Whole Element Method (WEM) [50]. WEM was extended for the clamped thick plates by Rosales, Filipich and Andreu Torras [51].

$$w = 0, v = 0, \text{ and } \sigma_x = 0 \qquad (4.1)$$

$$u = 0, v = 0 \text{ and } w = 0 \qquad (4.2)$$

$$\sigma_x = 0, \tau_{xy} = 0, \text{ and } \tau_{xz} = 0 \qquad (4.3)$$

To the author's knowledge, however, the Superposition Method has not been utilised for thick plates with basis of the three-dimensional theory. Considering the rapid rate of convergence shown by the Superposition Method for all the problems studied so far, it is believed that accurate results for thick plates based on exact three-dimensional theory could be obtained more efficiently using the Superposition Method.
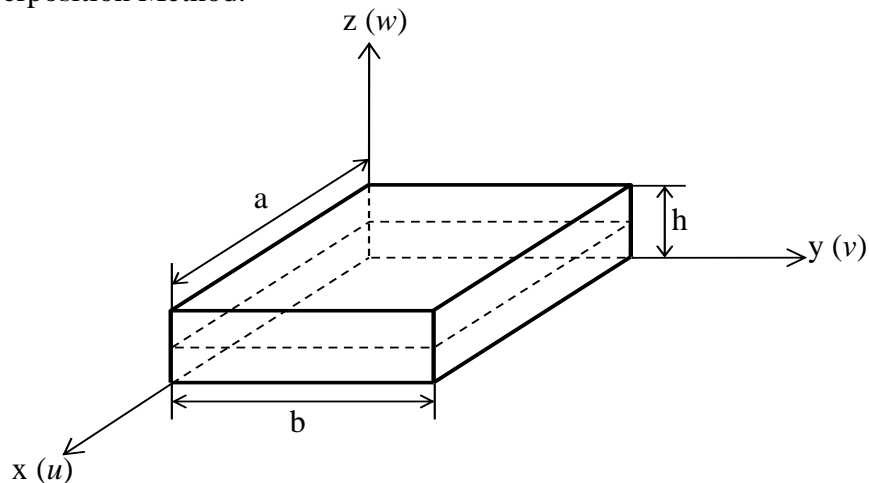
Fig. 4. 1 Reference coordinates and dimension of thick rectangular plate

References

[1] A.W. Leissa, *Vibration of plates*. NASA SP-160, 1969.

[2] D.J. Gorman, *Free vibration analysis of rectangular plates*. Elsevier North Holland, New York, 1982.

[3] D.J. Gorman, Accurate free vibration analysis of clamped orthotropic plates by the method of superposition. *Journal of Sound and Vibration* 140 (1990)391-441.

[4] D.J. Gorman, A general solution for the free vibration of rectangular plates resting on uniform elastic edge supports. *Journal of Sound and Vibration* 139 (1990)325-335.

[5] D.J. Gorman, Accurate free vibration analysis of the completely free orthotropic rectangular plate by the method of superposition. *Journal of Sound and Vibration* 165 (1993)409-420.

[6] D.J. Gorman, A general solution for the free vibration of rectangular plates with arbitrarily distributed lateral and rotational elastic edge support. *Journal of Sound and Vibration* 174 (1994)451-459.

[7] D.J. Gorman, *Vibration analysis of plates by the superposition method*. World Scientific Publishing, Singapore, 1999.

[8] D.J. Gorman, Free in-plane vibration analysis of rectangular plates by the method of superposition. *Journal of Sound and Vibration* 272 (2004)831-851.

[9] D.J. Gorman, Accurate analytical type solutions for the free in-plane vibration of clamped and simply supported rectangular plates. *Journal of Sound and Vibration* 276 (2004)311-333.

[10] D.J. Gorman, R. Singhal, Steady-state response of a cantilever plate subjected to harmonic displacement excitation at the base. *Journal of Sound and Vibration* 323 (2009)1003-1015.

[11] D.J. Gorman, W. Wing, The Superposition-Galerkin method for free vibration analysis of rectangular plates. *Journal of Sound and Vibration* 194 (1996)187-198.

[12] D.J. Gorman, Free vibration analysis of completely free rectangular plates by the Superposition-Galerkin method. *Journal of Sound and Vibration* 237 (2000)901-914.

[13]   S.D. Yu, W.L. Cleghorn, R.G. Fenton, On the accurate analysis of free vibration of open circular cylindrical shells. *Journal of Sound and Vibration* 188 (1995)315-336.

[14] A.W. Leissa, *Vibration of shells*. NASA SP-288, 1973.

[15] M.S. Qatu, Review of shallow shell vibration research. *Shock and Vibration Digest* 24 (1992)3-15.

[16] K.M. Liew, C.W. Lim, S. Kitipornchai, Vibration of shallow shells: a review with bibliography. *Applied Mechanics Reviews* 50 (1997)431-444.

[17]   E.M. Forsyth, G.B. Warburton, Transient vibration of rectangular plates. *Journal Mechanical Engineering Science* 2 (1960)325-330.

[18]   A. Craggs, Transient vibration analysis of linear systems using transition matrices, NASA, 1968.

[19]   K. Nagaya, Transient response of a continuous plate on elastic supports. *Journal of Sound and Vibration* 47 (1976)359-370.

[20] T. Rock, E. Hinton, Free vibration and transient response of thick and thin plates using the finite element method. *Earthquake Engineering and Structural Dynamics* 3 (1974)51-63.

[21] J.R. Coleby, J. Mazumdar, Non-linear vibrations of elastic plates subjected to transient pressure loading. *Journal of Sound and Vibration* 80 (1982)193-201.

[22]   Z. Celep, On the time-response of square plates on unilateral support. *Journal of Sound and Vibration* 125 (1988)305-312.

[23]   Y. Nath, K.K. Shukla, Non-linear transient analysis of moderately thick laminated composite plates. *Journal of Sound and Vibration* 247 (2001)509-526.

[24] S. Abrate, Transient response of beams, plates, and shells to impulsive loads, *2007 ASME International Mechanical Engineering Congress and Exposition,* Seattle, Washington, USA, November 11-15, pp.107-116.

[25] Y. Mochida, Bounded eigenvalues of fully clamped and completely free rectangular plates. , University of Waikato, 2008.

[26] Y. Mochida, S. Ilanko, Bounded eigenvalues of completely free rectangular plates *The 6th International Symposium on Vibrations of Continuous Systems,* Squaw Valley, U.S.A., July 22-24 2007, pp.22-24.

[27]   Y. Mochida, S. Ilanko, Bounded natural frequencies of completely free rectangular plates *Journal of Sound and Vibration* 311 (2008)1-8.

[28] Y. Mochida, S. Ilanko, Transient vibration analysis of a completely free plate using modes obtained by Gorman's superposition method *Journal of Sound and Vibration* 329 (2010)1890-1900

[29] D. Young, Vibration of rectangular plates by the Ritz method. *Journal of Applied Mechanics* 17 (1950)448–453.

[30] S.F. Bassily, S.M. Dickinson, On the use of beam functions for problems of plates involving free edges. *Journal of Applied Mechanics* 42 (1975)858-864.

[31] F.W. Williams, W.H. Wittrick, An automatic computational procedure for calculating natural frequencies of skeletal structures. *International Journal of Mechanical Sciences* 12 (1970)781-791.

[32] W.H. Wittrick, F.W. Williams, A general algorithm for computing natural frequencies of elastic structures. *Quarterly Journal of Mechanics and Applied Mathematics* 24 (1971)263-284.

[33] W.H. Wittrick, F.W. Williams, An algorithm for computing critical buckling loads of elastic structures. *Journal of Structural Mechanics* 1 (1973)497-518.

[34] S. Timochenko, S. Woinowsky-Krieger, *Theory of plates and shells*, Second ed. McGraw-Hill, Inc., Singapore, 1959.

[35] A.W. Leissa, A.S. Kadi, Curvature effects on shallow shell vibrations. *Journal of Sound and Vibration* 16 (1971)173-187.

[36] E. Ventsel, T. Krauthammer, *Thin Plates and Shells: Theory, Analysis, and Applications*. Marcel Dekker, Inc., New York, 2001.

[37] C.W. Lim, S. Kitipornchai, K.M. Liew, Comparative accuracy of shallow and deep shell theories for vibration of cylindrical shells. *Journal of Vibration and Control* 3 (1997)119-143.

[38] L.E. Monterrubio, Free vibration of shallow shells using the Rayleigh-Ritz method and penalty parameters. *Proceedings of the Institution of Mechanical Engineers, Part C: Journal of Mechanical Engineering Science* 223 (2009)2263-2272.

[39] S. Ilanko, S.M. Dickinson, Asymptotic modelling of rigid boundaries and connections in the Rayleigh-Ritz method *Journal of Sound and Vibration* 219 (1999)370-378

[40] K.M. Liew, C.W. Lim, Vibration of doubly-curved shallow shells. *Acta Mechanica* 114 (1996)95-119.

[41]   The Japan Society of Mechanical Engineers, *Handbook for vibration and buckling of shells (in Japanese)*. Gihodo Shuppan Co., Ltd., Tokyo, 2003.

[42]   Y. Narita, P. Robinson, Maximizing the fundamental frequency of laminated cylindrical panels using layerwise optimization. *International Journal of Mechanical Sciences* 48 (2006)1516-1524.

[43]   K.M. Liew, Y. Xiang, S. Kitipornchai, Research on thick plate vibration: A literature survey. *Journal of Sound and Vibration* 180 (1995)163-176.

[44]   R.D. Mindlin, Influence of rotatory inertia and shear on flexural motions of isotropic, elastic plates. *Journal of Applied Mechanics* 18 (1951)31-38.

[45]   D.J. Gorman, Free vibration analysis of mindlin plates with uniform elastic edge support by the superposition method. *Journal of Sound and Vibration* 207 (1997)335-350.

[46]   D.J. Gorman, Accurate free vibration analysis of point supported mindlin plates by the superposition method. *Journal of Sound and Vibration* 219 (1999)265-277.

[47]   D.J. Gorman, W. Ding, Accurate free vibration analysis of the completely free rectangular mindlin plate. *Journal of Sound and Vibration* 189 (1996)341-353.

[48] S. Srinivas, C.V.J. Rao, A.K. Rao, An exact analysis for vibration of simply-supported homogeneous and laminated thick rectangular plates. *Journal of Sound and Vibration* 12 (1970)187-199.

[49] K.M. Liew, K.C. Hung, M.K. Lim, A continuum three-dimensional vibration analysis of thick rectangular plates. *International Journal of Solids and Structures* 30 (1993)33357-3379.

[50]   C.P. Filipich, M.B. Rosales, P.M. Bellés, Natural vibration of rectangular plates considered as tridimensional solids. *Journal of Sound and Vibration* 212 (1998)599-610.

[51]   M.B. Rosales, C.P. Filipich, A.A. Torras, Clamped plates considered as three-dimensional solids: a method to find arbitrary precision frequencies. *Journal of Sound and Vibration* 248 (2001)955-962.

[52]   K. Suzuki, G. Yamada, Y. Narita, T. Saito, *Introduction to Vibrations of Shells (in Japanese)*. Corona Publishing Co., Ltd., Tokyo, 1996.

Appendix I: Theory of Thin shallow shell

Ventsel and Krauthammer explain the thin shallow shell theory in terms of out-of-plane displacement and the Airy stress function [36]. Suzuki et al. take a different approach and describe the thin shallow shell theory in terms of out-of-plane and in-plane displacements in their book [52]. For convenience and completeness, the relevant parts in the derivations for thin shallow shells based on Donnell-Mushtari-Vlasov (DMV) Theory are presented here. The key assumptions are listed below, in which (a) and (b) are the Kirchhoff-Love hypotheses and (c) and (d) are additional assumptions in the DMV theory [36]

(a) *"Normals to the undeformed middle surface remain straight and normal to the deformed middle surface and undergo no extension, i.e. all the strain components (normal and shear) in the direction of the normal to the middle surface vanish."*

(b) *"The transverse normal stress is small compared with other normal stress components and may be neglected."*

(c) *"The effect of the transverse shear in the in-plane is negligible."*

(d) *"The influence of the out-plane deflections, w, will predominate over the influences of the in-plane displacements u and v in the bending response of the shell."*

Consider the case of a thin shallow shell on a rectangular planform shown as Fig. A1. 1. The shape of the middle surface of the shell is defined by Eq. (A1. 1).

$$z = -\frac{1}{2}\left(\frac{x^2}{R_x} + \frac{y^2}{R_y}\right) \qquad (A1.1)$$

It is assumed that the radii of curvature, R_x and R_y are constant in the x and y directions respectively.
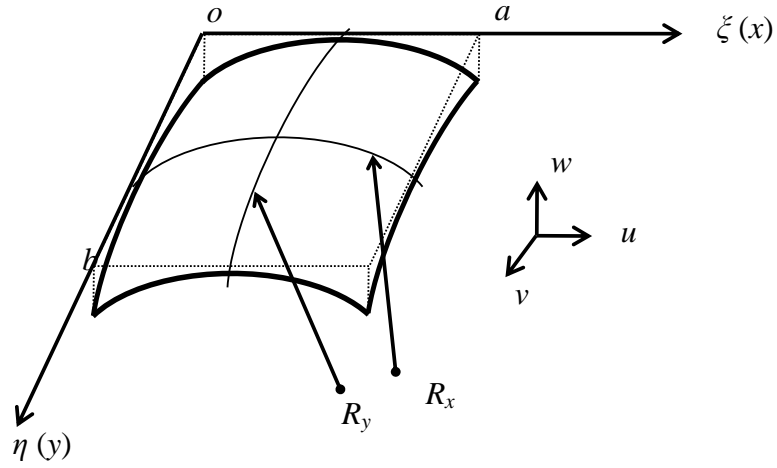
Fig. A1. 1 A shallow shell on rectangular planform

The stresses on a surface at the distance of z from the middle surface, neglecting the stresses in z-direction, are given by the Eq. (A1. 2).

$$\left. \begin{aligned} \sigma'_x &= \frac{E}{1-v^2}\left(\varepsilon'_x + v\varepsilon'_y\right) \\ \sigma'_y &= \frac{E}{1-v^2}\left(\varepsilon'_y + v\varepsilon'_x\right) \\ \gamma'_{xy} &= G\tau'_{xy} \end{aligned} \right\}$$
(A1. 2)

The normal forces per unit length are given by integrating Eq. (A1. 2) through the thickness of shell, which are expressed in Eq. (A1. 3).

$$\begin{Bmatrix} N_{xx} \\ N_{yy} \\ N_{xy} \end{Bmatrix} = \int_{-\frac{h}{2}}^{\frac{h}{2}} \begin{Bmatrix} \sigma'_x \\ \sigma'_y \\ \gamma'_{xy} \end{Bmatrix} dz = \frac{Eh}{1-v^2} \begin{bmatrix} 1 & v & 0 \\ v & 1 & 0 \\ 0 & 0 & \frac{1-v}{2} \end{bmatrix} \begin{Bmatrix} \varepsilon_x \\ \varepsilon_y \\ \gamma_{xy} \end{Bmatrix}$$
(A1. 3)

where

$$\left. \begin{aligned} \varepsilon_x &= \frac{\partial u}{\partial x} + \frac{w}{R_x} \\ \varepsilon_y &= \frac{\partial v}{\partial y} + \frac{w}{R_y} \\ \gamma_{xy} &= \frac{\partial u}{\partial y} + \frac{\partial v}{\partial x} \end{aligned} \right\}$$
(A1. 4)

ε_x, ε_y and τ_{xy} are strains and u, v, and w are displacements at the middle surface.

Similarly, the moments per unit length are given by integrating the relevant stresses in Eq. (A1. 4) multiplied by z and infinitesimal thickness dz (Eq. (A1. 5)).

$$\begin{Bmatrix} M_{xx} \\ M_{yy} \\ M_{xy} \end{Bmatrix} = \int_{-\frac{h}{2}}^{\frac{h}{2}} \begin{Bmatrix} \sigma'_x \\ \sigma'_y \\ \gamma'_{xy} \end{Bmatrix} z\,dz = = \frac{Eh^3}{12(1-v^2)} \begin{bmatrix} 1 & v & 0 \\ v & 1 & 0 \\ 0 & 0 & \frac{1-v}{2} \end{bmatrix} \begin{Bmatrix} \kappa_x \\ \kappa_y \\ \kappa_{xy} \end{Bmatrix} \quad (A1.5)$$

where

$$\left. \begin{aligned} \kappa_x &= -\frac{\partial^2 w}{\partial x^2} \\ \kappa_y &= -\frac{\partial^2 w}{\partial y^2} \\ \kappa_{xy} &= -2\frac{\partial^2 w}{\partial x \partial y} \end{aligned} \right\} \quad (A1.6)$$

Next, let us consider the equilibrium of the forces and moments acting on the middle surface of the shell. Fig. A1. 2 (a) shows an element $\delta x \times \delta y$ of the shell on which normal forces per unit length are working. The bending and twisting moments, and out-of-plane shear forces, Q_x and Q_y, acting on the element are also shown in Fig. A1. 2 (b). Normal forces, N's and moments, M's are given by Eqs. (A1. 3) and (A1. 5) respectively. From Fig. A1. 2 (a), the sum of normal forces in x-direction is

$$\left[\left(N_{xx} + \frac{\partial N_{xx}}{\partial x}dx\right) - N_{xx}\right]dy + \left[\left(N_{xy} + \frac{\partial N_{xy}}{\partial y}dy\right) - N_{xy}\right]dx$$

$$= \frac{\partial N_{xx}}{\partial x}dxdy + \frac{\partial N_{xy}}{\partial y}dxdy \quad (A1.7)$$

Applying Newton's 2nd law in the x-direction gives

$$\frac{\partial N_{xx}}{\partial x}dxdy + \frac{\partial N_{xy}}{\partial y}dxdy = \rho h dxdy \times \frac{\partial^2 u}{\partial t^2} \quad (A1.8)$$

i.e.

$$\frac{\partial N_{xx}}{\partial x} + \frac{\partial N_{xy}}{\partial y} = \rho h \frac{\partial^2 u}{\partial t^2} \quad (A1.9)$$

Similarly in the y-direction, we get

$$\frac{\partial N_{xy}}{\partial x} + \frac{\partial N_{yy}}{\partial y} = \rho h \frac{\partial^2 v}{\partial t^2} \qquad (A1.10)$$

(a)

(b)
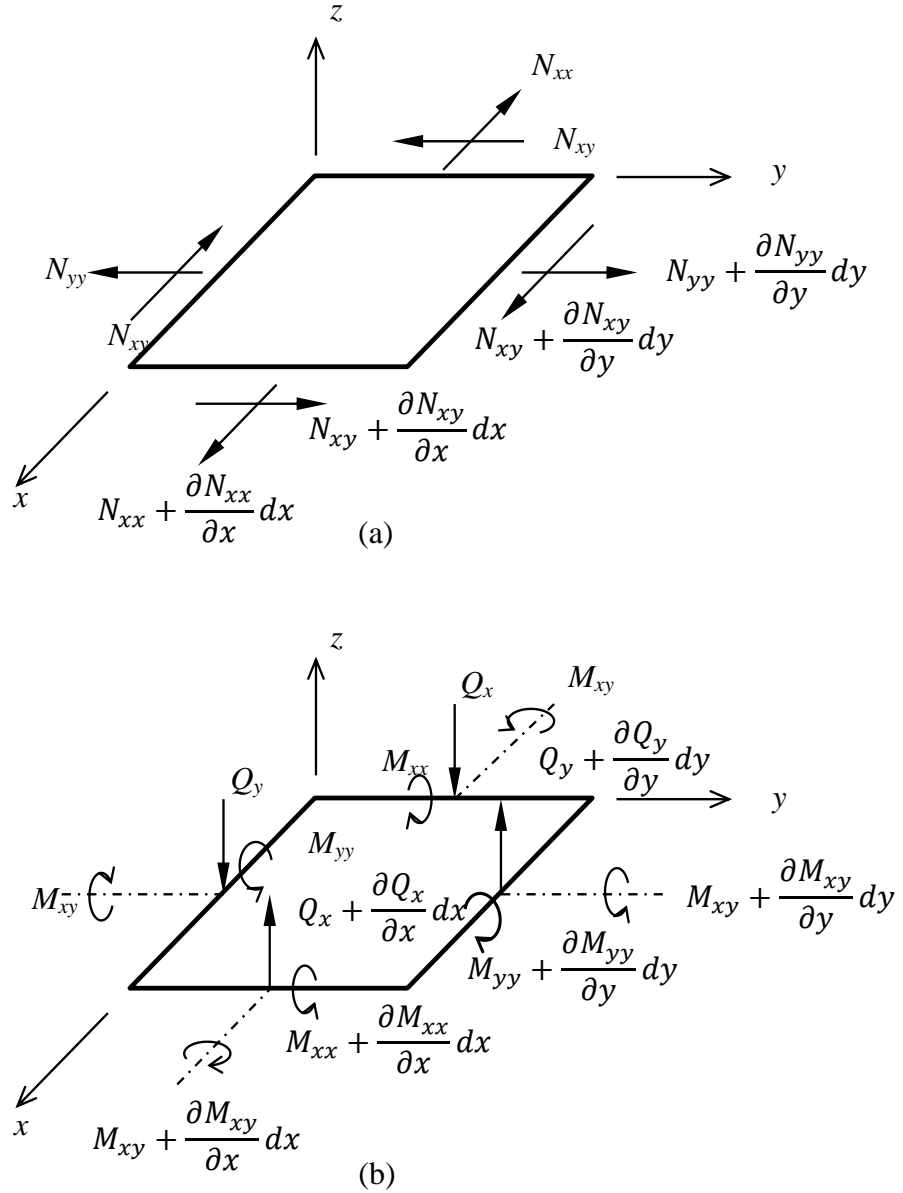
Fig. A1. 2 Equilibrium of (a) in-plane forces, (b) out-of-plane forces and moments

By applying Newton's second law in the z-direction to the element in Fig. A1. 2 (b) gives

66

$$\frac{\partial Q_x}{\partial x} + \frac{\partial Q_y}{\partial y} = \rho h \frac{\partial^2 w}{\partial t^2} \qquad (A1.11)$$

By applying Newton's second law in the about the x- and y-axes and neglecting the rotary inertia gives Eq. (A1. 12) and (A1. 13) respectively.

$$\frac{\partial M_{xx}}{\partial x} + \frac{\partial M_{xy}}{\partial y} - Q_x = 0 \qquad (A1.12)$$

$$\frac{\partial M_{xy}}{\partial x} + \frac{\partial M_{yy}}{\partial y} - Q_y = 0 \qquad (A1.13)$$

If substituting Q_x and Q_y obtained from Eqs (A1. 12) and (A1. 13) into Eq. (A1. 11) one will get the following equation.

$$\frac{\partial^2 M_{xx}}{\partial x^2} + 2\frac{\partial^2 M_{xy}}{\partial x \partial y} + \frac{\partial^2 M_{yy}}{\partial y^2} = \rho h \frac{\partial^2 w}{\partial t^2} \qquad (A1.14)$$

These derived equations of motion in x-, y- and z-direction do not include terms counting the curvatures of the shell. In DMV theory, the terms for transverse shear in the in–plane, which should be included in Eqs. (A1. 9) and (A1.10) in general shell theory, are neglected (Assumption (c)). However, the relationship of between the in-plane strains (i.e. in-plane forces) and the out-of-plane deflections, as expressed in Eq. (A1. 4), need to be counted in Eq. (A1. 14). The components of normal forces in z-direction as shown in Fig. A1. 3 are given by Eq. (A1. 15).

$$N_x' = -N_{xx}dy\sin\left(\frac{d\theta}{2}\right) - \left[N_{xx} + \left(\frac{\partial N_{xx}}{\partial x}\right)dx\right]dy\sin\left(\frac{d\theta}{2}\right) \quad (A1.15)$$

When $d\theta$ is small the following approximation is valid.

$$\sin\left(\frac{d\theta}{2}\right) = \frac{d\theta}{2} \text{ and } \frac{d\theta}{2} = \frac{dx}{2R_x} \qquad (A1.16)$$
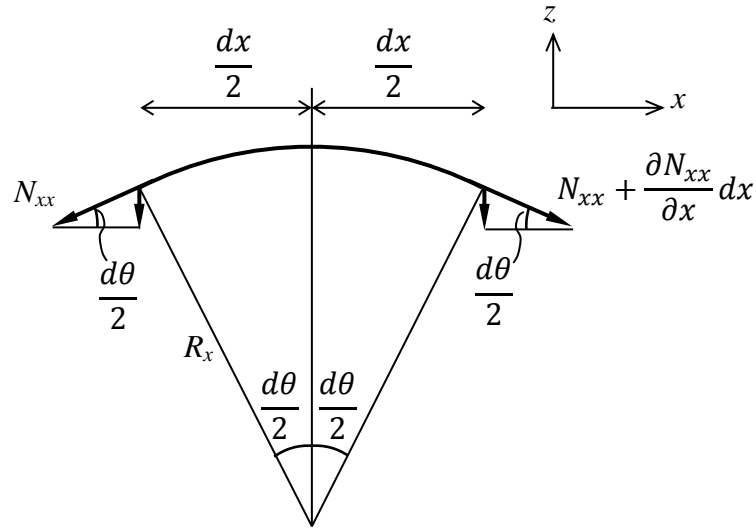
Fig. A1. 3 The components of normal forces in *z*-direction

Then, Eq. (A1. 15) is rearranged, neglecting the third order infinitesimal component, $dxdyd\theta$, as

$$N_x' = -\left(\frac{N_{xx}}{R_x}\right)dxdy \qquad (A1.17)$$

Similarly in *y*-direction,

$$N_y' = -\left(\frac{N_{yy}}{R_y}\right)dxdy \qquad (A1.18)$$

Including terms expressed by Eqs. (A1. 17) and (A1. 18) in Eq. (A1. 14) gives,

$$\frac{\partial^2 M_{xx}}{\partial x^2} + 2\frac{\partial^2 M_{xy}}{\partial x \partial y} + \frac{\partial^2 M_{yy}}{\partial y^2} - \frac{N_{xx}}{R_x} - \frac{N_{yy}}{R_y} = \rho h\frac{\partial^2 w}{\partial t^2} \qquad (A1.19)$$

Now, let the displacement, *u*, *v* and *w*, be the following functions.

$$\left.\begin{array}{l} u(x,y,t) = u(x,y)\sin\omega t \\ v(x,y,t) = v(x,y)\sin\omega t \\ w(x,y,t) = w(x,y)\sin\omega t \end{array}\right\} \qquad (A1.20)$$

Then, the derivatives of these functions in terms of time, t, would be given by Eq. (A1. 21).

$$\left.\begin{array}{l} \dfrac{\partial^2 u}{\partial t^2} = -\omega^2 u \\[6pt] \dfrac{\partial^2 v}{\partial t^2} = -\omega^2 v \\[6pt] \dfrac{\partial^2 w}{\partial t^2} = -\omega^2 w \end{array}\right\} \qquad (A1.21)$$

Finally, by substituting Eqs. (A1. 3) ~ (A1. 6), and (A1. 21) into Eqs. (A1. 9), (A1.10), and (A1. 19), the governing equations of vibration of thin shallow shell are expressed by Eq. (A1. 22) and (A1. 23).

$$\begin{bmatrix} L_{11} & L_{12} & L_{13} \\ L_{12} & L_{22} & L_{23} \\ L_{13} & L_{23} & L_{33} \end{bmatrix} \begin{Bmatrix} u \\ v \\ w \end{Bmatrix} - \omega^2 \begin{bmatrix} -\rho h & 0 & 0 \\ 0 & -\rho h & 0 \\ 0 & 0 & \rho h \end{bmatrix} \begin{Bmatrix} u \\ v \\ w \end{Bmatrix} = 0 \qquad (A1.22)$$

$$\left.\begin{array}{l} L_{11} = E_p \dfrac{\partial^2}{\partial x^2} + Gh \dfrac{\partial^2}{\partial y^2} \\[10pt] L_{12} = (E_p v + Gh) \dfrac{\partial^2}{\partial x \partial y} \\[10pt] L_{13} = E_p \left(\dfrac{1}{R_x} + \dfrac{v}{R_y}\right) \dfrac{\partial}{\partial x} \\[10pt] L_{22} = Gh \dfrac{\partial^2}{\partial x^2} + E_p \dfrac{\partial^2}{\partial y^2} \\[10pt] L_{23} = E_p \left(\dfrac{v}{R_x} + \dfrac{1}{R_y}\right) \dfrac{\partial}{\partial y} \\[10pt] L_{33} = D \left(\dfrac{\partial^4}{\partial x^4} + 2\dfrac{\partial^4}{\partial x^2 \partial y^2} + \dfrac{\partial^4}{\partial y^4}\right) + E_p \left(\dfrac{1}{R_x{}^2} + \dfrac{2v}{R_x R_y} + \dfrac{1}{R_y{}^2}\right) \end{array}\right\} \qquad (A1.23)$$

where

$$E_p = \frac{Eh}{(1-v^2)} \qquad G = \frac{E}{2(1+v)} \qquad D = \frac{Eh^3}{12(1-v^2)} \qquad (A1.24)$$

The dimensionless forms of the governing equations are also given as follows.

$$
\begin{bmatrix} L'_{11} & L'_{12} & L'_{13} \\ L'_{12} & L'_{22} & L'_{23} \\ L'_{13} & L'_{23} & L'_{33} \end{bmatrix} \begin{Bmatrix} U \\ V \\ W \end{Bmatrix} + \frac{1}{12\delta^2} \begin{bmatrix} \Omega^2 & 0 & 0 \\ 0 & \Omega^2 & 0 \\ 0 & 0 & -\Omega^2 \end{bmatrix} \begin{Bmatrix} U \\ V \\ W \end{Bmatrix} = 0 \quad (A1.25)
$$

$$
\left.\begin{aligned}
L'_{11} &= \frac{\partial^2}{\partial \xi^2} + \frac{\bar{v}}{\Phi^2}\frac{\partial^2}{\partial \eta^2} \\
L'_{12} &= \frac{(v + \bar{v})}{\Phi}\frac{\partial^2}{\partial \xi \partial \eta} \\
L'_{13} &= \beta(1 + v\gamma)\frac{\partial}{\partial \xi} \\
L'_{22} &= \bar{v}\frac{\partial^2}{\partial \xi^2} + \frac{1}{\Phi^2}\frac{\partial^2}{\partial \eta^2} \\
L'_{23} &= \frac{\beta}{\Phi}(v + \gamma)\frac{\partial}{\partial \eta} \\
L'_{33} = \frac{1}{12\delta^2}\left(\frac{\partial^4}{\partial \xi^4} + \frac{2}{\Phi^2}\frac{\partial^4}{\partial \xi^2 \partial \eta^2} + \frac{1}{\Phi^4}\frac{\partial^4}{\partial \eta^4}\right) &+ \beta^2(1 + 2v\gamma + \gamma^2)
\end{aligned}\right\} \quad (A1.26)
$$

where $\Omega = \omega a^2\sqrt{\rho h/D}$.

Appendix II: The results for transient responses of the completely free plates
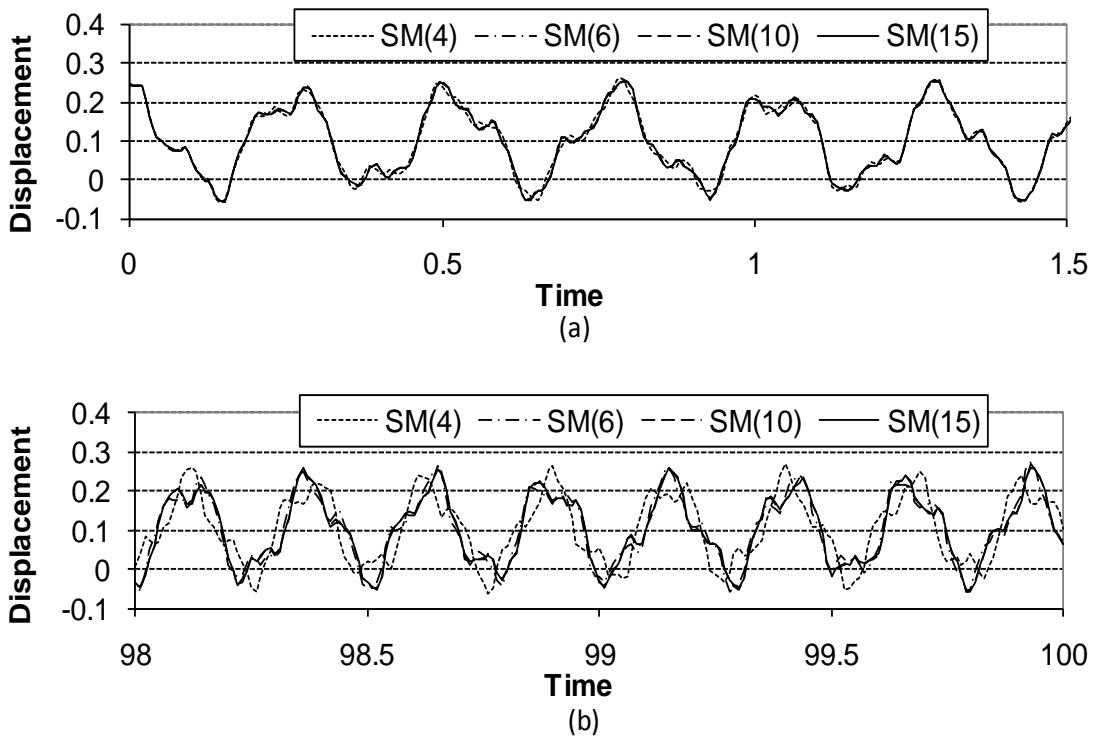
Fig. A2. 1 The transient response of the completely free square plate at the centre, based on the natural frequencies and modes given by the Superposition Method at the time of (a) 0 to 1.5 and (b) 98 to 100.
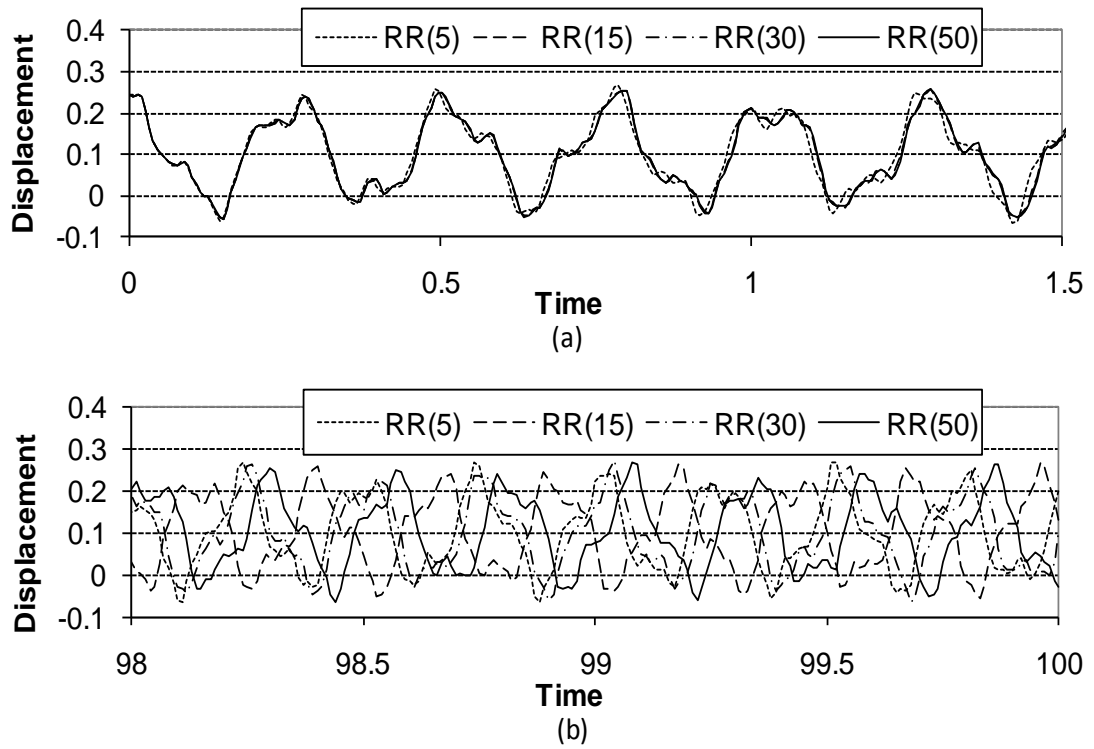
Fig. A2. 2 The transient response of the completely free square plate at the centre, based on the natural frequencies and modes given by the Rayleigh-Ritz method with the ordinary beam functions at the time of (a) 0 to 1.5 and (b) 98 to 100.
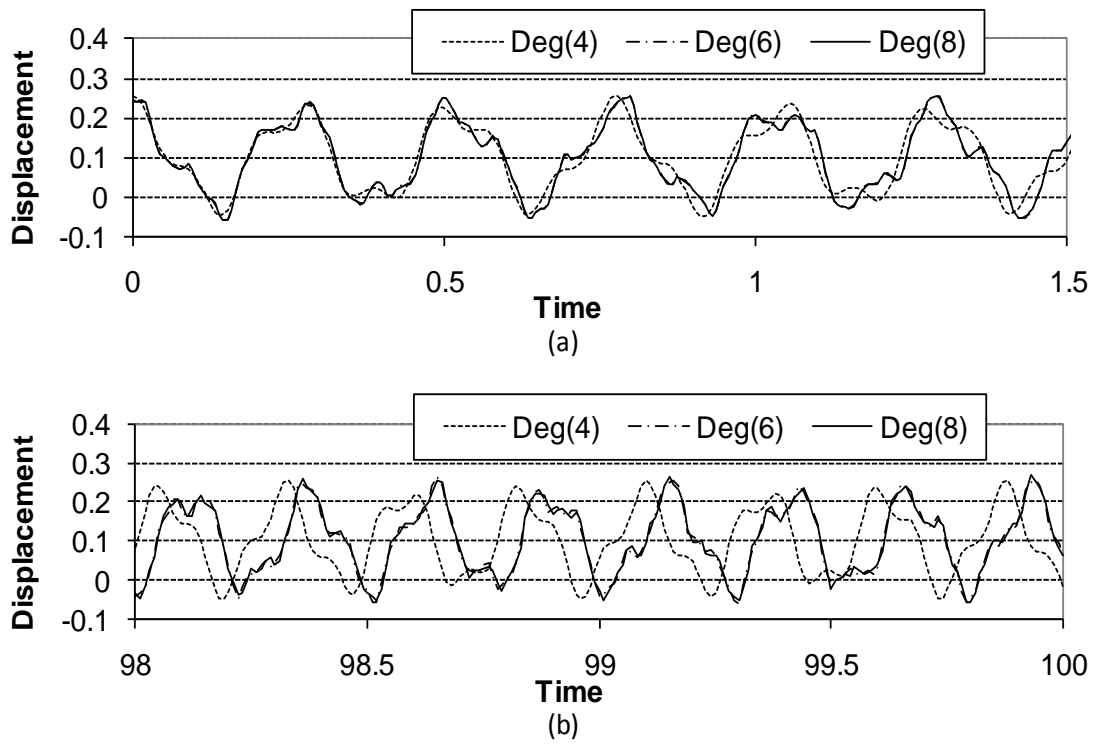
Fig. A2. 3 The transient response of the completely free square plate at the centre, based on the natural frequencies and modes given by the Rayleigh-Ritz method with the degenerated beam functions at the time of (a) 0 to 1.5 and (b) 98 to 100.
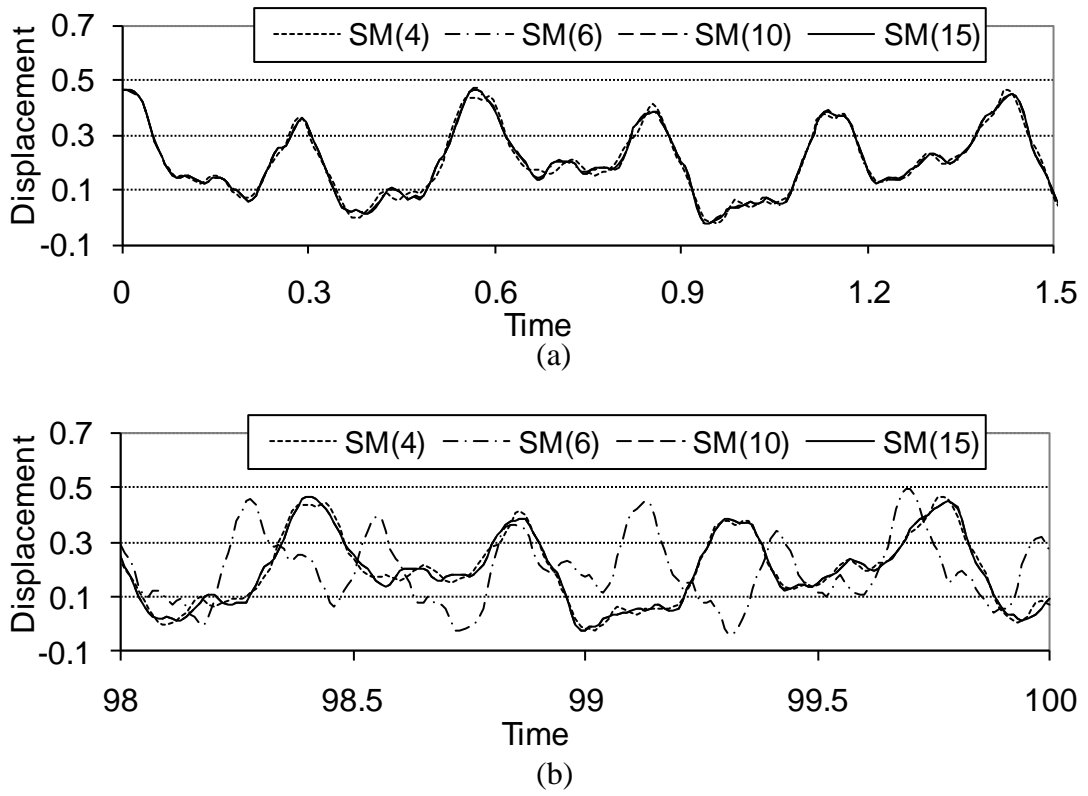
Fig. A2. 4 The transient response of the completely free rectangular plate (Φ = 1.5) at the centre, based on the Superposition Method at the time of (a) 0 to 1.5 and (b) 98 to 100.

74
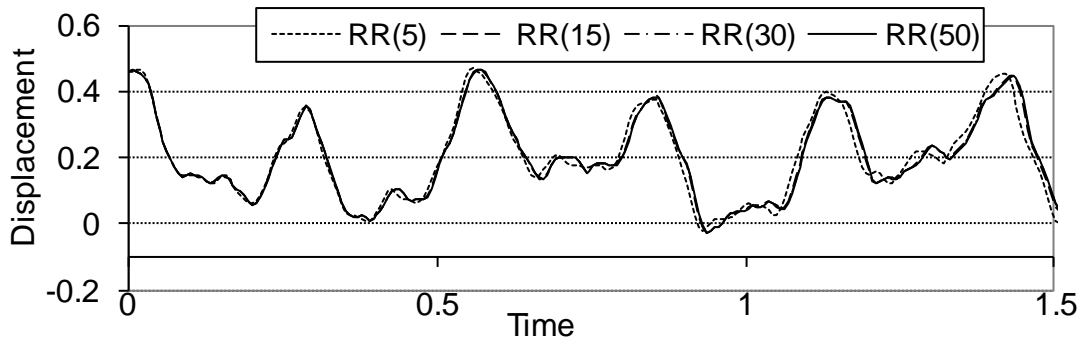
(a)
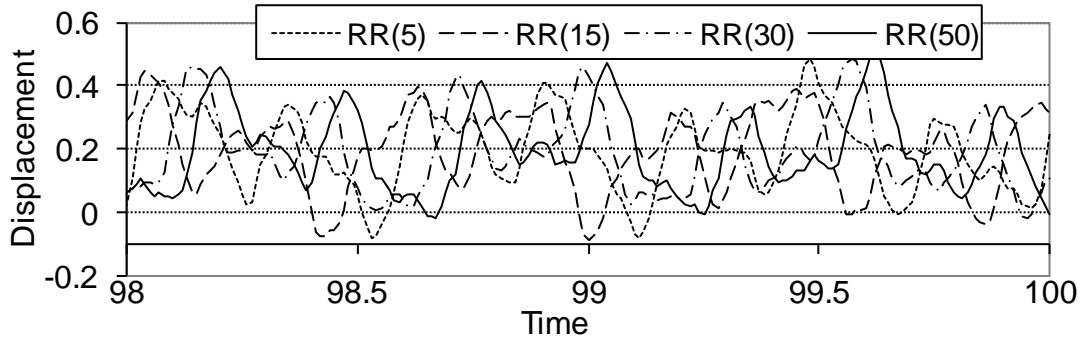
(b)

Fig. A2. 5The transient response of the completely free rectangular plate （Φ = 1.5) at the centre, based on the Rayleigh-Ritz method with the ordinary beam functions at the time of (a) 0 to 1.5 and (b) 98 to 100.
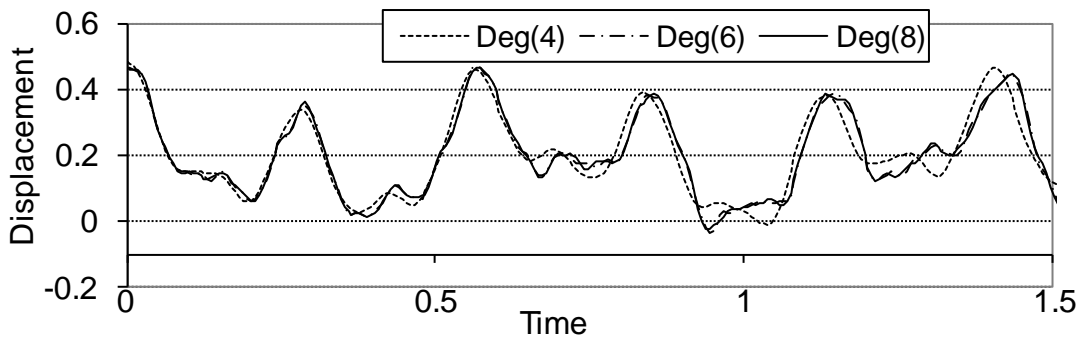
(a)
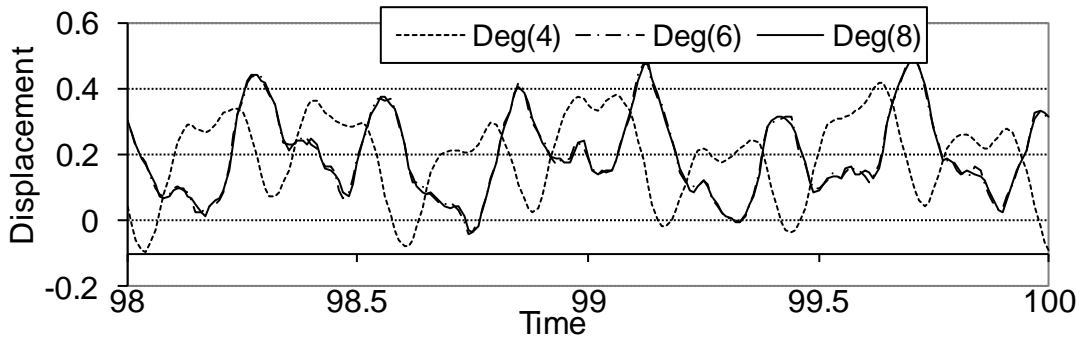
(b)

Fig. A2. 6 The transient response of the completely free rectangular plate（Φ = 1.5) at the centre, based on the Rayleigh-Ritz method with the degenerated beam functions at the time of (a) 0 to 1.5 and (b) 98 to 100.
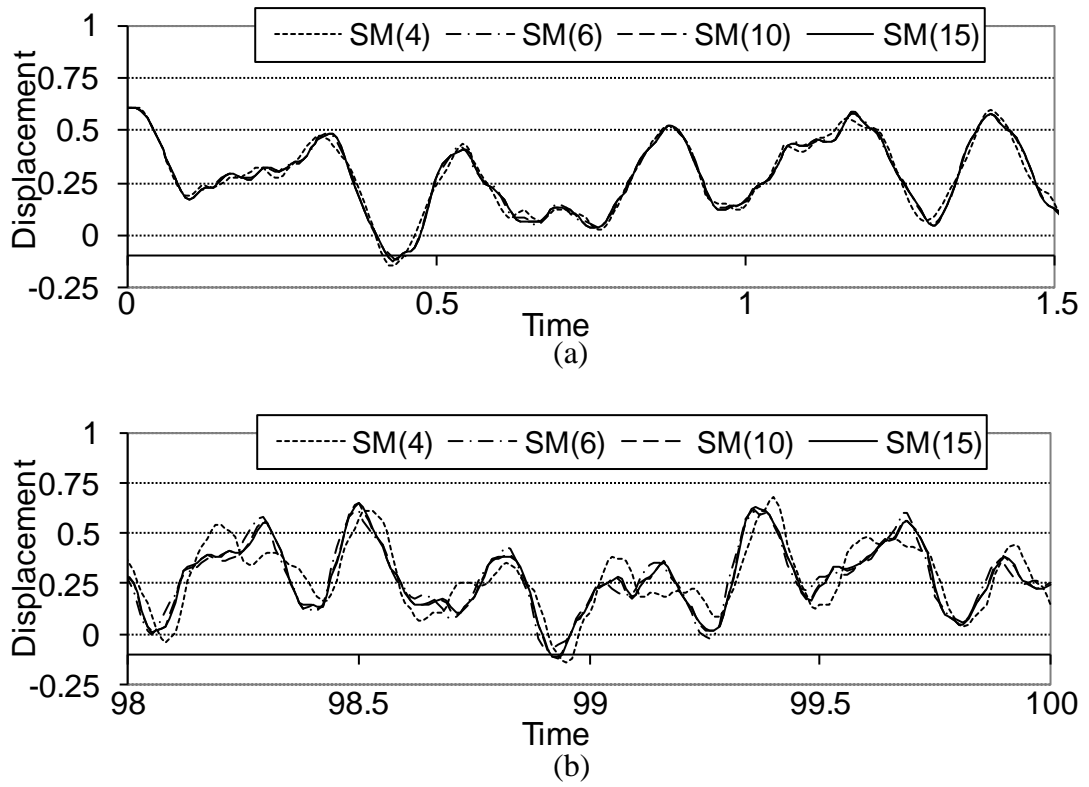
Fig. A2. 7 The transient response of the completely free rectangular plate （Φ = 2.0) at the centre, based on the Superposition Method at the time of (a) 0 to 1.5 and (b) 98 to 100.
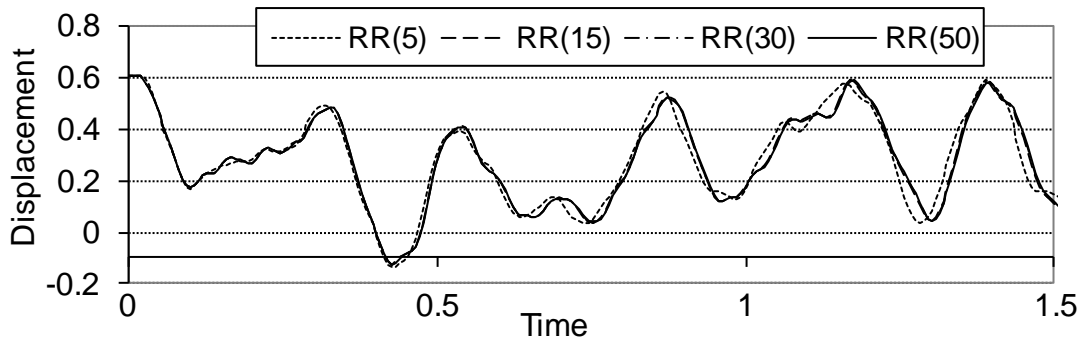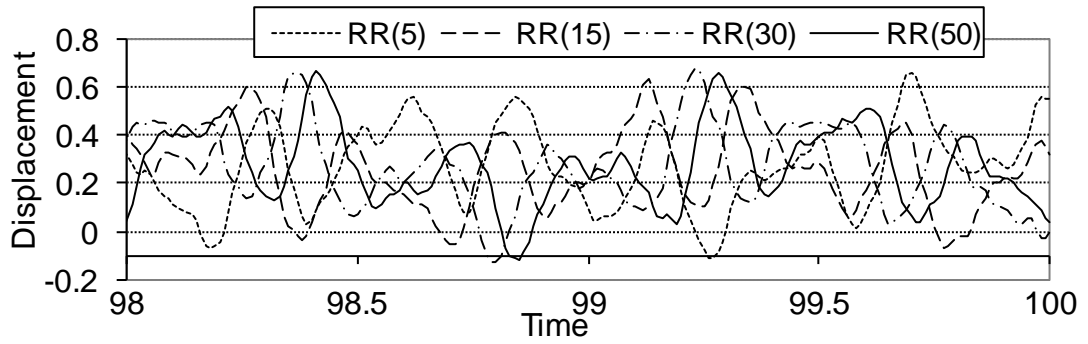
Fig. A2. 8 The transient response of the completely free rectangular plate（Φ = 2.0) at the centre, based on t the Rayleigh-Ritz method with the ordinary beam functions at the time of (a) 0 to 1.5 and (b) 98 to 100.
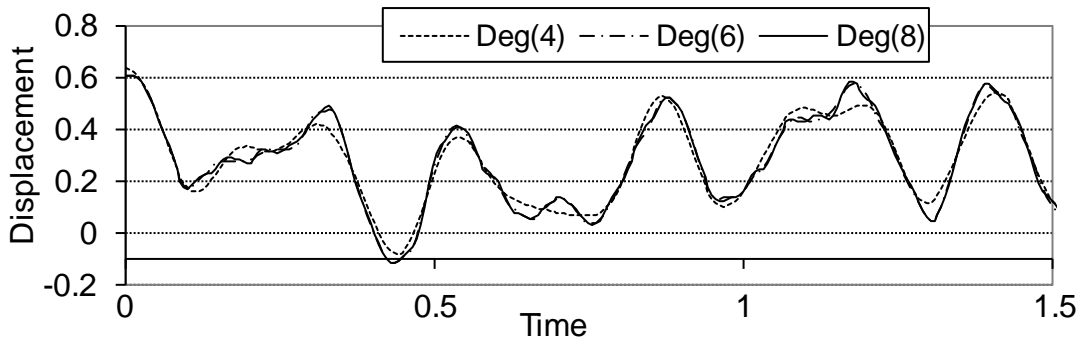
(a)
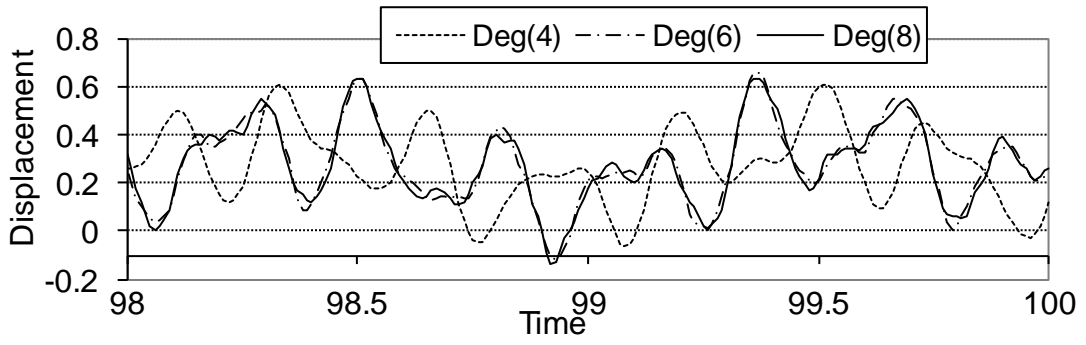
(b)

Fig. A2. 9 The transient response of the completely free rectangular plate (Φ = 2.0) at the centre, based on by the Rayleigh-Ritz method with the degenerated beam functions at the time of (a) 0 to 1.5 and (b) 98 to 100.
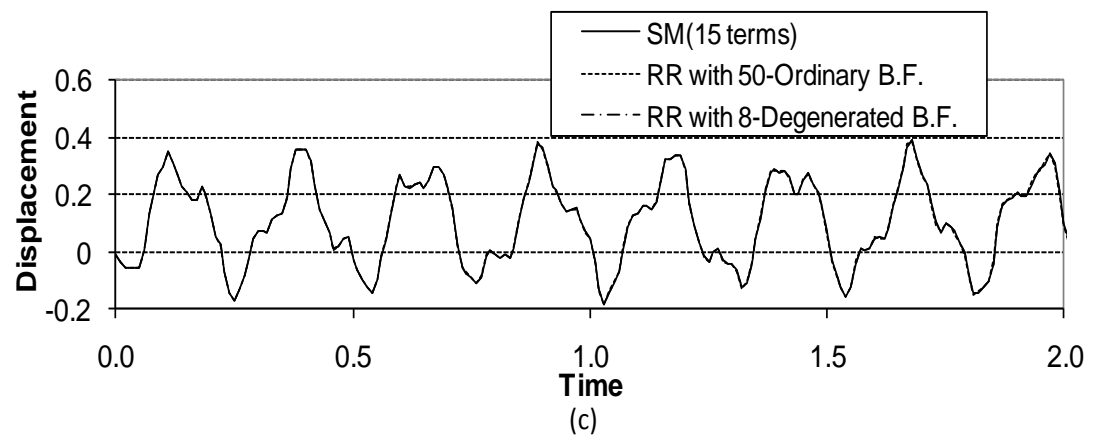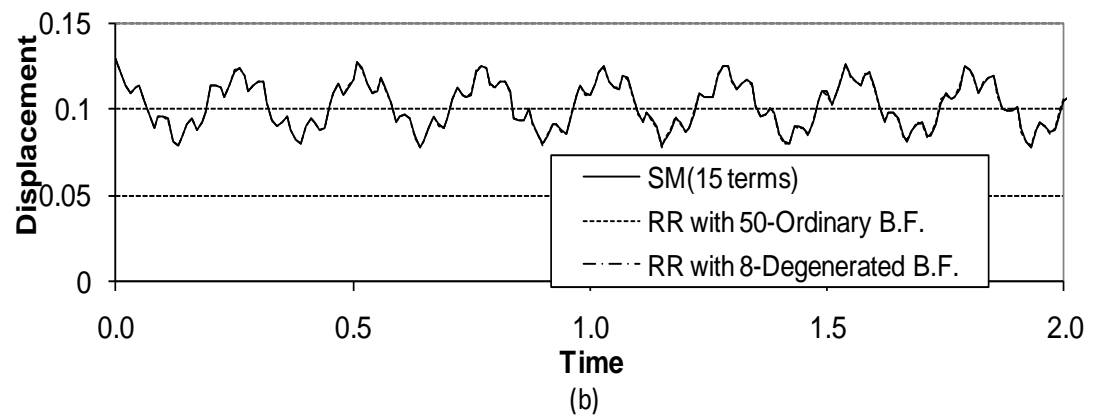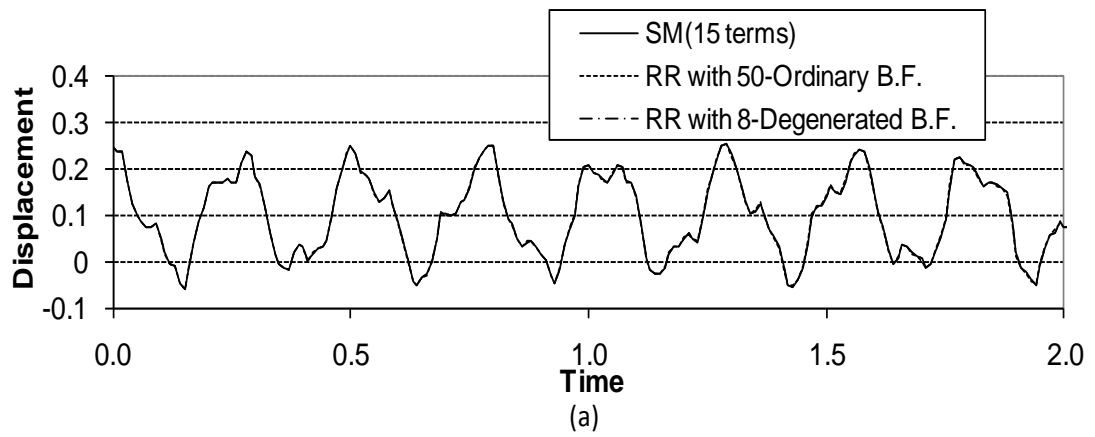
Fig. A2. 10 The transient response of the completely free square plate at (a) the centre, (b) the point *x=0.75a y=0.75*b and (c) the corner, for the duration of 0 to 2.0.
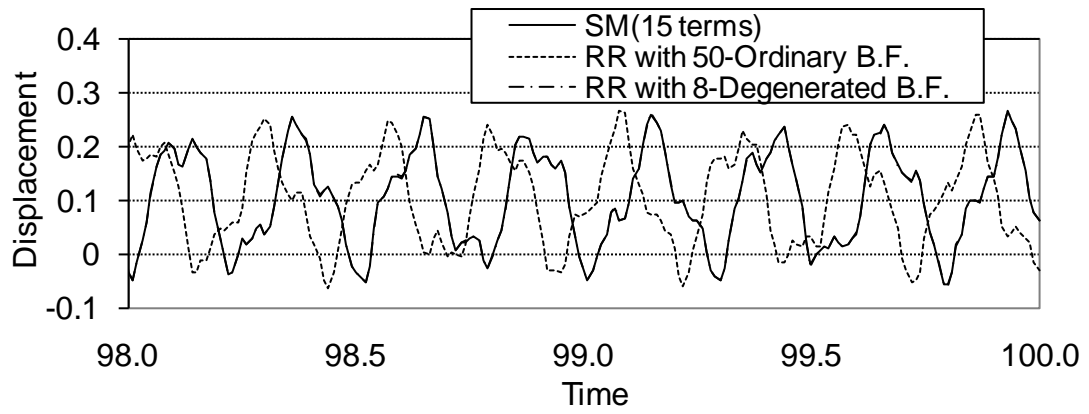
(a)
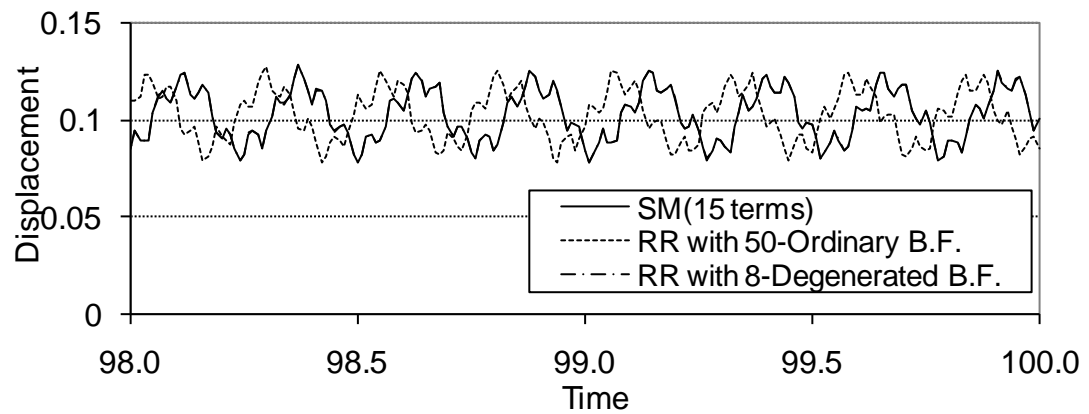
(b)
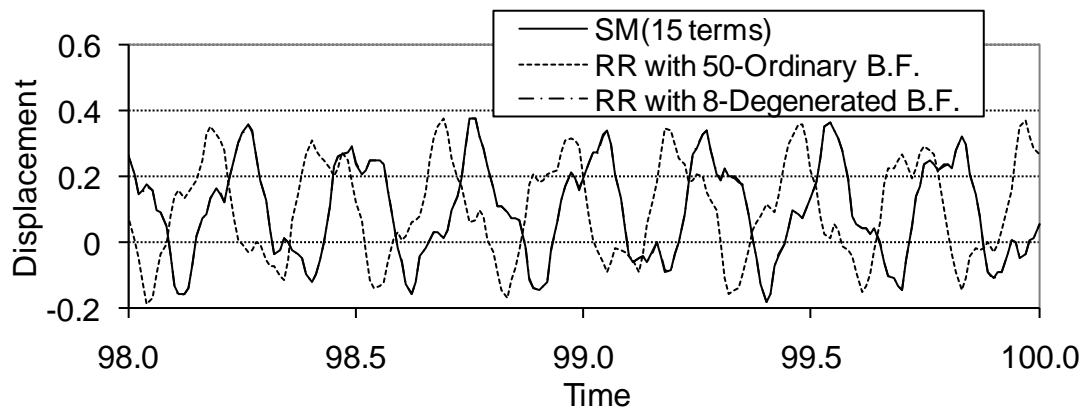
(c)

Fig. A2. 11 The transient response of the completely free square plate at (a) the centre, (b) the point *x=0.75a y=0.75b* and (c) for the duration of 98 to 100.

(a)

Displacement

0.8
0.6
0.4
0.2
0
-0.2

0.0 0.5 1.0 1.5
Time

SM(15 terms)
RR with 50-Ordinary B.F.
RR with 8-Degenerated B.F.

(a)

(b)

Displacement

0.3
0.2
0.1
0

0.0 0.5 1.0 1.5
Time

SM(15 terms)
RR with 50-Ordinary B.F.
RR with 8-Degenerated B.F.

(b)

(c)

Displacement

1.2
1
0.8
0.6
0.4
0.2
0
-0.2

0.0 0.5 1.0 1.5
Time

SM(15 terms)
RR with 50-Ordinary B.F.
RR with 8-Degenerated B.F.

(c)
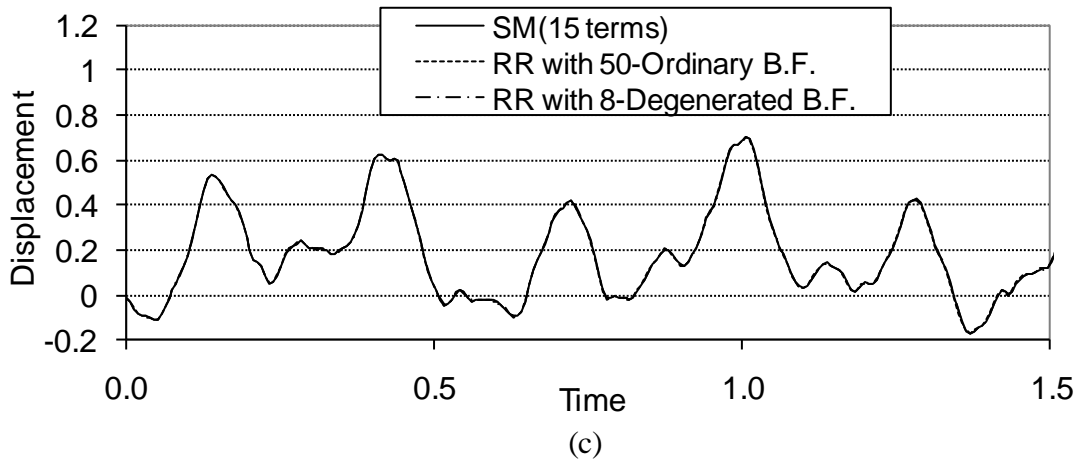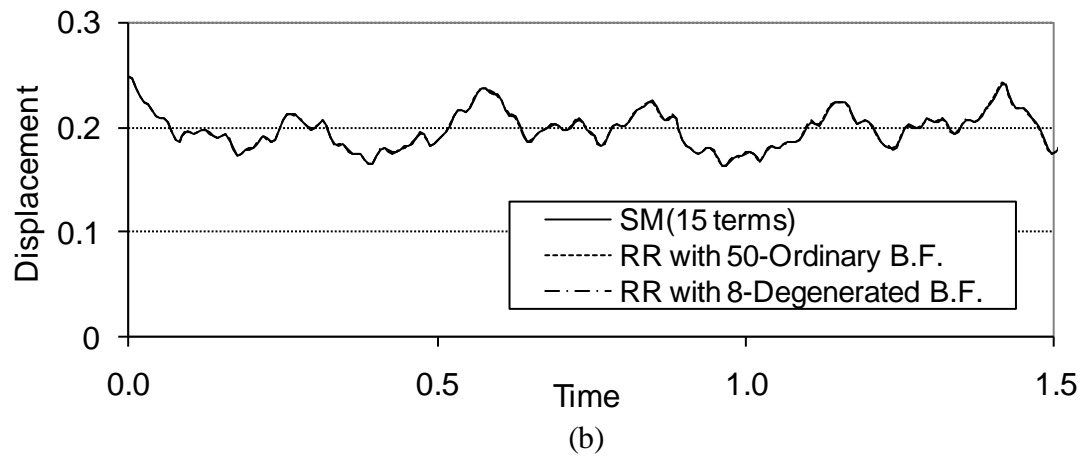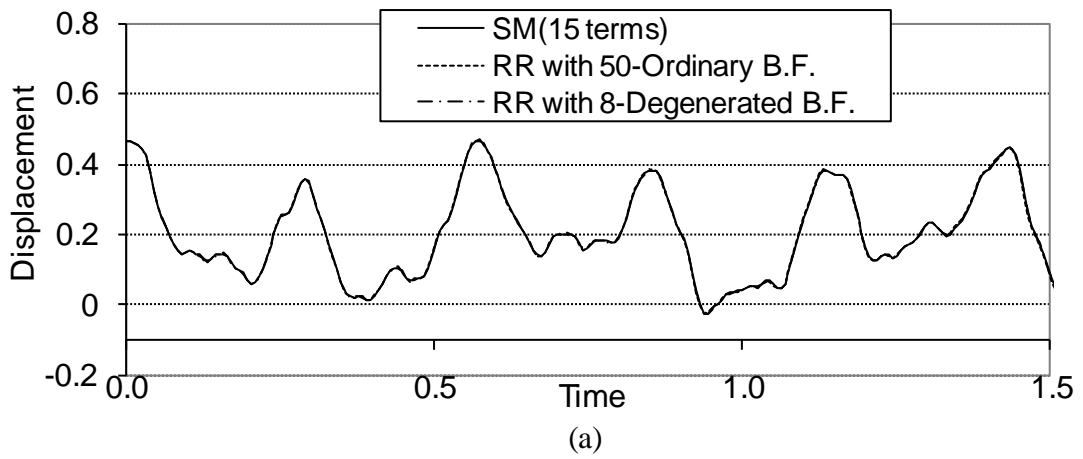
Fig. A2. 12 The transient response of the completely free rectangular plate (Φ = 1.5) at (a) the centre, (b) the point *x=0.75a y=0.75b* and (c) the corner, for the duration of 0 to 1.5.

(a)

(b)

(c)
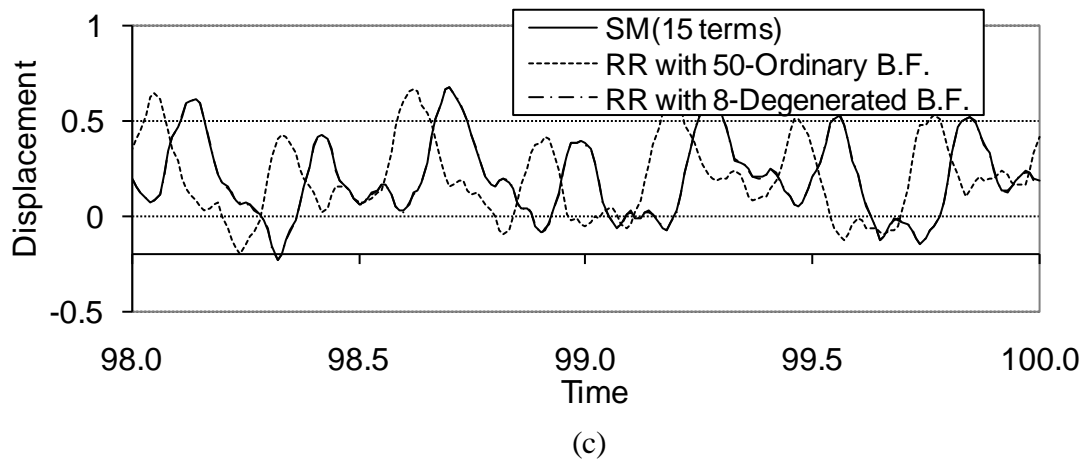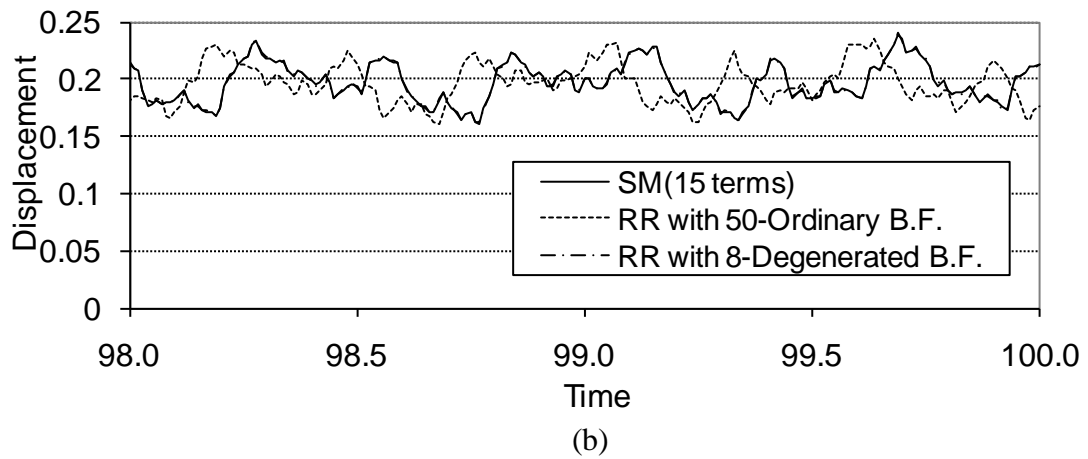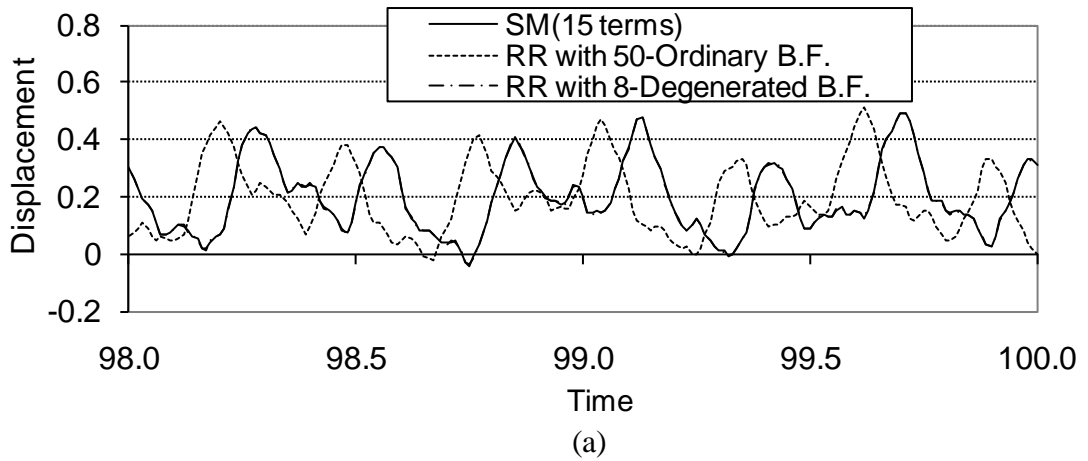
Fig. A2. 13 The transient response of the completely free rectangular plate (Φ = 1.5) at (a) the centre, (b) the point *x=0.75a y=0.75b* and (c) for the duration of 98 to 100.
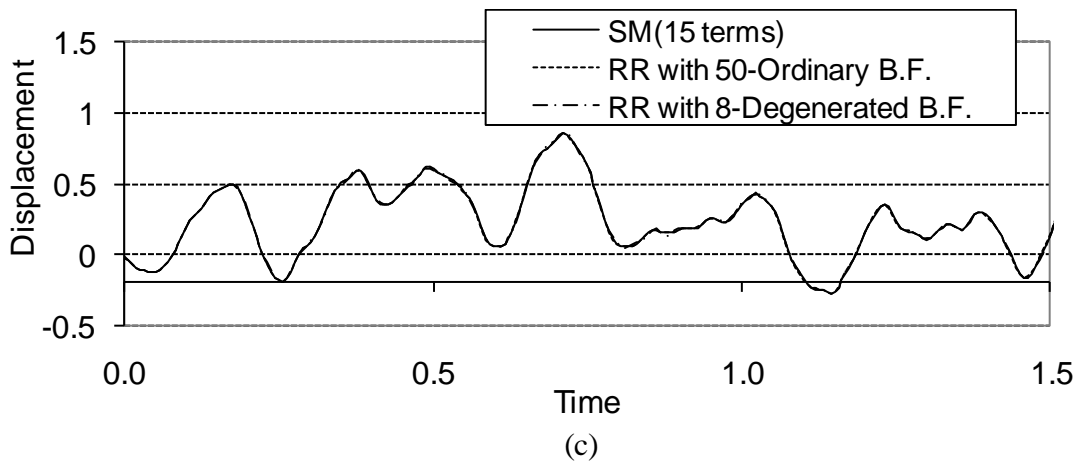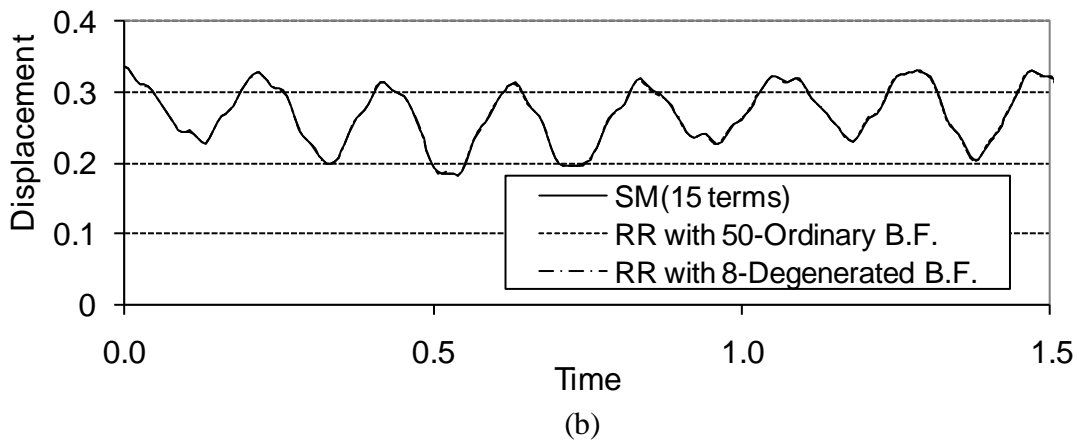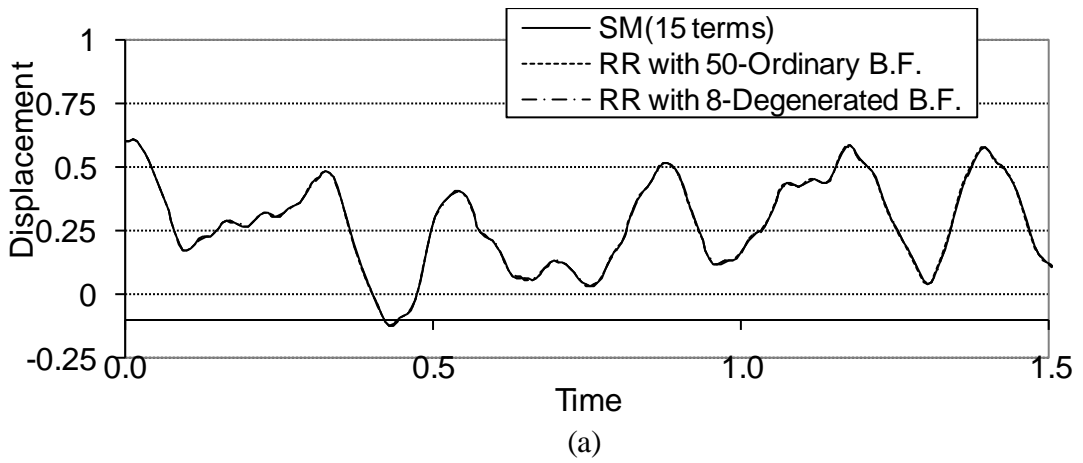
Fig. A2. 14 The transient response of the completely free rectangular plate (Φ = 2.0) at (a) the centre, (b) the point *x=0.75a y=0.75b* and (c) the corner, for the duration of 0 to 1.5.
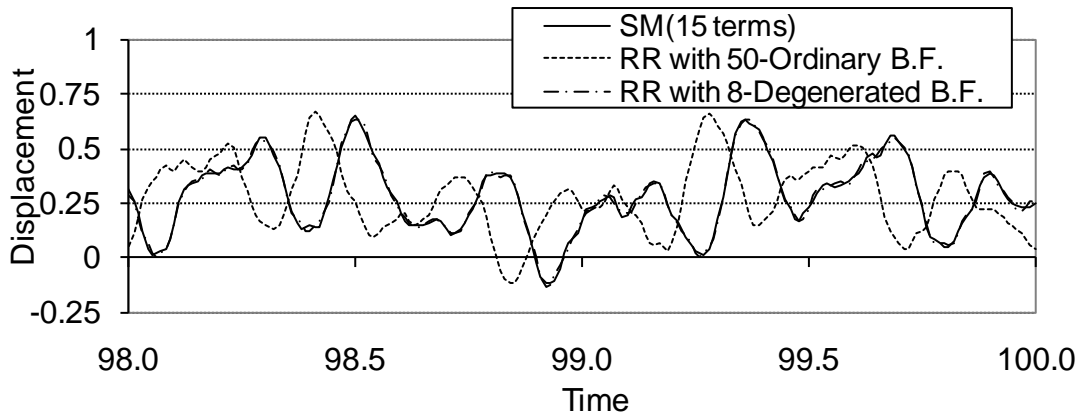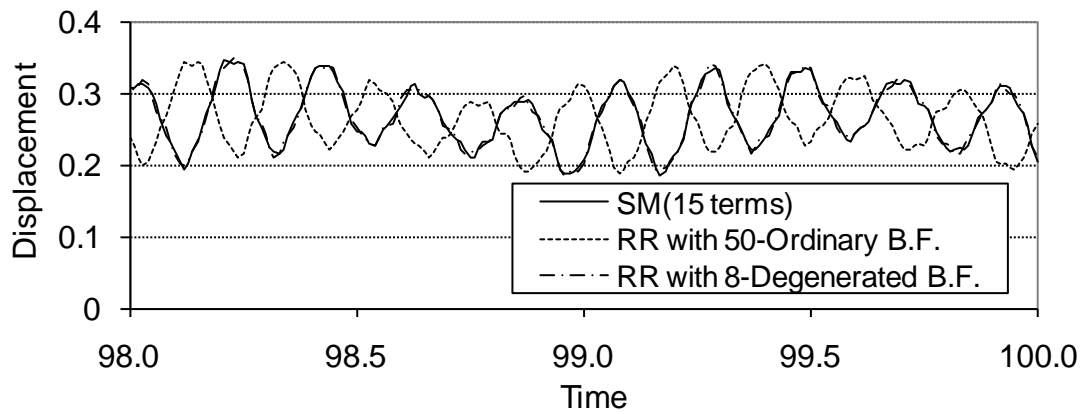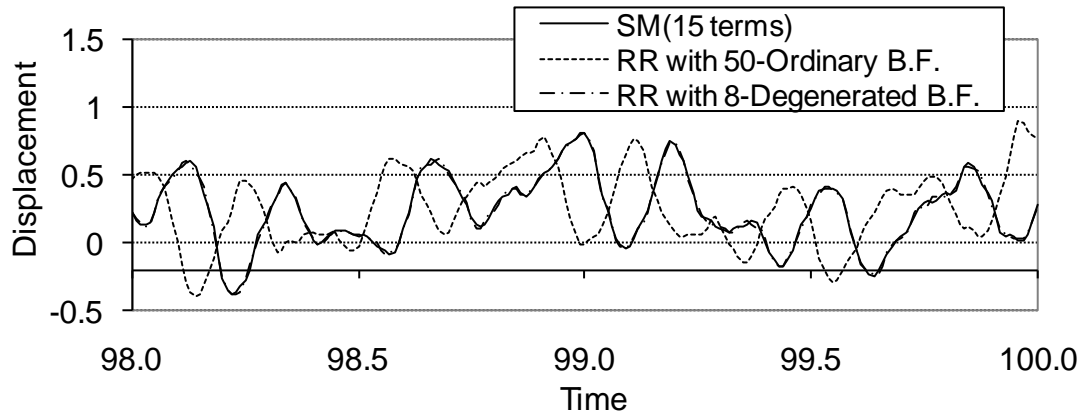
Fig. A2. 15 The transient response of the completely free rectangular plate (Φ = 1.5) at (a) the centre, (b) the point *x=0.75a y=0.75b* and (c) for the duration of 98 to 100.

Appendix III: Convergence study for the natural frequency parameters of the shallow shells

Table A3. 1 Convergence study for the natural frequency parameters of the CSCS cylindrical shallow shell on the square planform (Φ= 1.0, $R_y/R_x = 0$)

	k	Ω_1	Ω_2	Ω_3	Ω_4	Ω_5	Ω_6	Ω_7	Ω_8	Ω_9	Ω_{10}	Ω_{11}	Ω_{12}
$a/R_x = 0.1$	3	34.03	55.51	74.27	96.14	102.3	132.5	140.6	156.5		200.5		210.7
	4	34.03	55.51	74.27	96.14	102.3	132.5	140.6	156.5	170.4	200.5	206.8	210.7
	5	34.03	55.51	74.27	96.14	102.3	132.5	140.6	156.5	170.4	200.5	206.8	210.7
	6	34.03	55.51	74.27	96.14	102.3	132.5	140.6	156.5	170.4	200.5	206.8	210.7
	7	34.03	55.51	74.27	96.14	102.3	132.5	140.6	156.5	170.4	200.5	206.8	210.7
	8	34.03	55.51	74.27	96.14	102.3	132.5	140.6	156.5	170.4	200.5	206.8	210.7
	9	34.03	55.51	74.27	96.14	102.3	132.5	140.6	156.5	170.4	200.5	206.8	210.7
	10	34.03	55.51	74.27	96.14	102.3	132.5	140.6	156.5	170.4	200.5	206.8	210.7
	11	34.03	55.51	74.27	96.14	102.3	132.5	140.6	156.5	170.4	200.5	206.8	210.7
	12	34.03	55.51	74.27	96.14	102.3	132.5	140.6	156.5	170.4	200.5	206.8	210.7
$a/R_x = 0.3$	3	60.66	61.31	103.5	105.7	107.9	144.3	156.9	169.6		206.2		228.2
	4	60.66	61.31	103.5	105.7	107.9	144.3	156.9	169.6	170.6	206.2	208.0	228.2
	5	60.66	61.31	103.5	105.7	107.9	144.3	156.9	169.6	170.6	206.2	208.0	228.2
	6	60.66	61.31	103.5	105.7	107.9	144.3	156.9	169.6	170.6	206.2	208.0	228.2
	7	60.66	61.31	103.5	105.7	107.9	144.3	156.9	169.6	170.6	206.2	208.0	228.2
	8	60.66	61.31	103.5	105.7	107.9	144.3	156.9	169.6	170.6	206.2	208.0	228.2
	9	60.66	61.31	103.5	105.7	107.9	144.3	156.9	169.6	170.6	206.2	208.0	228.2
	10	60.66	61.31	103.5	105.7	107.9	144.3	156.9	169.6	170.6	206.2	208.0	228.2
	11	60.66	61.31	103.5	105.7	107.9	144.3	156.9	169.6	170.6	206.2	208.0	228.2
	12	60.66	61.31	103.5	105.7	107.9	144.3	156.9	169.6	170.6	206.2	208.0	228.2

Table A3. 2 Convergence study for the natural frequency parameters of the CSCS cylindrical shallow shell on the square planform ($\Phi=$ 1.0, $R_y/R_x = 0$) -continued

	k	Ω_1	Ω_2	Ω_3	Ω_4	Ω_5	Ω_6	Ω_7	Ω_8	Ω_9	Ω_{10}	Ω_{11}	Ω_{12}
$a/R_x = 0.5$	3	71.32	92.63	105.7	127.9	149.8	151.3	193.1	196.9			217.2	259.8
	4	71.32	92.63	105.7	127.9	149.8	151.3	171.1	193.1	196.9	210.3	217.2	259.8
	5	71.32	92.63	105.7	127.9	149.8	151.3	171.1	193.1	196.9	210.3	217.2	258.8
	6	71.32	92.63	105.7	127.9	149.8	151.3	171.1	193.1	196.9	210.3	217.2	258.8
	7	71.32	92.63	105.7	127.9	149.8	151.3	171.1	193.1	196.9	210.3	217.2	258.8
	8	71.32	92.63	105.7	127.9	149.8	151.3	171.1	193.1	196.9	210.3	217.2	258.8
	9	71.32	92.63	105.7	127.9	149.8	151.3	171.1	193.1	196.9	210.3	217.2	258.8
	10	71.32	92.63	105.7	127.9	149.8	151.3	171.1	193.1	196.9	210.3	217.2	258.8
	11	71.32	92.63	105.7	127.9	149.8	151.3	171.1	193.1	196.9	210.3	217.2	258.8
	12	71.32	92.63	105.7	127.9	149.8	151.3	171.1	193.1	196.9	210.3	217.2	258.8

Table A3. 3 Convergence study for the natural frequency parameters of the CSCS spherical shallow shell on the square planform (Φ= 1.0, $R_y/R_x = 1$)

	k	Ω_1	Ω_2	Ω_3	Ω_4	Ω_5	Ω_6	Ω_7	Ω_8	Ω_9	Ω_{10}	Ω_{11}	Ω_{12}
$a/R_x = 0.1$	3	47.43	64.47	77.54	100.7	107.5	133.8	144.2	158.5		202.6		211.1
	4	47.43	64.47	77.54	100.7	107.5	133.8	144.2	158.5	173.5	202.6	209.3	211.1
	5	47.43	64.47	77.54	100.7	107.5	133.8	144.2	158.5	173.5	202.6	209.3	211.1
	6	47.43	64.47	77.54	100.7	107.5	133.8	144.2	158.5	173.5	202.6	209.3	211.1
	7	47.43	64.47	77.54	100.7	107.5	133.8	144.2	158.5	173.5	202.6	209.3	211.1
	8	47.43	64.47	77.54	100.7	107.5	133.8	144.2	158.5	173.5	202.6	209.3	211.1
	9	47.43	64.47	77.54	100.7	107.5	133.8	144.2	158.5	173.5	202.6	209.3	211.1
	10	47.43	64.47	77.54	100.7	107.5	133.8	144.2	158.5	173.5	202.6	209.3	211.1
	11	47.43	64.47	77.54	100.7	107.5	133.8	144.2	158.5	173.5	202.6	209.3	211.1
	12	47.43	64.47	77.54	100.7	107.5	133.8	144.2	158.5	173.5	202.6	209.3	211.1
$a/R_x = 0.3$	3	114.9	115.7	125.0	140.1	143.0	167.3	173.0	186.2		224.2		231.8
	4	114.9	115.7	125.0	140.1	143.0	167.3	173.0	186.2	197.2	224.2	229.6	231.8
	5	114.9	115.7	125.0	140.1	143.0	167.3	173.0	186.2	197.2	224.2	229.6	231.8
	6	114.9	115.7	125.0	140.1	143.0	167.3	173.0	186.2	197.2	224.2	229.6	231.8
	7	114.9	115.7	125.0	140.1	143.0	167.3	173.0	186.2	197.2	224.2	229.6	231.8
	8	114.9	115.7	125.0	140.1	143.0	167.3	173.0	186.2	197.2	224.2	229.6	231.8
	9	114.9	115.7	125.0	140.1	143.0	167.3	173.0	186.2	197.2	224.2	229.6	231.8
	10	114.9	115.7	125.0	140.1	143.0	167.3	173.0	186.2	197.2	224.2	229.6	231.8
	11	114.9	115.7	125.0	140.1	143.0	167.3	173.0	186.2	197.2	224.2	229.6	231.8
	12	114.9	115.7	125.0	140.1	143.0	167.3	173.0	186.2	197.2	224.2	229.6	231.8

Table A3. 4 Convergence study for the natural frequency parameters of the CSCS spherical shallow shell on the square planform (Φ= 1.0, $R_y/R_x = 1$) -continued

	k	Ω_1	Ω_2	Ω_3	Ω_4	Ω_5	Ω_6	Ω_7	Ω_8	Ω_9	Ω_{10}	Ω_{11}	Ω_{12}
$a/R_x = 0.5$	3	177.6	182.8	185.8	195.2	196.1	219.2	221.7	231.8		262.1		268.2
	4	177.6	182.8	185.8	195.2	196.1	219.2	221.7	231.8	237.5	262.1	265.6	268.2
	5	177.6	182.8	185.8	195.2	196.1	219.2	221.7	231.8	237.5	262.1	265.6	268.2
	6	177.6	182.8	185.8	195.2	196.1	219.2	221.7	231.8	237.5	262.1	265.6	268.2
	7	177.6	182.8	185.8	195.2	196.1	219.2	221.7	231.8	237.5	262.1	265.6	268.2
	8	177.6	182.8	185.8	195.2	196.1	219.2	221.7	231.8	237.5	262.1	265.6	268.2
	9	177.6	182.8	185.8	195.2	196.1	219.2	221.7	231.8	237.5	262.1	265.6	268.2
	10	177.6	182.8	185.8	195.2	196.1	219.2	221.7	231.8	237.5	262.1	265.6	268.2
	11	177.6	182.8	185.8	195.2	196.1	219.2	221.7	231.8	237.5	262.1	265.6	268.2
	12	177.6	182.8	185.8	195.2	196.1	219.2	221.7	231.8	237.5	262.1	265.6	268.2

Table A3. 5 Convergence study for the natural frequency parameters of the CSCS hyperbolic-paraboloidal shallow shell on the square planform (Φ= 1.0, R_y/R_x = -1)

	k	Ω_1	Ω_2	Ω_3	Ω_4	Ω_5	Ω_6	Ω_7	Ω_8	Ω_9	Ω_{10}	Ω_{11}	Ω_{12}
$a/R_x = 0.1$	3	41.52	61.49	73.03	96.18	106.27	132.3	141.6	156.0		200.3		210.5
	4	41.52	61.49	73.03	96.18	106.27	132.3	141.6	156.0	173.0	200.3	208.0	210.5
	5	41.52	61.49	73.03	96.18	106.27	132.3	141.6	156.0	173.0	200.3	208.0	210.5
	6	41.52	61.49	73.03	96.18	106.27	132.3	141.6	156.0	173.0	200.3	208.0	210.5
	7	41.52	61.49	73.03	96.18	106.27	132.3	141.6	156.0	173.0	200.3	208.0	210.5
	8	41.52	61.49	73.03	96.18	106.27	132.3	141.6	156.0	173.0	200.3	208.0	210.5
	9	41.52	61.49	73.03	96.18	106.27	132.3	141.6	156.0	173.0	200.3	208.0	210.5
	10	41.52	61.49	73.03	96.18	106.27	132.3	141.6	156.0	173.0	200.3	208.0	210.5
	11	41.52	61.49	73.03	96.18	106.27	132.3	141.6	156.0	173.0	200.3	208.0	210.5
	12	41.52	61.49	73.03	96.18	106.27	132.3	141.6	156.0	173.0	200.3	208.0	210.5
$a/R_x = 0.3$	3	92.02	97.58	98.13	108.0	133.6	152.5	156.4	166.5		205.2		226.4
	4	92.02	97.58	98.13	108.0	133.6	152.5	156.4	166.5	192.8	205.2	218.1	226.4
	5	92.02	97.58	98.13	108.0	133.6	152.5	156.4	166.5	192.8	205.2	218.1	226.4
	6	92.02	97.58	98.13	108.0	133.6	152.5	156.4	166.5	192.8	205.2	218.1	226.4
	7	92.02	97.58	98.13	108.0	133.6	152.5	156.4	166.5	192.8	205.2	218.1	226.4
	8	92.02	97.58	98.13	108.0	133.6	152.5	156.4	166.5	192.8	205.2	218.1	226.4
	9	92.02	97.58	98.13	108.0	133.6	152.5	156.4	166.5	192.8	205.2	218.1	226.4
	10	92.02	97.58	98.13	108.0	133.6	152.5	156.4	166.5	192.8	205.2	218.1	226.4
	11	92.02	97.58	98.13	108.0	133.6	152.5	156.4	166.5	192.8	205.2	218.1	226.4
	12	92.02	97.58	98.13	108.0	133.6	152.5	156.4	166.5	192.8	205.2	218.1	226.4

Table A3. 6 Convergence study for the natural frequency parameters of the CSCS hyperbolic-paraboloidal shallow shell on the square planform (Φ= 1.0, R_y/R_x = -1) -continued

	k	Ω_1	Ω_2	Ω_3	Ω_4	Ω_5	Ω_6	Ω_7	Ω_8	Ω_9	Ω_{10}	Ω_{11}	Ω_{12}
$a/R_x = 0.5$	3	127.9	133.3	135.9	142.7	170.7	171.0	192.8	199.0	218.4			255.3
	4	127.9	133.3	135.9	142.7	170.7	171.0	192.8	199.0	218.4	226.0	236.3	255.3
	5	127.9	133.3	135.9	142.7	170.7	171.0	192.8	199.0	218.4	226.0	236.3	255.3
	6	127.9	133.3	135.9	142.7	170.7	171.0	192.8	199.0	218.4	226.0	236.3	255.3
	7	127.9	133.3	135.9	142.7	170.7	171.0	192.8	199.0	218.4	226.0	236.3	255.3
	8	127.9	133.3	135.9	142.7	170.7	171.0	192.8	199.0	218.4	226.0	236.3	255.3
	9	127.9	133.3	135.9	142.7	170.7	171.0	192.8	199.0	218.4	226.0	236.3	255.3
	10	127.9	133.3	135.9	142.7	170.7	171.0	192.8	199.0	218.4	226.0	236.3	255.3
	11	127.9	133.3	135.9	142.7	170.7	171.0	192.8	199.0	218.4	226.0	236.3	255.3
	12	127.9	133.3	135.9	142.7	170.7	171.0	192.8	199.0	218.4	226.0	236.3	255.3

Table A3. 7 Convergence study for the natural frequency parameters of the CCSS cylindrical shallow shell on the square planform (Φ= 1.0, $R_y/R_x = 0$)

	k	Ω_1	Ω_2	Ω_3	Ω_4	Ω_5	Ω_6	Ω_7	Ω_8	Ω_9	Ω_{10}	Ω_{11}	Ω_{12}
$a/R_x = 0.1$	3	34.45	62.00	66.69	94.75	114.8	118.4	146.1	147.5	187.5	190.0	197.7	215.3
	4	34.45	62.01	66.71	94.83	114.9	118.5	146.5	147.8	188.5	191.0	198.7	219.2
	5	34.45	62.02	66.71	94.85	114.9	118.5	146.5	147.9	188.6	191.1	198.8	219.4
	6	34.45	62.02	66.71	94.85	114.9	118.5	146.5	147.9	188.6	191.1	198.9	219.5
	7	34.45	62.02	66.71	94.86	114.9	118.5	146.5	147.9	188.6	191.1	198.9	219.5
	8	34.45	62.02	66.71	94.86	114.9	118.5	146.5	147.9	188.6	191.1	198.9	219.5
	9	34.45	62.02	66.71	94.86	114.9	118.5	146.5	147.9	188.6	191.1	198.9	219.5
	10	34.45	62.02	66.71	94.86	114.9	118.5	146.5	147.9	188.6	191.1	198.9	219.5
	11	34.45	62.02	66.71	94.86	114.9	118.5	146.5	147.9	188.6	191.1	198.9	219.5
	12	34.45	62.02	66.71	94.86	114.9	118.5	146.5	147.9	188.6	191.1	198.9	219.5
$a/R_x = 0.3$	3	59.36	78.76	99.85	111.7	118.1	145.7	151.5	162.5	188.4	204.2	209.5	217.6
	4	59.37	78.77	99.85	111.8	118.2	145.7	152.0	162.9	189.4	205.6	210.4	221.1
	5	59.37	78.77	99.85	111.8	118.3	145.7	152.1	162.9	189.5	205.7	210.5	221.5
	6	59.37	78.78	99.86	111.8	118.3	145.7	152.1	163.0	189.5	205.8	210.5	221.5
	7	59.37	78.78	99.86	111.8	118.3	145.7	152.1	163.0	189.5	205.8	210.5	221.5
	8	59.37	78.78	99.86	111.8	118.3	145.7	152.1	163.0	189.5	205.8	210.5	221.5
	9	59.37	78.78	99.86	111.8	118.3	145.7	152.1	163.0	189.5	205.8	210.5	221.5
	10	59.37	78.78	99.86	111.8	118.3	145.7	152.1	163.0	189.5	205.8	210.5	221.5
	11	59.37	78.78	99.86	111.8	118.3	145.7	152.1	163.0	189.5	205.8	210.5	221.5
	12	59.37	78.78	99.86	111.8	118.3	145.7	152.1	163.0	189.5	205.8	210.5	221.5

Table A3. 8 Convergence study for the natural frequency parameters of the CCSS cylindrical shallow shell on the square planform (Φ= 1.0, $R_y/R_x = 0$) -continued

	k	Ω_1	Ω_2	Ω_3	Ω_4	Ω_5	Ω_6	Ω_7	Ω_8	Ω_9	Ω_{10}	Ω_{11}	Ω_{12}
$a/R_x = 0.5$	3	72.35	105.5	127.2	132.8	147.4	167.7	184.6	190.9	191.7	217.4	222.6	243.6
	4	72.37	105.5	127.2	133.0	147.5	168.5	184.6	191.8	192.0	219.4	225.7	244.5
	5	72.37	105.5	127.2	133.0	147.5	168.6	184.6	191.9	192.1	219.6	226.1	244.5
	6	72.37	105.5	127.2	133.0	147.5	168.6	184.6	191.9	192.1	219.6	226.2	244.5
	7	72.37	105.5	127.2	133.0	147.5	168.6	184.6	191.9	192.1	219.7	226.2	244.5
	8	72.37	105.5	127.2	133.0	147.5	168.6	184.6	191.9	192.1	219.7	226.2	244.5
	9	72.37	105.5	127.2	133.0	147.5	168.6	184.6	191.9	192.1	219.7	226.2	244.5
	10	72.37	105.5	127.2	133.0	147.5	168.6	184.6	191.9	192.1	219.7	226.2	244.5
	11	72.37	105.5	127.2	133.0	147.5	168.6	184.6	191.9	192.1	219.7	226.2	244.5
	12	72.37	105.5	127.2	133.0	147.5	168.6	184.6	191.9	192.1	219.7	226.2	244.5

Table A3. 9 Convergence study for the natural frequency parameters of the CCSS spherical shallow shell on the square planform ($\Phi = 1.0$, $R_y/R_x = 1$)

	k	Ω_1	Ω_2	Ω_3	Ω_4	Ω_5	Ω_6	Ω_7	Ω_8	Ω_9	Ω_{10}	Ω_{11}	Ω_{12}
$a/R_x = 0.1$	3	45.18	69.57	70.34	98.96	119.4	119.6	149.2	149.6	190.2	190.6	199.8	217.3
	4	45.19	69.57	70.37	99.03	119.4	119.7	149.7	149.9	191.4	191.4	200.7	221.4
	5	45.19	69.57	70.38	99.05	119.4	119.7	149.7	150.0	191.4	191.5	200.9	221.7
	6	45.19	69.57	70.38	99.05	119.4	119.8	149.7	150.0	191.4	191.6	200.9	221.7
	7	45.19	69.57	70.38	99.05	119.4	119.8	149.7	150.0	191.4	191.6	200.9	221.7
	8	45.19	69.57	70.38	99.05	119.4	119.8	149.7	150.0	191.4	191.6	200.9	221.7
	9	45.19	69.57	70.38	99.05	119.4	119.8	149.7	150.0	191.4	191.6	200.9	221.7
	10	45.19	69.57	70.38	99.06	119.4	119.8	149.7	150.0	191.4	191.6	200.9	221.7
	11	45.19	69.57	70.38	99.06	119.4	119.8	149.7	150.1	191.4	191.6	200.9	221.7
	12	45.19	69.57	70.38	99.06	119.4	119.8	149.7	150.1	191.4	191.6	200.9	221.7
$a/R_x = 0.3$	3	108.3	119.1	123.6	139.1	153.0	154.7	177.7	178.1	212.5	213.4	221.5	237.1
	4	108.3	119.1	123.6	139.1	153.0	154.9	177.8	178.8	213.6	214.2	222.6	241.3
	5	108.3	119.1	123.6	139.1	153.0	154.9	177.8	178.8	213.6	214.3	222.7	241.4
	6	108.3	119.1	123.6	139.1	153.0	154.9	177.8	178.9	213.6	214.3	222.7	241.4
	7	108.3	119.1	123.6	139.1	153.0	154.9	177.8	178.9	213.6	214.3	222.7	241.4
	8	108.3	119.1	123.6	139.1	153.0	154.9	177.8	178.9	213.6	214.3	222.8	241.4
	9	108.3	119.1	123.6	139.1	153.0	154.9	177.8	178.9	213.6	214.3	222.8	241.4
	10	108.3	119.1	123.6	139.1	153.0	154.9	177.8	178.9	213.6	214.3	222.8	241.4
	11	108.3	119.1	123.6	139.1	153.0	154.9	177.8	178.9	213.6	214.3	222.8	241.4
	12	108.3	119.1	123.6	139.1	153.0	154.9	177.8	178.9	213.6	214.3	222.8	241.4

Table A3. 10 Convergence study for the natural frequency parameters of the CCSS spherical shallow shell on the square planform ($\Phi=$ 1.0, $R_y/R_x = 1$) -continued

	k	Ω_1	Ω_2	Ω_3	Ω_4	Ω_5	Ω_6	Ω_7	Ω_8	Ω_9	Ω_{10}	Ω_{11}	Ω_{12}
$a/R_x = 0.5$	3	171.6	180.3	187.0	195.3	204.0	210.0	223.4	225.1	251.0	253.4	259.6	272.3
	4	171.6	180.3	187.0	195.3	204.0	210.1	223.5	225.9	252.1	254.1	260.7	276.4
	5	171.6	180.3	187.0	195.3	204.1	210.1	223.5	226.0	252.1	254.2	260.9	276.4
	6	171.6	180.3	187.0	195.3	204.1	210.1	223.5	226.0	252.1	254.2	260.9	276.5
	7	171.6	180.3	187.0	195.3	204.1	210.1	223.5	226.0	252.1	254.2	260.9	276.5
	8	171.6	180.3	187.0	195.3	204.1	210.1	223.5	226.0	252.1	254.2	260.9	276.5
	9	171.6	180.3	187.0	195.3	204.1	210.1	223.5	226.0	252.1	254.2	260.9	276.5
	10	171.6	180.3	187.0	195.3	204.1	210.1	223.5	226.0	252.1	254.2	260.9	276.5
	11	171.6	180.3	187.0	195.3	204.1	210.1	223.5	226.0	252.1	254.2	260.9	276.5
	12	171.6	180.3	187.0	195.3	204.1	210.1	223.5	226.0	252.1	254.2	260.9	276.5

Table A3. 11 Convergence study for the natural frequency parameters of the CCSS hyperbolic-paraboloidal shallow shell on the square planform ($\Phi= 1.0$, $R_y/R_x = -1$)

	k	Ω_1	Ω_2	Ω_3	Ω_4	Ω_5	Ω_6	Ω_7	Ω_8	Ω_9	Ω_{10}	Ω_{11}	Ω_{12}
$a/R_x = 0.1$	3	35.59	65.68	65.83	94.49	117.9	118.0	146.5	147.0	189.6	189.9	197.4	215.7
	4	35.59	65.71	65.83	94.58	118.0	118.1	147.1	147.2	190.7	190.8	198.4	220.3
	5	35.59	65.72	65.83	94.60	118.0	118.1	147.1	147.3	190.8	190.9	198.5	220.4
	6	35.59	65.72	65.83	94.60	118.0	118.1	147.1	147.3	190.8	190.9	198.6	220.4
	7	35.59	65.72	65.83	94.60	118.0	118.1	147.1	147.3	190.8	190.9	198.6	220.4
	8	35.59	65.72	65.83	94.60	118.0	118.1	147.1	147.3	190.8	190.9	198.6	220.4
	9	35.59	65.72	65.83	94.60	118.0	118.1	147.1	147.3	190.8	190.9	198.6	220.4
	10	35.59	65.72	65.83	94.61	118.0	118.1	147.1	147.3	190.8	190.9	198.6	220.4
	11	35.59	65.72	65.83	94.61	118.0	118.1	147.1	147.3	190.8	190.9	198.6	220.4
	12	35.59	65.72	65.83	94.61	118.0	118.1	147.1	147.3	190.8	190.9	198.6	220.4
$a/R_x = 0.3$	3	69.31	92.45	97.59	112.5	141.6	142.1	156.6	158.1	201.1	207.1	207.9	223.9
	4	69.31	92.45	97.59	112.7	141.6	142.1	157.7	158.2	203.2	208.5	208.7	229.1
	5	69.31	92.45	97.60	112.7	141.7	142.1	157.8	158.2	203.4	208.6	208.7	229.7
	6	69.31	92.45	97.60	112.7	141.7	142.1	157.9	158.2	203.4	208.7	208.7	229.8
	7	69.31	92.45	97.60	112.7	141.7	142.1	157.9	158.2	203.4	208.7	208.7	229.8
	8	69.31	92.45	97.60	112.7	141.7	142.1	157.9	158.2	203.4	208.7	208.7	229.8
	9	69.31	92.45	97.60	112.7	141.7	142.1	157.9	158.2	203.4	208.7	208.8	229.8
	10	69.31	92.45	97.60	112.7	141.7	142.1	157.9	158.2	203.4	208.7	208.8	229.8
	11	69.31	92.45	97.60	112.7	141.7	142.1	157.9	158.2	203.4	208.7	208.8	229.8
	12	69.31	92.45	97.60	112.7	141.7	142.1	157.9	158.2	203.4	208.7	208.8	229.8

Table A3. 12 Convergence study for the natural frequency parameters of the CCSS hyperbolic-paraboloidal shallow shell on the square planform ($\Phi= 1.0$, $R_y/R_x = -1$) -continued

	k	Ω_1	Ω_2	Ω_3	Ω_4	Ω_5	Ω_6	Ω_7	Ω_8	Ω_9	Ω_{10}	Ω_{11}	Ω_{12}
$a/R_x = 0.5$	3	94.15	122.4	136.9	149.2	172.9	173.0	182.2	187.0	211.5	238.0	238.8	240.0
	4	94.17	122.4	137.0	149.2	173.0	173.6	183.1	187.1	215.8	239.0	239.3	247.1
	5	94.18	122.4	137.0	149.2	173.0	173.6	183.1	187.1	216.2	239.0	239.3	247.7
	6	94.18	122.4	137.0	149.2	173.0	173.6	183.1	187.1	216.2	239.0	239.3	247.8
	7	94.18	122.4	137.0	149.2	173.0	173.6	183.1	187.1	216.3	239.0	239.3	247.8
	8	94.18	122.4	137.0	149.2	173.0	173.6	183.1	187.1	216.3	239.0	239.3	247.8
	9	94.18	122.4	137.0	149.2	173.0	173.6	183.1	187.1	216.3	239.0	239.3	247.8
	10	94.18	122.4	137.0	149.2	173.0	173.6	183.1	187.1	216.3	239.0	239.3	247.8
	11	94.18	122.4	137.0	149.2	173.0	173.6	183.1	187.1	216.3	239.0	239.3	247.8
	12	94.18	122.4	137.0	149.2	173.0	173.6	183.1	187.1	216.3	239.0	239.3	247.8

Table A3. 13 Convergence study for the natural frequency parameters of the CCCC cylindrical shallow shell on the square planform (Φ= 1.0, $R_y/R_x = 0$)

	k	Ω_1	Ω_2	Ω_3	Ω_4	Ω_5	Ω_6	Ω_7	Ω_8	Ω_9	Ω_{10}	Ω_{11}	Ω_{12}
$a/R_x = 0.1$	3	46.26	74.44	79.10	109.2	132.3	135.3	164.3	165.5	208.6	210.8	218.9	232.9
	4	46.26	74.61	79.25	110.2	132.3	135.3	165.1	166.3	210.4	212.6	218.9	242.2
	5	46.28	74.63	79.27	110.2	132.5	135.5	165.6	166.8	210.5	212.7	220.6	242.2
	6	46.28	74.64	79.28	110.3	132.5	135.5	165.7	166.8	210.6	212.8	220.6	242.7
	7	46.28	74.65	79.28	110.3	132.5	135.5	165.7	166.9	210.6	212.8	220.8	242.7
	8	46.28	74.65	79.28	110.3	132.5	135.5	165.7	166.9	210.6	212.9	220.8	242.7
	9	46.28	74.65	79.28	110.3	132.5	135.5	165.7	166.9	210.6	212.9	220.8	242.7
	10	46.28	74.65	79.28	110.3	132.5	135.5	165.7	166.9	210.6	212.9	220.8	242.7
	11	46.28	74.65	79.28	110.3	132.5	135.5	165.8	166.9	210.6	212.9	220.8	242.7
	12	46.28	74.65	79.28	110.3	132.5	135.5	165.8	166.9	210.6	212.9	220.8	242.7
$a/R_x = 0.3$	3	67.67	78.06	94.46	134.8	145.5	166.8	171.1	208.9	217.6	221.6	234.6	241.8
	4	67.67	78.25	94.57	116.3	134.8	145.5	167.6	172.1	210.8	219.6	221.6	243.2
	5	67.68	78.27	94.60	116.3	135.0	145.7	168.1	172.5	210.9	219.6	223.4	243.2
	6	67.68	78.28	94.60	116.4	135.0	145.7	168.2	172.6	211.0	219.8	223.4	243.7
	7	67.68	78.29	94.60	116.4	135.0	145.7	168.2	172.6	211.0	219.8	223.6	243.7
	8	67.68	78.29	94.61	116.4	135.0	145.7	168.3	172.6	211.0	219.8	223.6	243.8
	9	67.68	78.29	94.61	116.4	135.0	145.8	168.3	172.7	211.0	219.8	223.6	243.8
	10	67.68	78.29	94.61	116.4	135.0	145.8	168.3	172.7	211.0	219.8	223.6	243.8
	11	67.68	78.29	94.61	116.4	135.0	145.8	168.3	172.7	211.0	219.8	223.6	243.8
	12	67.68	78.29	94.61	116.4	135.0	145.8	168.3	172.7	211.0	219.8	223.6	243.8

Table A3. 14 Convergence study for the natural frequency parameters of the CCCC cylindrical shallow shell on the square planform ($\Phi= 1.0$, $R_y/R_x = 0$) -continued

	k	Ω_1	Ω_2	Ω_3	Ω_4	Ω_5	Ω_6	Ω_7	Ω_8	Ω_9	Ω_{10}	Ω_{11}	Ω_{12}
$a/R_x = 0.5$	3	98.89	118.9	149.4	156.2	172.3	190.7	201.6	205.4	211.7	240.9	242.6	260.2
	4	99.22	118.9	151.1	156.2	172.3	191.6	201.6	207.3	213.7	240.9	250.4	262.7
	5	99.25	119.0	151.1	156.3	172.5	192.3	201.7	207.6	213.8	243.2	250.4	262.8
	6	99.26	119.0	151.1	156.3	172.5	192.4	201.7	207.7	213.9	243.2	251.0	262.9
	7	99.26	119.0	151.1	156.3	172.5	192.4	201.7	207.8	213.9	243.4	251.0	262.9
	8	99.26	119.0	151.1	156.3	172.5	192.4	201.7	207.8	213.9	243.4	251.1	262.9
	9	99.26	119.0	151.1	156.3	172.5	192.4	201.7	207.8	213.9	243.4	251.1	262.9
	10	99.26	119.0	151.1	156.3	172.5	192.4	201.7	207.8	213.9	243.4	251.1	262.9
	11	99.27	119.0	151.1	156.3	172.5	192.4	201.7	207.8	213.9	243.4	251.1	262.9
	12	99.27	119.0	151.1	156.3	172.5	192.4	201.7	207.8	213.9	243.4	251.1	262.9

Table A3. 15 Convergence study for the natural frequency parameters of the CCCC spherical shallow shell on the square planform (Φ= 1.0, $R_y/R_x = 1$)

	k	Ω_1	Ω_2	Ω_3	Ω_4	Ω_5	Ω_6	Ω_7	Ω_8	Ω_9	Ω_{10}	Ω_{11}	Ω_{12}
$a/R_x = 0.1$	3	46.26	74.44	79.10	109.2	132.3	135.3	164.3	165.5	208.6	210.8	218.9	232.9
	4	46.26	74.61	79.25	110.2	132.3	135.3	165.1	166.3	210.4	212.6	218.9	242.2
	5	46.28	74.63	79.27	110.2	132.5	135.5	165.6	166.8	210.5	212.7	220.6	242.2
	6	46.28	74.64	79.28	110.3	132.5	135.5	165.7	166.8	210.6	212.8	220.6	242.7
	7	46.28	74.65	79.28	110.3	132.5	135.5	165.7	166.9	210.6	212.8	220.8	242.7
	8	46.28	74.65	79.28	110.3	132.5	135.5	165.7	166.9	210.6	212.9	220.8	242.7
	9	46.28	74.65	79.28	110.3	132.5	135.5	165.7	166.9	210.6	212.9	220.8	242.7
	10	46.28	74.65	79.28	110.3	132.5	135.5	165.7	166.9	210.6	212.9	220.8	242.7
	11	46.28	74.65	79.28	110.3	132.5	135.5	165.8	166.9	210.6	212.9	220.8	242.7
	12	46.28	74.65	79.28	110.3	132.5	135.5	165.8	166.9	210.6	212.9	220.8	242.7
$a/R_x = 0.3$	3	67.67	78.06	94.46	134.8	145.5	166.8	171.1	208.9	217.6	221.6	234.6	241.8
	4	67.67	78.25	94.57	116.3	134.8	145.5	167.6	172.1	210.8	219.6	221.6	243.2
	5	67.68	78.27	94.60	116.3	135.0	145.7	168.1	172.5	210.9	219.6	223.4	243.2
	6	67.68	78.28	94.60	116.4	135.0	145.7	168.2	172.6	211.0	219.8	223.4	243.7
	7	67.68	78.29	94.60	116.4	135.0	145.7	168.2	172.6	211.0	219.8	223.6	243.7
	8	67.68	78.29	94.61	116.4	135.0	145.7	168.3	172.6	211.0	219.8	223.6	243.8
	9	67.68	78.29	94.61	116.4	135.0	145.8	168.3	172.7	211.0	219.8	223.6	243.8
	10	67.68	78.29	94.61	116.4	135.0	145.8	168.3	172.7	211.0	219.8	223.6	243.8
	11	67.68	78.29	94.61	116.4	135.0	145.8	168.3	172.7	211.0	219.8	223.6	243.8
	12	67.68	78.29	94.61	116.4	135.0	145.8	168.3	172.7	211.0	219.8	223.6	243.8

Table A3. 16 Convergence study for the natural frequency parameters of the CCCC spherical shallow shell on the square planform (Φ= 1.0, $R_y/R_x = 1$) -continued

	k	Ω_1	Ω_2	Ω_3	Ω_4	Ω_5	Ω_6	Ω_7	Ω_8	Ω_9	Ω_{10}	Ω_{11}	Ω_{12}
$a/R_x = 0.5$	3	98.89	118.9	149.4	156.2	172.3	190.7	201.6	205.4	211.7	240.9	242.6	260.2
	4	99.22	118.9	151.1	156.2	172.3	191.6	201.6	207.3	213.7	240.9	250.4	262.7
	5	99.25	119.0	151.1	156.3	172.5	192.3	201.7	207.6	213.8	243.2	250.4	262.8
	6	99.26	119.0	151.1	156.3	172.5	192.4	201.7	207.7	213.9	243.2	251.0	262.9
	7	99.26	119.0	151.1	156.3	172.5	192.4	201.7	207.8	213.9	243.4	251.0	262.9
	8	99.26	119.0	151.1	156.3	172.5	192.4	201.7	207.8	213.9	243.4	251.1	262.9
	9	99.26	119.0	151.1	156.3	172.5	192.4	201.7	207.8	213.9	243.4	251.1	262.9
	10	99.26	119.0	151.1	156.3	172.5	192.4	201.7	207.8	213.9	243.4	251.1	262.9
	11	99.27	119.0	151.1	156.3	172.5	192.4	201.7	207.8	213.9	243.4	251.1	262.9
	12	99.27	119.0	151.1	156.3	172.5	192.4	201.7	207.8	213.9	243.4	251.1	262.9

Table A3. 17 Convergence study for the natural frequency parameters of the CCCC hyperbolic-paraboloidal shallow shell on the square planform (Φ= 1.0, R_y/R_x = -1)

	k	Ω_1	Ω_2	Ω_3	Ω_4	Ω_5	Ω_6	Ω_7	Ω_8	Ω_9	Ω_{10}	Ω_{11}	Ω_{12}
$a/R_x = 0.1$	3	46.26	74.44	79.10	109.2	132.3	135.3	164.3	165.5	208.6	210.8	218.9	232.9
	4	46.26	74.61	79.25	110.2	132.3	135.3	165.1	166.3	210.4	212.6	218.9	242.2
	5	46.28	74.63	79.27	110.2	132.5	135.5	165.6	166.8	210.5	212.7	220.6	242.2
	6	46.28	74.64	79.28	110.3	132.5	135.5	165.7	166.8	210.6	212.8	220.6	242.7
	7	46.28	74.65	79.28	110.3	132.5	135.5	165.7	166.9	210.6	212.8	220.8	242.7
	8	46.28	74.65	79.28	110.3	132.5	135.5	165.7	166.9	210.6	212.9	220.8	242.7
	9	46.28	74.65	79.28	110.3	132.5	135.5	165.7	166.9	210.6	212.9	220.8	242.7
	10	46.28	74.65	79.28	110.3	132.5	135.5	165.7	166.9	210.6	212.9	220.8	242.7
	11	46.28	74.65	79.28	110.3	132.5	135.5	165.8	166.9	210.6	212.9	220.8	242.7
	12	46.28	74.65	79.28	110.3	132.5	135.5	165.8	166.9	210.6	212.9	220.8	242.7
$a/R_x = 0.3$	3	67.67	78.06	94.46	134.8	145.5	166.8	171.1	208.9	217.6	221.6	234.6	241.8
	4	67.67	78.25	94.57	116.3	134.8	145.5	167.6	172.1	210.8	219.6	221.6	243.2
	5	67.68	78.27	94.60	116.3	135.0	145.7	168.1	172.5	210.9	219.6	223.4	243.2
	6	67.68	78.28	94.60	116.4	135.0	145.7	168.2	172.6	211.0	219.8	223.4	243.7
	7	67.68	78.29	94.60	116.4	135.0	145.7	168.2	172.6	211.0	219.8	223.6	243.7
	8	67.68	78.29	94.61	116.4	135.0	145.7	168.3	172.6	211.0	219.8	223.6	243.8
	9	67.68	78.29	94.61	116.4	135.0	145.8	168.3	172.7	211.0	219.8	223.6	243.8
	10	67.68	78.29	94.61	116.4	135.0	145.8	168.3	172.7	211.0	219.8	223.6	243.8
	11	67.68	78.29	94.61	116.4	135.0	145.8	168.3	172.7	211.0	219.8	223.6	243.8
	12	67.68	78.29	94.61	116.4	135.0	145.8	168.3	172.7	211.0	219.8	223.6	243.8

Table A3. 18 Convergence study for the natural frequency parameters of the CCCC hyperbolic-paraboloidal shallow shell on the square planform (Φ= 1.0, R_y/R_x = -1) -continued

	k	Ω_1	Ω_2	Ω_3	Ω_4	Ω_5	Ω_6	Ω_7	Ω_8	Ω_9	Ω_{10}	Ω_{11}	Ω_{12}
$a/R_x = 0.5$	3	98.89	118.9	149.4	156.2	172.3	190.7	201.6	205.4	211.7	240.9	242.6	260.2
	4	99.22	118.9	151.1	156.2	172.3	191.6	201.6	207.3	213.7	240.9	250.4	262.7
	5	99.25	119.0	151.1	156.3	172.5	192.3	201.7	207.6	213.8	243.2	250.4	262.8
	6	99.26	119.0	151.1	156.3	172.5	192.4	201.7	207.7	213.9	243.2	251.0	262.9
	7	99.26	119.0	151.1	156.3	172.5	192.4	201.7	207.8	213.9	243.4	251.0	262.9
	8	99.26	119.0	151.1	156.3	172.5	192.4	201.7	207.8	213.9	243.4	251.1	262.9
	9	99.26	119.0	151.1	156.3	172.5	192.4	201.7	207.8	213.9	243.4	251.1	262.9
	10	99.26	119.0	151.1	156.3	172.5	192.4	201.7	207.8	213.9	243.4	251.1	262.9
	11	99.27	119.0	151.1	156.3	172.5	192.4	201.7	207.8	213.9	243.4	251.1	262.9
	12	99.27	119.0	151.1	156.3	172.5	192.4	201.7	207.8	213.9	243.4	251.1	262.9

Table A3. 19 Convergence study for the natural frequency parameters of the CCCC cylindrical shallow shell on the rectangular planform (Φ= 2.0, $R_y/R_x = 0$)

	k	Ω_1	Ω_2	Ω_3	Ω_4	Ω_5	Ω_6	Ω_7	Ω_8	Ω_9	Ω_{10}	Ω_{11}	Ω_{12}
$a/R_x = 0.1$	3	37.74	42.69	53.25	64.28	64.53	71.58	84.28	88.06	88.33	117.0	123.8	129.6
	4	37.74	42.94	53.25	64.31	69.75	72.19	84.52	88.33	102.3	113.1	117.1	117.1
	5	37.75	42.95	53.50	64.33	69.78	72.19	85.06	92.16	102.3	117.1	117.1	123.9
	6	37.75	42.96	53.50	64.34	70.00	72.25	85.07	92.16	102.9	120.2	123.9	125.2
	7	37.75	42.96	53.52	64.34	70.00	72.25	85.14	92.36	102.9	120.2	123.9	125.7
	8	37.75	42.97	53.52	64.34	70.02	72.26	85.14	92.36	103.0	120.3	123.9	125.7
	9	37.75	42.97	53.53	64.34	70.02	72.26	85.15	92.38	103.0	120.3	123.9	125.8
	10	37.75	42.97	53.53	64.34	70.02	72.27	85.16	92.38	103.0	120.4	123.9	125.8
	11	37.75	42.97	53.53	64.34	70.02	72.27	85.16	92.39	103.0	120.4	123.9	125.8
	12	37.75	42.97	53.53	64.34	70.03	72.27	85.16	92.39	103.0	120.4	123.9	125.8
$a/R_x = 0.3$	3	67.06	80.40	83.64	87.96	96.18	98.07	99.13	100.3	119.7	127.0	132.7	135.4
	4	67.09	81.04	83.64	88.19	96.18	98.37	108.4	118.6	119.7	127.0	132.7	138.2
	5	67.13	81.04	83.64	88.19	96.35	98.89	108.4	118.6	125.5	132.7	138.3	141.8
	6	67.13	81.11	83.64	88.20	96.35	98.91	108.6	119.1	125.5	132.7	138.5	141.9
	7	67.14	81.11	83.64	88.20	96.35	98.97	108.6	119.1	125.7	132.7	138.5	142.4
	8	67.14	81.12	83.64	88.20	96.35	98.98	108.6	119.2	125.7	132.7	138.5	142.4
	9	67.15	81.12	83.64	88.20	96.35	98.99	108.6	119.2	125.7	132.7	138.5	142.5
	10	67.15	81.13	83.64	88.20	96.35	98.99	108.6	119.2	125.7	132.7	138.5	142.5
	11	67.15	81.13	83.64	88.20	96.35	99.00	108.6	119.2	125.7	132.7	138.5	142.5
	12	67.15	81.13	83.64	88.20	96.35	99.00	108.6	119.2	125.7	132.7	138.6	142.5

Table A3. 20 Convergence study for the natural frequency parameters of the CCCC cylindrical shallow shell on the rectangular planform (Φ= 2.0, $R_y/R_x = 0$) -continued

	k	Ω_1	Ω_2	Ω_3	Ω_4	Ω_5	Ω_6	Ω_7	Ω_8	Ω_9	Ω_{10}	Ω_{11}	Ω_{12}
$a/R_x = 0.5$	3	72.15	95.00	106.4	116.2	119.9	120.9	131.8	144.0	144.8	150.8	164.3	168.7
	4	72.19	95.68	106.4	116.3	120.4	131.8	144.7	150.5	150.8	164.3	168.7	170.1
	5	72.24	95.68	106.4	116.3	120.8	131.9	144.7	150.5	168.5	169.5	170.0	170.2
	6	72.25	95.76	106.4	116.4	120.9	131.9	145.1	150.6	168.5	169.5	170.0	170.3
	7	72.26	95.76	106.4	116.4	120.9	132.0	145.1	150.6	168.5	169.9	170.0	170.3
	8	72.26	95.78	106.4	116.4	120.9	132.0	145.2	150.6	168.5	169.9	170.0	170.3
	9	72.27	95.78	106.4	116.4	120.9	132.0	145.2	150.6	168.5	170.0	170.0	170.3
	10	72.27	95.78	106.4	116.4	120.9	132.0	145.2	150.6	168.5	170.0	170.0	170.3
	11	72.27	95.78	106.4	116.4	120.9	132.0	145.2	150.6	168.5	170.0	170.0	170.3
	12	72.27	95.78	106.4	116.4	120.9	132.0	145.2	150.6	168.5	170.0	170.0	170.3

Table A3. 21 Convergence study for the natural frequency parameters of the CCCC spherical shallow shell on the rectangular planform ($\Phi= 2.0$, $R_y/R_x = 1$)

	k	Ω_1	Ω_2	Ω_3	Ω_4	Ω_5	Ω_6	Ω_7	Ω_8	Ω_9	Ω_{10}	Ω_{11}	Ω_{12}
$a/R_x = 0.1$	3	50.73	51.52	59.06	68.40	72.35	78.61	89.67	90.51	92.86	116.3	118.2	128.5
	4	51.09	51.52	59.06	72.38	72.53	79.26	89.89	90.51	106.1	116.3	118.3	128.5
	5	51.09	51.53	59.36	72.40	72.55	79.26	90.45	93.86	106.1	118.3	127.7	128.6
	6	51.11	51.53	59.36	72.40	72.78	79.31	90.46	93.86	106.7	121.1	127.8	128.6
	7	51.11	51.54	59.38	72.41	72.79	79.31	90.52	94.07	106.7	121.1	128.3	128.6
	8	51.11	51.54	59.38	72.41	72.81	79.32	90.52	94.07	106.8	121.3	128.4	128.6
	9	51.11	51.54	59.38	72.41	72.81	79.32	90.54	94.09	106.8	121.3	128.4	128.6
	10	51.11	51.54	59.38	72.41	72.81	79.32	90.54	94.09	106.8	121.3	128.4	128.6
	11	51.11	51.54	59.38	72.41	72.81	79.32	90.54	94.10	106.8	121.3	128.4	128.6
	12	51.11	51.54	59.38	72.41	72.81	79.32	90.54	94.10	106.8	121.3	128.4	128.6
$a/R_x = 0.3$	3	113.4	115.2	119.8	125.6	126.2	127.9	133.9	134.0	140.4	151.1	152.7	165.7
	4	115.2	116.6	119.8	126.9	127.9	127.9	134.1	140.4	145.4	151.2	153.1	170.0
	5	115.5	116.6	119.8	126.9	127.9	130.1	135.1	141.7	145.4	153.1	161.4	170.1
	6	115.5	116.6	119.8	127.0	128.3	130.1	135.1	141.7	146.2	155.7	161.5	170.1
	7	115.5	116.6	119.8	127.0	128.3	130.1	135.1	141.8	146.2	155.7	162.1	170.1
	8	115.5	116.6	119.8	127.0	128.3	130.1	135.1	141.8	146.2	155.9	162.1	170.1
	9	115.5	116.6	119.8	127.0	128.3	130.1	135.1	141.8	146.2	155.9	162.2	170.1
	10	115.5	116.6	119.8	127.0	128.3	130.1	135.1	141.8	146.2	155.9	162.2	170.1
	11	115.5	116.6	119.8	127.0	128.3	130.1	135.1	141.8	146.2	155.9	162.2	170.1
	12	115.5	116.6	119.8	127.0	128.3	130.1	135.1	141.8	146.2	155.9	162.2	170.1

Table A3. 22 Convergence study for the natural frequency parameters of the CCCC spherical shallow shell on the rectangular planform (Φ= 2.0, R_y/R_x = 1) -continued

	k	Ω_1	Ω_2	Ω_3	Ω_4	Ω_5	Ω_6	Ω_7	Ω_8	Ω_9	Ω_{10}	Ω_{11}	Ω_{12}
$a/R_x = 0.5$	3	175.1	179.3	179.4	184.6	187.4	191.0	192.0	192.1	199.5	204.2	204.9	213.3
	4	179.3	179.4	179.8	187.4	187.8	191.5	192.3	199.5	201.0	204.3	205.9	221.4
	5	179.4	179.8	180.5	187.8	189.5	191.5	194.5	200.2	201.0	205.9	212.9	221.4
	6	179.4	179.9	180.5	187.9	189.5	192.4	194.5	200.2	202.4	208.0	213.0	222.2
	7	179.4	179.9	180.5	187.9	189.6	192.4	194.5	200.4	202.4	208.0	213.9	224.4
	8	179.4	179.9	180.5	187.9	189.6	192.5	194.5	200.4	202.5	208.1	213.9	224.4
	9	179.4	179.9	180.5	187.9	189.6	192.5	194.5	200.4	202.5	208.1	214.0	224.5
	10	179.4	179.9	180.5	187.9	189.6	192.5	194.5	200.4	202.5	208.1	214.0	224.5
	11	179.4	179.9	180.5	187.9	189.6	192.5	194.5	200.4	202.5	208.1	214.0	224.5
	12	179.4	179.9	180.5	187.9	189.6	192.5	194.5	200.4	202.5	208.1	214.0	224.5

Table A3. 23 Convergence study for the natural frequency parameters of the CCCC hyperbolic-paraboloidal shallow shell on the rectangular planform (Φ= 2.0, R_y/R_x = -1)

	k	Ω_1	Ω_2	Ω_3	Ω_4	Ω_5	Ω_6	Ω_7	Ω_8	Ω_9	Ω_{10}	Ω_{11}	Ω_{12}
$a/R_x = 0.1$	3	43.56	44.14	53.69	63.19	70.88	74.33	85.01	87.48	87.83	112.2	116.4	127.5
	4	43.56	44.82	53.69	69.47	70.89	75.51	85.26	87.48	102.1	112.3	116.5	127.5
	5	43.58	44.83	54.12	69.50	70.93	75.51	86.06	91.87	102.1	116.5	124.6	127.6
	6	43.58	44.85	54.12	69.77	70.93	75.59	86.08	91.87	102.8	119.9	124.7	127.6
	7	43.58	44.85	54.15	69.78	70.94	75.59	86.16	92.09	102.8	119.9	125.3	127.6
	8	43.58	44.85	54.15	69.80	70.94	75.60	86.16	92.09	102.9	120.1	125.3	127.6
	9	43.58	44.85	54.15	69.80	70.94	75.60	86.18	92.12	102.9	120.1	125.4	127.6
	10	43.58	44.85	54.15	69.80	70.94	75.61	86.18	92.12	102.9	120.1	125.4	127.6
	11	43.58	44.85	54.16	69.80	70.94	75.61	86.19	92.12	102.91	120.1	125.4	127.6
	12	43.58	44.86	54.16	69.81	70.94	75.61	86.19	92.12	102.92	120.1	125.4	127.6
$a/R_x = 0.3$	3	83.66	87.04	94.21	99.67	102.5	106.8	109.1	109.3	120.1	125.1	139.6	141.0
	4	94.21	96.03	99.93	102.2	106.8	108.1	109.3	117.7	120.1	125.3	140.2	151.0
	5	94.89	96.03	102.2	102.5	108.1	111.4	114.1	117.7	125.2	138.4	140.2	151.0
	6	94.89	96.03	102.2	102.5	108.7	111.4	114.1	120.4	125.2	138.5	146.2	158.1
	7	94.90	96.03	102.2	102.6	108.7	111.4	114.2	120.4	125.6	139.9	146.2	158.1
	8	94.90	96.03	102.3	102.6	108.8	111.4	114.2	120.5	125.6	139.9	146.4	158.1
	9	94.90	96.03	102.3	102.6	108.8	111.4	114.2	120.5	125.6	140.0	146.4	158.1
	10	94.90	96.03	102.3	102.6	108.8	111.4	114.2	120.6	125.6	140.0	146.4	158.1
	11	94.90	96.03	102.3	102.6	108.8	111.4	114.2	120.6	125.6	140.0	146.4	158.1
	12	94.90	96.03	102.3	102.6	108.8	111.4	114.2	120.6	125.6	140.0	146.4	158.1

Table A3. 24 Convergence study for the natural frequency parameters of the CCCC hyperbolic-paraboloidal shallow shell on the rectangular planform ($\Phi= 2.0$, $R_y/R_x = -1$) -continued

	k	Ω_1	Ω_2	Ω_3	Ω_4	Ω_5	Ω_6	Ω_7	Ω_8	Ω_9	Ω_{10}	Ω_{11}	Ω_{12}
$a/R_x = 0.5$	3	95.54	114.1	119.1	137.6	140.0	142.1	149.1	150.0	157.9	164.6	169.8	171.9
	4	114.3	130.7	137.6	139.8	140.3	142.8	149.1	157.5	164.6	169.9	174.7	176.8
	5	130.7	130.9	139.2	139.8	142.8	154.6	157.6	159.0	171.0	174.7	176.8	183.2
	6	130.9	131.2	139.2	139.9	154.1	154.7	158.4	159.0	171.0	183.2	186.0	187.9
	7	131.0	131.2	139.2	139.9	154.1	155.5	158.4	159.0	175.0	183.5	186.0	187.9
	8	131.0	131.2	139.2	139.9	154.3	155.5	158.4	159.0	175.0	183.5	186.1	189.7
	9	131.0	131.2	139.2	139.9	154.3	155.5	158.4	159.0	175.1	183.5	186.1	189.7
	10	131.0	131.2	139.2	139.9	154.3	155.5	158.4	159.0	175.1	183.5	186.1	189.9
	11	131.0	131.2	139.2	139.9	154.3	155.5	158.4	159.0	175.1	183.5	186.1	189.9
	12	131.0	131.2	139.2	139.9	154.4	155.5	158.4	159.0	175.1	183.5	186.1	189.9

Appendix IV Matlab code

```
%%%%%%%%%%%%%%%%%%%%%%%%%%%%%%%%%%%%%%
% This programme is to calculate the natural frequency parameters of doubly      %
% curved fully clamped thin shells on a rectangular planform using the           %
% Superposition-Galerkin Method for different curvature ratios and aspect ratios. %
%%%%%%%%%%%%%%%%%%%%%%%%%%%%%%%%%%%%%%


clear all

k=input('Please enter the value for k=');  % No. of terms for driving coefficient
PHI=input('Please enter the value for b/a=');        % aspect ratio
beta=input('Please enter the value for a/Rx=');     % ratio of planform
                        % dimension to the radius of curvature
delta=input('Please enter the value for a/h=');       % thickness ratio
gamma=input('Please enter the value for Rx/Ry='); % Gaussian curvature
% 0:cylindrical 1:spherical -1:hyperbolic paraboloidal
almds=input('Please enter the trial value of Lambda to be begun almds=');
del0=input('Please enter the increment of Lambda del=');


BC=[1 1 1 1 1 1 1 1; 1 2 3 4 5 6 7 8];     % boundary condition matrix
                        % BC(2,m) stands for the mth building block
                        % 1:clamped
                        % 0: simply-supported or shear-diagraph (in-plane)
                        % at the its driving edge


PHIS = PHI^2;
POI = 0.3;      % Poisson's ratio
POIS = 2-POI;
POIb = (1-POI)/2;
kk = 20;         % No. of terms for series expansion
del = del0;

Ls = almds+del;
h = 1;
Dc = 1;
r = 1;
d1 = 0;
d2 = 0;
counter0 = 0;
l = 1;

ML=12;         % No. of frequency parameter to be obtained


% Solving vibration problem of the building blocks in terms of E's using Galerkin
% method.
```

```
while h <= ML

% First building block
    a = zeros(3);
    b = zeros(3,1);
    c = zeros(3,1);

    for m = 1:k
        emp = m*pi;

        for s = 1:kk
            esp = s*pi;

            a(1,1) = -12*delta^2*emp^2 - 12*delta^2*POIb/PHIS*esp^2 + Ls^2;
            a(1,2) = -12*delta^2*(1+POI)/2/PHI*emp*esp;
            a(1,3) = 12*delta^2*beta*(1+POI*gamma)*emp;
            a(2,1) = -12*delta^2*(1+POI)/2/PHI*emp*esp;
            a(2,2) = -12*delta^2*POIb*emp^2 - 12*delta^2/PHIS*esp^2 + Ls^2;
            a(2,3) = 12*delta^2*beta/PHI*(POI+gamma)*esp;
            a(3,1) = -12*delta^2*beta*(1+POI*gamma)*emp;
            a(3,2) = -12*delta^2*beta/PHI*(POI+gamma)*esp;
            a(3,3) = (emp^4 + 2/PHIS*emp^2*esp^2 + esp^4/PHIS^2)...
                + 12*delta^2*beta^2*(1+2*POI*gamma+gamma^2) - Ls^2;

            b(1,1) = -2*12*delta^2*beta*(1+POI*gamma)*emp*(-cos(esp)/esp^3);
            b(2,1) = -2*12*delta^2*beta/PHI*(POI+gamma)*(-cos(esp)/esp^2);
            b(3,1) = -2*(2/PHIS*emp^2*(-cos(esp)/esp)...
          + (emp^4 + 12*delta^2*beta^2*(1+2*POI*gamma+gamma^2) - Ls^2)...
          *(-cos(esp)/esp^3));

            c(1,1) = -2*6*(1+POI)*delta^2/PHI*emp*(-cos(esp)/esp);
            c(2,1) = -2*(-12*delta^2*POIb*emp^2 + Ls^2)*(cos(esp)/esp^2);
            c(3,1) = -2*12*delta^2*beta/PHI*(gamma+POI)*(-cos(esp)/esp);

            Em(:,s,m) = a\b;
            Fm(:,s,m) = a\c;
        end
        Em(2,2:kk,m) = Em(2,1:kk-1,m);
        Em(2,1,m) = 0;
        Fm(2,2:kk,m) = Fm(2,1:kk-1,m);
        Fm(2,1,m) = ((12*delta^2*POIb*emp^2 - Ls^2)/6 - 12*delta^2/PHIS)...
                    /(-12*delta^2*POIb*emp^2 + Ls^2);
    end


% Second building block
    a = zeros(3);
    b = zeros(3,1);
    c = zeros(3,1);

    for n = 1:k
        enp = n*pi;

        for t = 1:kk
            etp = t*pi;
```

```matlab
            a(1,1) = -12*delta^2*etp^2 - 12*delta^2*POIb/PHIS*enp^2 + Ls^2;
            a(1,2) = -12*delta^2*(1+POI)/2/PHI*etp*enp;
            a(1,3) = 12*delta^2*beta*(1+POI*gamma)*etp;
            a(2,1) = -12*delta^2*(1+POI)/2/PHI*etp*enp;
            a(2,2) = -12*delta^2*POIb*etp^2 - 12*delta^2/PHIS*enp^2 + Ls^2;
            a(2,3) = 12*delta^2*beta/PHI*(POI+gamma)*enp;
            a(3,1) = -12*delta^2*beta*(1+POI*gamma)*etp;
            a(3,2) = -12*delta^2*beta/PHI*(POI+gamma)*enp;
            a(3,3) = (etp^4 + 2/PHIS*etp^2*enp^2 + enp^4/PHIS^2)...
                + 12*delta^2*beta^2*(1+2*POI*gamma+gamma^2) - Ls^2;

            b(1,1)=-2*12*delta^2*beta*(1+POI*gamma)*(-cos(etp)/etp^2);
            b(2,1)=-2*12*delta^2*beta/PHI*(POI+gamma)*enp*(-cos(etp)/etp^3);
            b(3,1)=-2*(2/PHIS*enp^2*(-cos(etp)/etp) + (enp^4/PHIS^2 ...
                + 12*delta^2*beta^2*(1+2*POI*gamma+gamma^2) - Ls^2)...
                *(-cos(etp)/etp^3));

            c(1,1)=-2*(-12*delta^2*POIb/PHIS*enp^2+ Ls^2)*(cos(etp)/etp^2);
            c(2,1)=-2*(6*(1+POI)*delta^2/PHI*enp)*(-cos(etp)/etp);
            c(3,1)=-2*(12*delta^2*beta*(1+gamma*POI))*(-cos(etp)/etp);

            En(:,t,n) = a\b;
            Fn(:,t,n) = a\c;
        end
        En(1,2:kk,n) = En(1,1:kk-1,n);
        En(1,1,n) = 0;
        Fn(1,2:kk,n) = Fn(1,1:kk-1,n);
        Fn(1,1,n) = ((12*delta^2*POIb/PHIS*enp^2 - Ls^2)/6 - 12*delta^2)...
            /(-12*delta^2*POIb/PHIS*enp^2 + Ls^2);
    end

    Ep = Em;
    Eq = En;
    Fp = Fm;
    Fq = Fn;


% Generating a coefficient matrix "A"
    A = zeros(8*k,8*k);

for m = 1:k
    emp = m*pi;

    for s = 1:kk
        esp = s*pi;
        espc = (s-1)*pi;

        A(m,m) = A(m,m)+Em(3,s,m)*esp*cos(esp);
        A(k+m,k+m) = A(k+m,k+m)+Fm(2,s,m)*cos(espc);
        A(4*k+m,4*k+m) = A(4*k+m,4*k+m)+Ep(3,s,m)*esp*cos(esp);
        A(5*k+m,5*k+m) = A(5*k+m,5*k+m)+Fp(2,s,m)*cos(espc);

        A(m,k+m) = A(m,k+m)+Fm(3,s,m)*esp*cos(esp);
        A(m,4*k+m) = A(m,4*k+m)+Ep(3,s,m)*esp;
```

```
      A(m,5*k+m) = A(m,5*k+m)+Fp(3,s,m)*esp;

      A(k+m,m) = A(k+m,m)+Em(2,s,m)*cos(espc);
      A(k+m,4*k+m) = A(k+m,4*k+m)+Ep(2,s,m);
      A(k+m,5*k+m) = A(k+m,5*k+m)+Fp(2,s,m);

      A(4*k+m,m) = A(4*k+m,m)+Em(3,s,m)*esp;
      A(4*k+m,k+m) = A(4*k+m,k+m)+Fm(3,s,m)*esp;
      A(4*k+m,5*k+m) = A(4*k+m,5*k+m)+Fp(3,s,m)*esp*cos(esp);

      A(5*k+m,m) = A(5*k+m,m)+Em(2,s,m);
      A(5*k+m,k+m) = A(5*k+m,k+m)+Fm(2,s,m);
      A(5*k+m,4*k+m) = A(5*k+m,4*k+m)+Ep(2,s,m)*cos(espc);
   end

   A(m,m) = (A(m,m)-1/3);
   A(k+m,k+m) = (A(k+m,k+m)+1/2);
   A(4*k+m,4*k+m) = (A(4*k+m,4*k+m)-1/3);
   A(5*k+m,5*k+m) = (A(5*k+m,5*k+m)+1/2);

   A(m,4*k+m) = (A(m,4*k+m)+1/6);
   A(4*k+m,m) = (A(4*k+m,m)+1/6);
end

for n = 1:k
   enp = n*pi;

   for t = 1:kk
      etp = t*pi;
      etpc = (t-1)*pi;

      A(2*k+n,2*k+n) = A(2*k+n,2*k+n)+En(3,t,n)*etp*cos(etp);
      A(3*k+n,3*k+n) = A(3*k+n,3*k+n)+Fn(1,t,n)*cos(etpc);
      A(6*k+n,6*k+n) = A(6*k+n,6*k+n)+Eq(3,t,n)*etp*cos(etp);
      A(7*k+n,7*k+n) = A(7*k+n,7*k+n)+Fq(1,t,n)*cos(etpc);

      A(2*k+n,3*k+n) = A(2*k+n,3*k+n)+Fn(3,t,n)*etp*cos(etp);
      A(2*k+n,6*k+n) = A(2*k+n,6*k+n)+Eq(3,t,n)*etp;
      A(2*k+n,7*k+n) = A(2*k+n,7*k+n)+Fq(3,t,n)*etp;

      A(3*k+n,2*k+n) = A(3*k+n,2*k+n)+En(1,t,n)*cos(etpc);
      A(3*k+n,6*k+n) = A(3*k+n,6*k+n)+Eq(1,t,n);
      A(3*k+n,7*k+n) = A(3*k+n,7*k+n)+Fq(1,t,n);

      A(6*k+n,2*k+n) = A(6*k+n,2*k+n)+En(3,t,n)*etp;
      A(6*k+n,3*k+n) = A(6*k+n,3*k+n)+Fn(3,t,n)*etp;
      A(6*k+n,7*k+n) = A(6*k+n,7*k+n)+Fq(3,t,n)*etp*cos(etp);

      A(7*k+n,2*k+n) = A(7*k+n,2*k+n)+En(1,t,n);
      A(7*k+n,3*k+n) = A(7*k+n,3*k+n)+Fn(1,t,n);
      A(7*k+n,6*k+n) = A(7*k+n,6*k+n)+Eq(1,t,n)*cos(etpc);
   end

   A(2*k+n,2*k+n) = (A(2*k+n,2*k+n)-1/3);
   A(3*k+n,3*k+n) = (A(3*k+n,3*k+n)+1/2);
```

```
    A(6*k+n,6*k+n) = (A(6*k+n,6*k+n)-1/3);
    A(7*k+n,7*k+n) = (A(7*k+n,7*k+n)+1/2);

    A(2*k+n,6*k+n) = (A(2*k+n,6*k+n)+1/6);
    A(6*k+n,2*k+n) = (A(6*k+n,2*k+n)+1/6);
end


for m = 1:k
    for n = 1:k
        p = m;
        q = n;

        if m > kk
            En3 = 0;
            Eq3 = 0;
            Fn3 = 0;
            Fq3 = 0;

            En2 = 0;
            Eq2 = 0;
            Fn2 = 0;
            Fq2 = 0;
        else
            En3 = En(3,m,n);
            Eq3 = Eq(3,m,q);
            Fn3 = Fn(3,m,n);
            Fq3 = Fq(3,m,q);

            En2 = En(2,m,n);
            Eq2 = Eq(2,m,q);
            Fn2 = Fn(2,m,n);
            Fq2 = Fq(2,m,q);
        end

        if n > kk
            Em3 = 0;
            Ep3 = 0;
            Fm3 = 0;
            Fp3 = 0;

            Em1 = 0;
            Ep1 = 0;
            Fm1 = 0;
            Fp1 = 0;
        else
            Em3 = Em(3,n,m);
            Ep3 = Ep(3,n,p);
            Fm3 = Fm(3,n,m);
            Fp3 = Fp(3,n,p);

            Em1 = Em(1,n,m);
            Ep1 = Ep(1,n,p);
            Fm1 = Fm(1,n,m);
            Fp1 = Fp(1,n,p);
```

```matlab
        end

        emp = m*pi;
        enp = n*pi;
        epp = p*pi;
        eqp = q*pi;

        A(m,2*k+n) = 2*enp*cos(enp)*(1/2*En3-cos(emp)/emp^3);
        A(m,3*k+n) = 2*enp*cos(enp)*(1/2*Fn3);
        A(m,6*k+q) = -2*eqp*cos(eqp)*(-1/2*Eq3*cos(emp)+1/emp^3);
        A(m,7*k+q) = -2*eqp*cos(eqp)*(-1/2*Fq3*cos(emp));

        A(k+m,2*k+n) = 2*cos(enp)*(1/2*En2);
        A(k+m,3*k+n) = 2*cos(enp)*(1/2*Fn2);
        A(k+m,6*k+q) = -2*cos(eqp)*(-1/2*Eq2*cos(emp));
        A(k+m,7*k+q) = -2*cos(eqp)*(-1/2*Fq2*cos(emp));

        A(2*k+n,m) = 2*emp*cos(emp)*(1/2*Em3-cos(enp)/enp^3);
        A(2*k+n,k+m) = 2*emp*cos(emp)*(1/2*Fm3);
        A(2*k+n,4*k+p) = -2*epp*cos(epp)*(-1/2*Ep3*cos(enp)+1/enp^3);
        A(2*k+n,5*k+p) = -2*epp*cos(epp)*(-1/2*Fp3*cos(enp));

        A(3*k+n,m) = 2*cos(emp)*(1/2*Em1);
        A(3*k+n,k+m) = 2*cos(emp)*(1/2*Fm1);
        A(3*k+n,4*k+p) = -2*cos(epp)*(-1/2*Ep1*cos(enp));
        A(3*k+n,5*k+p) = -2*cos(epp)*(-1/2*Fp1*cos(enp));

        A(4*k+p,2*k+n) = 2*enp*(1/2*En3-cos(epp)/epp^3);
        A(4*k+p,3*k+n) = 2*enp*(1/2*Fn3);
        A(4*k+p,6*k+q) = -2*eqp*(-1/2*Eq3*cos(epp)+1/epp^3);
        A(4*k+p,7*k+q) = -2*eqp*(-1/2*Fq3*cos(epp));

        A(5*k+p,2*k+n) = 2*(1/2*En2);
        A(5*k+p,3*k+n) = 2*(1/2*Fn2);
        A(5*k+p,6*k+q) = -2*(-1/2*Eq2*cos(epp));
        A(5*k+p,7*k+q) = -2*(-1/2*Fq2*cos(epp));

        A(6*k+q,m) = 2*emp*(1/2*Em3-cos(eqp)/eqp^3);
        A(6*k+q,k+m) = 2*emp*(1/2*Fm3);
        A(6*k+q,4*k+p) = -2*epp*(-1/2*Ep3*cos(eqp)+1/eqp^3);
        A(6*k+q,5*k+p) = -2*epp*(-1/2*Fp3*cos(eqp));

        A(7*k+q,m) = 2*(1/2*Em1);
        A(7*k+q,k+m) = 2*(1/2*Fm1);
        A(7*k+q,4*k+p) = -2*(-1/2*Ep1*cos(eqp));
        A(7*k+q,5*k+p) = -2*(-1/2*Fp1*cos(eqp));
    end
end

AA = A;


% if the driving edge of a building block is simply-supported (out of plane) or
% shear diaphragm (in-plane) the corresponding row and column are removed.
bm = 0;
```

```
   for m = 1:8
      if BC(1,m) == 0
         bc = BC(2,m)-bm;
         A((bc-1)*k+1:bc*k,:) = [];
         A(:,(bc-1)*k+1:bc*k) = [];
         bm = bm+1;
      end
   end


% Gaussian elimination
   bn = 8-bm;
   for p = 1:bn*k
      for m = p+1:bn*k
         if A(m,p)~=0
            alp=A(m,p)/A(p,p);
            for n = p:bn*k
               A(m,n)=A(m,n)-A(p,n)*alp;
            end
         end
      end
   end


% Counting the negatives in diagonal and determining natural frequency parameters
   da=1;
   DA = diag(A);
   counter = 0;
   for m = 1: bn*k
      if DA(m)<0
         counter = counter+1;
      end
   end

   d = det(A)*10^6;
   D(l) = d;
   L(l) = Ls;
   C(l) = counter;
   l = l+1;

   if counter0 == 2
      if d1*d > 0
         if (abs(d3) > abs(d2)) && (abs(d) > abs(d1))
            LA(h,k) = Ls-1.5*Dc*del;
            LA(h+1,k) = Ls-1.5*Dc*del;
            h = h+2;
            Ls = Ls+Dc*del;
         else
            Ls = Ls+Dc*del;
         end
      elseif ((d1*d< 0) && (abs(d2) > abs(d1)))
         LA(h,k) = Ls-Dc*del/2;
         h = h+1;
         Ls = Ls+Dc*del;
      else
```

117

```
        Ls = Ls+Dc*del;
      end
      counter0 = 1;

  elseif ((d1*d< 0) && (abs(d2) > abs(d1)))
     LA(h,k) = Ls-Dc*del/2;
     h = h+1;
     Ls = Ls+Dc*del;
  else
     Ls = Ls+Dc*del;
  end


  if counter0 == 0
     counter0 = 1;
     counter1 = counter;
     d2 = d1;
     d1 = d;

  elseif PHI == 1 && abs(counter1-counter) == 2
     counter0 = 2;
     counter1 = counter;
     d3 = d2;
     d2 = d1;
     d1 = d;
  else
     counter1 = counter;
     d2 = d1;
     d1 = d;
  end

  if Ls > (10^(r+1)-Dc*del);
     Dc = 10^r;
     r = r+1;
  end
end

Eigenvalues = LA
```